UNIVERSITÉ DU QUÉBEC À MONTRÉAL

THÈSE PRÉSENTÉE À L'UNIVERSITÉ DU QUÉBEC À CHICOUTIMI
COMME EXIGENCE PARTIELLE DU

DOCTORAT EN RESSOURCES MINÉRALES

OFFERT À L'UNIVERSITÉ DU QUÉBEC À MONTRÉAL
EN VERTU D'UN PROTOCOLE D'ENTENTE
AVEC
L'UNIVERSITÉ DU QUÉBEC À CHICOUTIMI

PAR
ANDRE POIRIER

GÉOCHIMIE ISOTOPIQUE Re-Os et Pb-Pb : APPROCHES ENVIRONNEMENTALE ET MÉTÉORITIQUE

JUILLET 2005

Bibliothèque Paul-Émile-Boulet

UQAC Université du Québec à Chicoutimi

Mise en garde/Advice

Afin de rendre accessible au plus grand nombre le résultat des travaux de recherche menés par ses étudiants gradués et dans l'esprit des règles qui régissent le dépôt et la diffusion des mémoires et thèses produits dans cette Institution, **l'Université du Québec à Chicoutimi (UQAC)** est fière de rendre accessible une version complète et gratuite de cette œuvre.

Motivated by a desire to make the results of its graduate students' research accessible to all, and in accordance with the rules governing the acceptation and diffusion of dissertations and theses in this Institution, the **Université du Québec à Chicoutimi (UQAC)** is proud to make a complete version of this work available at no cost to the reader.

L'auteur conserve néanmoins la propriété du droit d'auteur qui protège ce mémoire ou cette thèse. Ni le mémoire ou la thèse ni des extraits substantiels de ceux-ci ne peuvent être imprimés ou autrement reproduits sans son autorisation.

The author retains ownership of the copyright of this dissertation or thesis. Neither the dissertation or thesis, nor substantial extracts from it, may be printed or otherwise reproduced without the author's permission.

UNIVERSITÉ DU QUÉBEC À MONTRÉAL

THESIS PRESENTED AT UNIVERSITÉ DU QUÉBEC À CHICOUTIMI
AS PARTIAL FULFILMENT TO OBTAIN THE GRADE OF

DOCTOR IN MINERAL RESSOURCES

OFFERED AT UNIVERSITÉ DU QUÉBEC À MONTRÉAL
IN AGREEMENT WITH
UNIVERSITÉ DU QUÉBEC À CHICOUTIMI

BY
ANDRE POIRIER

Re-Os & Pb-Pb ISOTOPE GEOCHEMISTRY: ENVIRONMENTAL AND METEORITICS EXAMPLES

JULY 2005

RÉSUMÉ

Le sujet principal de cette thèse est le traceur isotopique rhénium-osmium (Re-Os). Depuis 1991, année de publication d'une technique efficace pour en faire l'analyse, grâce à la thermo-ionisation à polarité inversée, le système isotopique Re-Os a permis d'étendre les connaissances dans de nombreuses branches des géosciences. Cependant, beaucoup d'aspects du comportement chimique de ces deux éléments chalco-sidérophiles demeurent incompris, que ce soit en géochimie environnementale ou en ce qui a trait aux météorites. Ces lacunes limitent la portée des interprétations faites à partir des données Re-Os. L'objectif de la présente thèse vise à combler certaines de ces lacunes et à faire ainsi progresser l'état des connaissances du système Re-Os. A cette fin, celui-ci est comparé avec un second système isotopique, connu depuis plus longtemps, celui du plomb. Trois domaines d'application sont explorés à partir d'études de cas: le domaine "classique" des météorites, celui des apports anthropiques et enfin le domaine de la géologie environnementale et sédimentaire.

Le premier chapitre porte ainsi sur la météorite de St-Robert, une chondrite de type pétrographique H5. Son système Pb-Pb a livré un âge de 4.56 Ga, soit l'âge accepté de la formation des corps rocheux du système solaire. Les résultats du système Re-Os sur des fragments rocheux présentent des perturbations par rapport à l'isochrone de l'âge de l'échantillon, comme c'est le cas dans la vaste majorité des études de chondrites rapportées dans la littérature scientifique. Nos résultats permettent d'avancer un échange de Re entre les diverses phases métalliques. Les croûtes de fusion, résultat de l'entrée atmosphérique du météore, présentent moins de perturbations que les autres fragments rocheux. Nous croyons que cela est du à l'homogénéisation des phases de divers rapports Re/Os dans la croûte, pendant la fusion de la surface du météoroïde.

Le deuxième chapitre porte sur certains apports anthropiques en Os. Quelques études passée sont fait mention de la possibilité que les voitures équipées de convertisseurs catalytiques dans leur système d'échappement renvoient de l'osmium dans l'environnement. Les pots catalytiques automobiles contiennent des platinoïdes (Pd-Pt-Rh); ces métaux étant nécessaires à la conversion des gaz d'échappement (CO, NO_x, hydrocarbure) en composés moins nocifs (CO_2, N_2, H_20). Il a été démontré que les vibrations d'une voiture en opération causent l'attrition du matériel catalytique, et que les particules ainsi libérées sont évacuées par l'échappement, accumulant des platinoïdes sur les bords du réseau routier. Par nature, ces platinoïdes sont associés à de l'Os de composition isotopique non-radiogénique ($^{187}Os/^{188}Os < 0.2$). L'analyse de catalyseurs confirme qu'ils comportent, en impureté (jusqu'à 228 ppt), de l'Os de faible composition isotopique. Nous pensons que cette valeur est trop faible pour rendre compte d'une pollution significative en osmium par l'expulsion de poussière des catalyseurs. Par contre, nous avons examiné la possibilité que la volatilité de l'osmium oxydé permette une perte gazeuse de cet élément dans les conditions d'opération des pots catalytiques. Une simulation expérimentale a permis d'évaluer la volatilité de l'oxyde d'osmium ($OsO_{4(g)}$) : près de 95% de l'Os pourrait être évacué vers le milieu ambiant par les pots d'échappement des voitures. Par cette perte gazeuse, le parc automobile pourrait ainsi constituer une source majeure de pollution en Os nonradiogénique: plusieurs pico-grammes d'osmium par m_2 pourraient être déposés annuellement dans les zones de forte densité de voitures. Cette source de pollution viendrait s'ajouter aux quelques rares sources d'osmium anthropiques déjà inventoriées.

Le troisième chapitre porte sur les sédiments récents de Saanich Inlet, un fjord anoxique de la Cote Ouest du Canada, cité comme un possible analogue moderne de milieu de dépôt d'argilites noires *(black shales)*. Parmis d'autres sédiments anciens, les black shales ont été utilisés pour construire la courbe évolutive du $^{187}Os/^{188}Os$ des paléo-océans au Cénozoïque, et plus partiellement au Mézosoïque. L'interprétation de cette courbe permet d'établir des éléments d'appréciation d'événements géologiques passés et peut aider à une meilleure compréhension des phénomènes tectono-climatiques anciens. Nous avons voulu vérifier ici dans quelle mesure les sédiments récents déposés à Saanich Inlet s'avéraient susceptibles d'enregistrer la composition en $^{187}Os/^{188}Os$ actuelle de l'océan. Nous constatons que ces sédiments ne rendent pas compte de la composition de l'osmium océanique et que leurs teneurs en Os restent faibles (55-60 ppt). Cela semble être le résultat combiné d'un faible enrichissement en osmium marin des sédiments du fjord et à un apport local en Os non-radiogénique (détritique et/ou dissous). L'analyse de niveaux stratigraphiques pré-anthropiques permet le rejet de la possibilité d'un apport lié à la pollution humaine en Os pour expliquer les valeurs non-radiogéniques. Les isotopes du plomb des sédiments rendent par ailleurs compte de l'impact environnemental de l'utilisation de tétra-éthyl de Pb comme additif anti-détonant aux carburants automobiles, entre les années ~1930 et ~1980. La signature isotopique en Pb des sédiments de Saanich Inlet, durant cette période, permet de démontrer que ce fjord fut grandement affecté pas les apports de plomb atmosphérique originaire des Etats-Unis et provenant du parc automobile.

Mots clés : Re-Os, Pb-Pb, géochimie isotopique, cosmochimie, météorite de St-Robert, contamination en métaux lourds, convertisseur catalytique, sédiments anoxiques, fjord de Saanich Inlet.

ABSTRACT

The rhenium-osmium (Re-Os) isotopic tracer is the main subject of this thesis. Since the discovery of an efficient technique to analyze these two elements in 1991 (negative ion thermal ionization mass spectrometry), this isotopic system has allowed us to improve our understanding in many geoscientific topics. However, lots of poorly understood issues remain about the chemical behavior of these chalco-siderophile elements. These issues cover a wide range of subjects (from meteoritics to environmental studies) and hinder the scope of the interpretation accessible to the use of the Re-Os couple. The main objective of this thesis was to solve some of these unresolved issues. For that, we compare the Re-Os with the Pb-Pb isotopic scheme, that last one being used since much longer time. Three areas are investigated throughout this thesis: the "classical" case of meteorite study, the anthropogenic input problem and Os behavior in the context of sedimentary geology.

The first chapter reports the isotopic study of the St-Robert H5 chondrite. This meteorite yields a Pb-Pb age of 4.56 Ga, comparable to the accepted age of most chondrites. These results imply that no major perturbation affected the Pb-Pb systematics of this meteorite's parent body within the first few billion years following its accretion. Re and Os isotopic data of whole-rock fragments, surface fusion crusts and metal phases show perturbation, although most data plot near the 4.56 Ga reference isochron. From the fusion crust results, we rule out the possibility that atmospheric entry caused the perturbations in the Re-Os system, since melted crust analysis yields amongst the most concordant datapoints. Evidence from metal phases suggests that a very recent process perturbed the isochron, relocating Re from kamacite towards troilite.

The second chapter examines the importance of anthropogenic input from automobile catalytic converters in the Os budget. Higher osmium concentrations and lower $^{187}Os/^{188}Os$ ratios in sediments from urban areas have been linked to anthropogenic osmium sources and automobile catalytic converters that use platinum group metals (PGM) are a potential source for this Os pollution. We present the first direct Os concentrations and isotopic measurements of catalytic converters for major automobile brands in order to test the assumption that car catalysts release Os with a distinct signature in the environment. The analysis of 4 new catalytic converters yield similar low $^{187}Os/^{188}Os$ ratios (0.1-0.2), suggesting a similar source for the PGM. The Os concentrations measured are in the ppt range (6-228 ppt). From our results, the osmium contribution of the car catalysts to the environment through *attrition* (wearing and grinding down of the catalyst by friction) is predicted to be low; < 0.2 pg Os/m^2/year in highly urbanized environment. We show that Os loss from catalysts as volatile OsO_4 is important at car catalyst operating temperatures. Moreover, we estimate that car catalysts may be responsible for up to ~120 pg Os/m^2 deposited per year in urban areas, and that part of it may be exported to sedimentary sinks. Car catalytic converters are thus an important anthropogenic osmium source in densely populated areas. The NIST car catalyst standard (SRM-2557, made from recycled catalysts) yields higher concentrations (up to 721 ppt Os) and a more radiogenic isotopic composition (~0.38), perhaps indicative of Os contamination during its preparation.

The third chapter investigates the capability of anoxic sediments (from the fjord of Saanich Inlet, B.C.) to record the osmium isotopic composition of the ocean. From core top to 61 cm downcore, spanning approximately the last 100 years of sedimentation, $^{187}Os/^{188}Os$

ratio and Os concentration decrease respectively from ~0.9 to ~0.8, and 60 to 55 ppt, whereas the Re concentration increase from 2800 to 4000 ppt. ^{204}Pb-normalized lead isotope ratios increase from sediment surface down to 7 cm down-core, then decrease steadily to pre-industrial levels at ~ 50 cm downcore. This pattern illustrates the contamination from leaded gasoline until the recent past. The measured Pb isotopic ratios point toward an atmospheric lead source primarily from the USA. The osmium isotopic values measured are significantly lower than those of modern seawater-Os (1.06; Levasseur et al. 1998). In comparison with other anoxic environments, the osmium content of Saanich Inlet sediments is low, suggesting prominent inputs from unradiogenic, detrital and/or dissolved sources. Thus, the bulk sediment of Saanich Inlet does not appear to record ^{187}Os/^{188}Os composition of the marine end-member of the only slightly below normal salinity, fjord water. The low seawater-derived Os content of the sediment, coupled with unradiogenic Os inputs from local sources, explain the overall low isotopic values observed. As a consequence, such near-shore anoxic sediments are unlikely to record changes in the past ocean Os isotopic composition.

Keywords : Re-Os, Pb-Pb, isotope geochemistry, cosmochemistry, St-Robert meteorite, heavy metal contamination, catalytic converters, anoxic sediments, Saanich Inlet.

REMERCIEMENTS

Mes premiers remerciements se doivent d'aller à mon directeur de thèse, Clément Gariépy, qui a succombé à la maladie en avril 2004. Je lui dois énormément, autant au plan humain qu'au point de vue scientifique... Merci Clem!

Des remerciements sincères vont aux membres du jury pour avoir accepté d'évaluer cette thèse : MM. Jean-Louis Birck, Thomas Pedersen, Daniele Pinti et C. Hillaire-Marcel. Un double remerciement va à ce dernier, pour avoir accepté la tâche de me relire, en tant que superviseur pour le dernier droit de cette thèse.

Merci à Jean David pour son aide, ses encouragements et son entendement. Merci à Raynald Lapointe pour son soutien technique essentiel et ses discussions.

Beaucoup de gens qui me sont extrêmement chers ne savent pratiquement rien du contenu des pages suivantes. Et c'est pour cette raison que je les apprécie tant : il y a tellement plus que la Science dans la vie!

Le Fonds Québécois de Recherche sur la Nature et les Technologies (FQRNT), de même que le Conseil de Recherches en Sciences Naturelles et en Génie (CRSNG) sont remerciés pour le financement qu'ils m'ont accordé pour réaliser cette thèse.

TABLE DES MATIÈRES

LISTE DES FIGURES

LISTE DES TABLEAUX

INTRODUCTION

En tant que traceur et chronomètre de processus géologiques, le couple rhénium-osmium a permis d'approfondir les connaissances dans le domaines de Sciences de le Terre et de l'Univers. L'utilisation généralisée de ce système radioactif est encore relativement récente. Les difficultés techniques liées à l'analyse de l'osmium, difficile à ioniser par les techniques classiques de spectrométrie de masse, ont eu pour effet d'en ralentir les progrès. C'est au début des années 1990, alors que l'on saisit enfin comment analyser l'osmium de manière efficace, par thermo-ionisation à polarité négative (Creaser et al. 1991; Völkening et al. 1991), que l'utilisation à grande échelle du couple Re-Os a débuté. Malgré la grande quantité d'études aujourd'hui réalisées, le comportement chimique de ces deux éléments chalcosidérophiles (i.e., présentant des affinités avec les comportements du soufre et du fer), reste encore obscur, à certains niveaux. Des interrogations persistent en ce qui a trait à plusieurs facettes de ce système isotopique. En géochimie environnementale par exemple, les sources éventuelles de pollution en Os sont encore peu connues (par ex. Ravizza et Bothner, 1996); son comportement en milieu estuarien reste équivoque et son temps de séjour océanique mal connu (Martin et al. 2001; Peucker-Ehrenbrink et Ravizza, 2000; Oxburg, 1998). Dans les météorites, les résultats obtenus sur les chondrites sont mal expliqués, au même titre que l'impact de l'altération, en milieu terrestre, sur la distribution du Re-Os. La présente étude se fixe ainsi pour objectif de répondre à certaines de ces questions. Pour y parvenir, le système Re-Os sera comparé avec celui des isotopes du plomb, connu depuis plus longtemps. Du fait de leurs comportements cosmochimique et géochimique différents, le couplage de ces deux systèmes est en effet susceptible d'apporter des informations complémentaires sur les phénomènes étudiés.

Trois thèmes seront abordés dans cette thèse; ils touchent aux extrémités de la trame historique de notre planète. Le premier chapitre consacré à l'examen d'une météorite non différenciée concerne les premiers instants de sa formation, il y a 4.56 milliards d'années. Les deux autres chapitres traitent de phénomènes actuels, en l'occurrence de certaines parties du cycle exogène de l'osmium; ils visent d'une part à quantifier la pollution anthropogénique en osmium et, d'autre part, le comportement de cet élément en milieu sédimentaire anoxique, dans le fjord de Saanich Inlet, en Colombie-Britannique.

Rappel sommaire sur les systèmes isotopiques utilisés

Cette section se veut un rappel sur certains aspects de la géochimie des systèmes Pb-Pb et Re-Os, utilisés dans cette étude doctorale. L'aspect analytique étant traité dans le premier chapitre, il ne sera pas abordé ici.

Système Pb –Pb

Le système Pb-Pb est en fait un sous-système du système U-Pb. Nous aborderons d'abord ce dernier afin d'en faire ressortir le premier. Les isotopes de masses 235 et 238 de l'uranium, après une suite de désintégrations en chaîne, aboutissent à deux isotopes stables du plomb. Nous ne nous intéresserons pas ici aux produits intermédiaires de ces chaînes de désintégrations; seuls les éléments extrêmes seront considérés. Ainsi, ^{238}U (période radioactive de 4.47 Ga) donne le ^{206}Pb et ^{235}U (période radioactive de 704 Ma), le ^{207}Pb (Dickin, 1995). Des quatre isotopes stables du plomb, seule l'abondance du plomb 204 n'a pas varié depuis la formation du système solaire; il est ainsi pratique de présenter les données isotopiques sous forme de rapports avec le plomb 204 comme dénominateur commun (équations 1 et 2). Les isotopes de plomb de masses 206, 207 et 208 ont tous trois vu leur abondance croître par la désintégration radioactive d'ascendants (les 2 uranium déjà mentionnés et le ^{232}Th se désintégrant en ^{208}Pb, éq. 3). Les abondances relatives des isotopes stables du plomb peuvent donc varier d'un environnement géologique à l'autre, en fonction de la quantité de U et Th présente, relativement à la quantité de Pb, de même qu'en fonction du temps écoulé; ce temps ayant permis à la radioactivité de faire son effet.

Équation 1
$$\left(\frac{^{207}Pb}{^{204}Pb}\right)_{actuel} = \left(\frac{^{207}Pb}{^{204}Pb}\right)_{initial} + \frac{^{235}U}{^{204}Pb}\left(e^{\lambda 235 t} - 1\right)$$

Équation 2
$$\left(\frac{^{206}Pb}{^{204}Pb}\right)_{actuel} = \left(\frac{^{206}Pb}{^{204}Pb}\right)_{initial} + \frac{^{238}U}{^{204}Pb}\left(e^{\lambda 238 t} - 1\right)$$

Équation 3
$$\left(\frac{^{208}Pb}{^{204}Pb}\right)_{actuel} = \left(\frac{^{208}Pb}{^{204}Pb}\right)_{initial} + \frac{^{232}Th}{^{204}Pb}\left(e^{\lambda 232 t} - 1\right)$$

Où les λ_{xxx} sont les constantes de désintégration des isotopes ^{235}U, ^{238}U et ^{232}Th.

D'un point de vue cosmochimique, l'uranium est un élément réfractaire, c'est-à-dire qu'il se condense rapidement et reste difficile à volatiliser sous la forme élémentaire. Lors du refroidissement de la nébuleuse présolaire, il fut parmi les premiers éléments à condenser (température de 50% de condensation = *ca.* 1580 K, ce qui représente la température à laquelle une moitié du stock de l'élément est gazeux et l'autre condensée, liquide ou solide). Le plomb est plutôt un élément volatil (température de 50% de condensation = *ca.* 520 K). Le Pb est demeuré ainsi plus longtemps en phase gazeuse avant de passer finalement en phase solide et de "fixer" ainsi la composition isotopique initiale du système solaire ($^{206}Pb/^{204}Pb$ = 9.307; $^{207}Pb/^{204}Pb$ = 10.294, Tasumoto et al. 1973). Ce fractionnement entre U et Pb fait en sorte que certaines phases riches en éléments réfractaires présentes dans les météorites possèdent aujourd'hui des compositions isotopiques du Pb extrêmement radiogéniques (par exemple les inclusions de calcium et aluminium) alors que d'autres phases minérales ont conservé la composition isotopique primordiale (par exemple les troïlites).

Dans le premier chapitre, le système Pb-Pb sera utilisé pour déterminer l'âge d'une météorite non-différenciée et s'assurer de l'absence de perturbation majeure affectant cet échantillon à la suite de l'accrétion du corps parent (i.e. un astéroïde ou une proto-planète) d'où il provient. Pour une telle application géochronologique, la concentration en uranium, l'élément père, n'est pas une donnée nécessaire lorsque nous utilisons le système Pb-Pb, contrairement aux systèmes isotopiques classiques U-Pb. En divisant l'une par l'autre les équations de désintégration des deux isotopes de l'uranium (éq. 1et 2), une nouvelle équation est obtenue (éq. 4) dans laquelle se retrouve le rapport isotopique actuel de l'uranium naturel (i.e., $^{238}U/^{235}U$ = 137.88), permettant de s'affranchir totalement de la mesure de la teneur en uranium. Mentionnons un corollaire avantageux: s'il s'est produit un changement *récent* du rapport élémentaire U/Pb dans l'échantillon, la composition isotopique actuelles du Pb n'en sera pas affectée et l'âge obtenu ne sera donc pas perturbé. Cette particularité fait du Pb-Pb un système robuste face à toute altération éventuelle récente des échantillons.

Équation 4

$$\frac{\left(\frac{^{207}Pb}{^{204}Pb}\right)_{actuel} - \left(\frac{^{207}Pb}{^{204}Pb}\right)_{initial}}{\left(\frac{^{206}Pb}{^{204}Pb}\right)_{actuel} - \left(\frac{^{206}Pb}{^{204}Pb}\right)_{initial}} = \frac{1}{137.88}\frac{\left(e^{\lambda 235 t} - 1\right)}{\left(e^{\lambda 238 t} - 1\right)}$$

Pour obtenir l'âge d'un échantillon, il suffit donc, d'un point de vue théorique, d'obtenir les compositions isotopiques actuelle et initiale en plomb, et de résoudre l'équation 4 pour l'âge *t*. Notons que la solution est établie par calcul itératif puisque l'équation est de nature transcendante. Un problème demeure: les compositions isotopiques initiales du Pb d'un échantillon sont rarement connues. Pour les météorites, on peut utiliser la valeur obtenue pour la troïlite de la météorite de fer de Cañon Diablo (CDT, Tatsumoto et al. 1973), valeur subséquemment démontrée comme reflétant un état initial uniforme du système solaire (Göpel et al. 1985). Par contre, dans la plupart des échantillons terrestres et météoritiques éventuellemennt perturbés, la composition isotopique initiale reste inconnue, puisque les processus géologiques subséquents sont susceptibles d'avoir ajouté du plomb radiogénique au plomb initial en proportions *a priori* inconnues. On pourra cependant contourner ce problème par une approche mathématique simple: le membre gauche de l'équation 4 correspondant directement à la pente de la droite $^{206}Pb/^{204}Pb$ vs $^{207}Pb/^{204}Pb$, dans l'espace géométrique (Fig.1). Donc, pour une série d'analyse d'échantillons syngénétiques, si l'on définit une droite dans un tel espace géométrique, on peut s'affranchir des valeurs isotopiques initiales en injectant la valeur de la pente de la droite de régression, dans l'équation, pour obtenir *t*, toujours par itération. L'évolution temporelle des compositions isotopiques est illustrée sur la figure 1. Il est à noter que, contrairement aux autres systèmes isotopiques traditionnels, le changement de pente, dans le temps, d'une isochrone Pb-Pb ne se fait pas vers des valeurs toujours plus grandes; cela est dû au fait que l'on n'utilise pas le rapport isotope père/isotope fils, en abscisse, lequel décroît dans le temps, mais bien un rapport isotope fils/isotope stable initial qui s'accroît dans le temps. Le même principe s'applique aux ordonnées, mais quoique avec un taux d'accroissement différent de celui du rapport porté en abscisse. La position d'un point donné, débutant avec la valeur de la troïlite CDT, évoluera ainsi sur une trajectoire courbe avec le temps (fig. 1). L'allure de cette courbe est fonction du rapport U/Pb de la phase analysée et des périodes radioactives de chacun des isotopes de l'uranium.

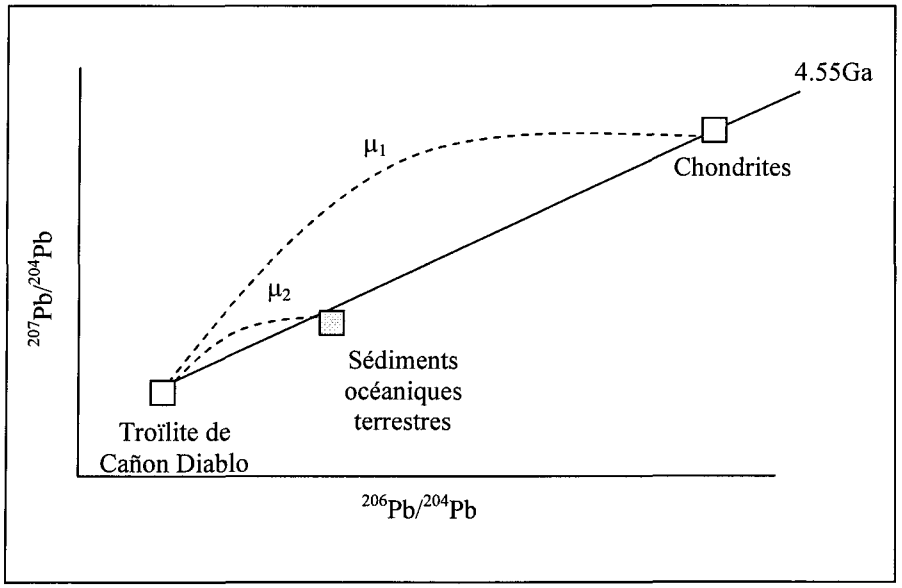

Figure 1. Évolutions des compositions isotopiques en Pb avec le temps, à partir de la valeur initiale du système solaire, en fonction de différents rapports $\mu = {}^{238}U/{}^{204}Pb$ (ici, $\mu_1 > \mu_2$). Il s'agit de la première étude donnant un âge 'valable' pour notre planète, par analogie à l'âge des météorites. Modifié de Patterson (1956).

Sur Terre, les Hommes exploitent les gisements de plomb depuis longtemps (à l'échelle temporelle humaine). Ces gisements sont les produits de concentrations anormales de ce métal dans la croûte terrestre et se sont mis en place à divers moments dans l'histoire géologique de la planète (le principal minerais de plomb est la galène, un sulfure contenant plus de 80% de plomb, en masse). Ces gisements ont des compositions isotopiques du Pb distinctes, en fonction de leur âge de mise en place. Lorsque l'activité anthropique résulte en une pollution de l'environnement par des composés plombifères, il est ainsi possible de retracer la (ou les) source(s) polluante(s) si l'on connaît sa (leurs) composition(s) isotopique(s). Dans le cas de sources multiples, advenant qu'elles proviennent de gisements avec des signatures isotopiques distinctes, celles-ci définissent alors autant de pôles de mélanges dans un diagramme isotopique.

Un cas classique illustre bien cette situation: l'addition de tétra-éthyl de Pb aux carburants automobiles, en Amérique du Nord, en tant qu'agent antidétonant (une pratique

maintenant abandonnée depuis le début des années 1980), à fait augmenter considérablement les teneurs en plomb des aérosols et, via leur dépôt en milieu aquatique, celles des sédiments récents. L'analyses isotopique de ce plomb dans des sédiments récents du Canada a permis de mettre en évidence: 1) que ce plomb de surface était distinct des apports pré-anthropiques enregistrés dans les sédiments profonds plus anciens et, 2) qu'une bonne partie de la contamination en Pb du Canada provenait des États-Unis (e.g., Sturges et Barrie, 1987). En effet, le plomb des Etats Unis, provenant en bonne partie des gisements de la vallée du Mississippi, possède une signature isotopique différente du Pb canadien, extrait du gisement de Bathurst (sulfure massif volcanogène du Nouveau-Brunswick).

Système Re-Os

Le rhénium possède 2 isotopes, de masses 185 et 187. Le plus lourd de ceux-ci est aussi le plus abondant (62.7%); il est également radioactif, avec une période de décroissance de 41.6 milliards d'années (Smoliar et al. 1996). La désintégration du ^{187}Re se fait par l'émission d'une particule bêta et d'un antineutrino, et devenant par le fait même un atome de ^{187}Os (éq. 4). Ce nouvel atome d'osmium viendra s'ajouter à ceux déjà présent naturellement.

Équation 5: $^{187}\mathrm{Re} \Rightarrow {}^{187}Os + \beta^{-} + \nu + \acute{e}nergie$ (2.75 keV)

L'osmium possède 7 isotopes stables répartis entre les masses 184 et 192 (fig. 2). Deux d'entre eux sont issus de processus radioactifs, soient les isotopes 186 et 187. Une petite partie de l'osmium 186 provient de la lente désintégration alpha d'un isotope mineur du platine (^{190}Pt, 0.012% du Pt élémentaire naturel). Dans la présente étude, on ne s'intéressera pas aux variations éventuelles en osmium 186, mais il importe de mentionner cet isotope puisque les études les plus anciennes (avant 1995) utilisaient cet isotope aux fins de normalisation des rapports isotopiques de l'élément. Cette pratique est abandonnée; on utilise maintenant ^{188}Os comme dénominateur des rapports isotopiques. La conversion des données ^{187}Os/^{186}Os en ^{187}Os/^{188}Os s'effectue en multipliant le premier par 0.12034, une valeur arbitraire distincte du rapport ^{186}Os/^{188}Os actuellement accepté de 0.11998 (Shirey et Walker, 1998).

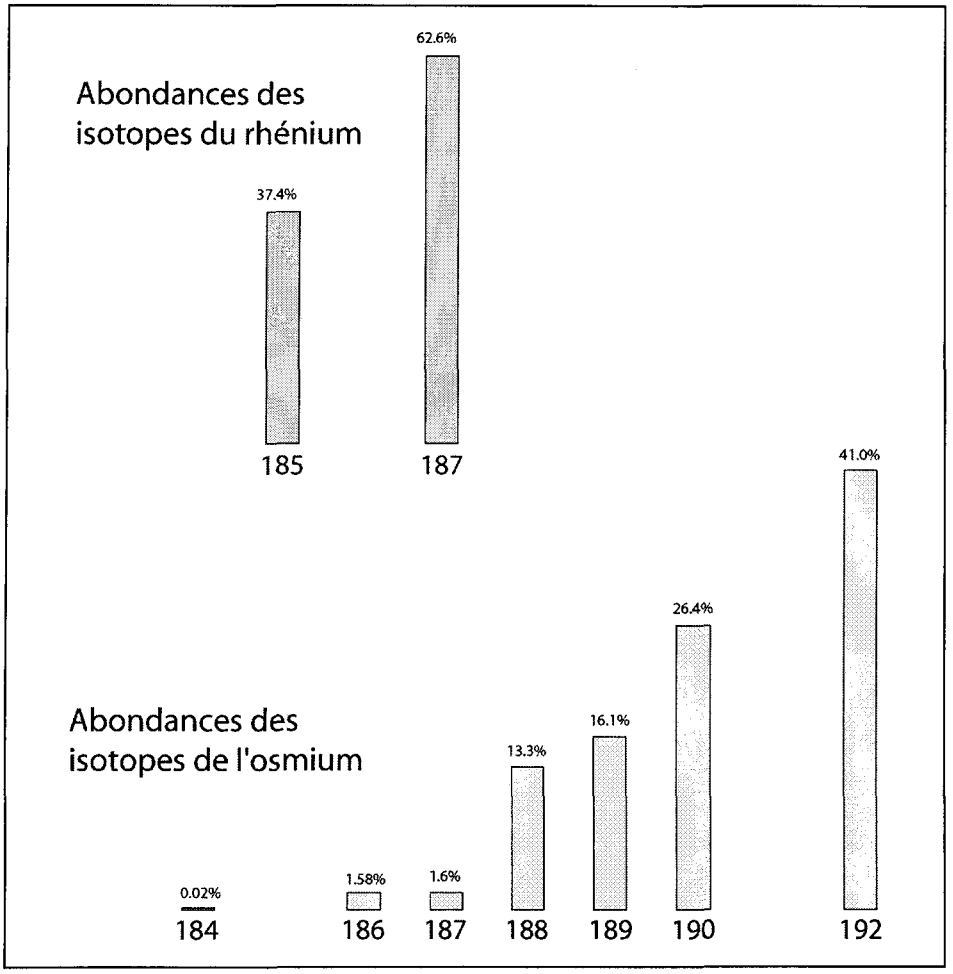

Figure 2: Abondances relatives des isotopes du rhénium et de l'osmium. Les isotopes 186 et 187 de l'osmium peuvent varier.

Les atomes de ^{187}Os présents dans un échantillon proviennent en partie de la désintégration du rhénium, parfois même en majorité, dans certains types d'échantillons (comme les molybdénites qui sont riches en rhénium et pauvres en osmium). Les divers réservoirs géochimiques (et cosmochimiques) verront ainsi leur teneur relative en osmium 187 différer, selon leur rapport Re/Os et le temps laissé au système pour accumuler du ^{187}Os radiogénique. C'est ici que prend forme la méthode isotopique Re-Os, tant comme géochronomètre que comme traceur. Du fait de leurs affinités chimiques chalco-sidérophiles, le Re et l'Os se rencontrent principalement dans des minéraux et lithologies différant de ceux où l'on retrouvera les couples U-Pb, Rb-Sr ou Sm-Nd. En conséquence, les applications du

système Re-Os seront souvent complémentaires de celles des autres systèmes. Le Re-Os est d'intérêt pour un large éventail d'applications. Les études publiées jusqu'à maintenant, dont le nombre augmente sans cesse, portent tant sur la cosmochimie (Walker et al. 2002), la géologie profonde (Brandon et al. 1998) et la géologie environnementale (Ravizza et Bothner, 1996), que sur la géologie économique (le Re-Os et l'un des rares systèmes à pouvoir dater directement une minéralisation aurifère; Arne et al. 2001).

Le rhénium et l'osmium sont des éléments réfractaires ayant condensé parmi les premiers dans la nébuleuse présolaire (température de 50% de condensation de ~1800 K pour Re et Os). Une partie du stock de ces éléments fut alors emprisonnée dans les inclusions de calcium et aluminium (CAI) fraîchement formés; le Re et l'Os étant des éléments hautement sidérophiles (HSE), une partie du stock élémentaire réagit ensuite avec le fer et nickel condensants. Cela eut pour conséquence de laisser peu de temps à une homogénéisation complète des compositions isotopiques $^{187}Os/^{188}Os$. Les chondrites, ces "roches sédimentaires cosmiques", sont des amalgames des telles phases de condensation précoce (CAI, FeNi, olivine, pyroxène) et de poussière de fin de cristallisation (matrice riche en éléments volatils) (McSween, 1999).

Sur Terre, les affinités chimiques de ces deux éléments impliquent qu'une grande part de leur inventaire doit être actuellement situé dans le noyau de la planète. L'osmium est un élément compatible lors d'événement de fusion dans le manteau terrestre, c'est-à-dire qu'il tend à demeurer dans le solide résiduel. Le rhénium est moins compatible, passant partiellement dans le liquide magmatique. Cela a pour effet que la croûte continentale s'est enrichie en Re, par rapport au manteau, lors de sa formation. Avec le temps, la signature isotopique en osmium de la croûte continentale a évoluée vers une composition radiogénique ($^{187}Os/^{188}Os > 1$), alors que le manteau a conservé une composition similaire de celle des chondrites ($^{187}Os/^{188}Os \sim 0.12$). Bien qu'ils se trouvent dans la croûte, les gisements de platinoïdes (le groupe comprenant les éléments : Pt, Pd, Rh, Ru, Os, et Ir) ont souvent des caractéristiques isotopiques d'osmium typiques du manteau. C'est qu'ils trouvent leurs origines dans les morceaux de manteau obductés sur la croûte (e.g., ophiolites de Thetford Mines) ou de magmatisme ultramafique (e.g., complexe du Stillwater). On trouve aussi des gisements de platinoïdes provenant de la re-mobilisation de minéraux lourds de platinoïdes sous forme de placers.

Le comportement de l'osmium en milieu océanique et sédimentaire est encore relativement peu connu, comparativement à celui du Re. Par sa plus grande abondance dans ce milieu, le Re est plus facile à analyser et a ainsi été étudié depuis plus longtemps. Les temps de séjour océanique de ces éléments sont estimé à ~750 000 ans pour le Re (Colodner et al. 1995) et entre 2000 et 35 000 ans pour l'osmium, selon les études (Oxburgh, 2001; Peucker-Ehrinbrink, 2002). L'importance relative des diverses sources et puits d'osmium est encore mal quantifiée, ce qui explique en partie les différences importantes des estimations dans le cas de l'osmium. La composition isotopique de l'osmium de l'océan est considérée comme homogène ($^{187}Os/^{188}Os \sim 1.06$; Levasseur et al., 1998); cependant, certains indices semblent démontrer que sa concentration puisse être hétérogène (Levasseur et al. 1998 ; Woodhouse et al. 1999). Le comportement de l'osmium en milieu estuarien, à l'interface entre les sources majeures fluviales d'osmium et l'océan, est très mal connu et semble varier selon les estuaires étudiés (par ex. : Levasseur et al. 2000 ; Martin et al. 2001). Parmi les environnements sédimentaires, les milieux réducteurs sont des puits importants, pour l'osmium marin. Leur étude a permis de générer une ébauche de courbe d'évolution isotopique de l'osmium marin au cours du Phanérozoïque, de manière analogue à celle du strontium. L'interprétation de cette courbe fait maintenant l'objet d'intenses recherches dans plusieurs laboratoires. Les comportements chimiques différents de l'osmium et du strontium ont pour effet que leurs courbes séculaires véhiculent des informations complémentaires (Ravizza, 1993), permettant éventuellement de mieux comprendre les processus tectono-climatiques anciens. Beaucoup d'échantillons ayant permis l'élaboration de la courbe de l'osmium ont été récupérés dans des séquences anciennes de *black shales*. Notons qu'il n'existe aucun analogue moderne réel pour vérifier directement la capacité de ce type d'environnement sédimentaire d'enregistrer, de façon univoque, la composition isotopique de l'osmium marin (Piper et Perkins, 2004).

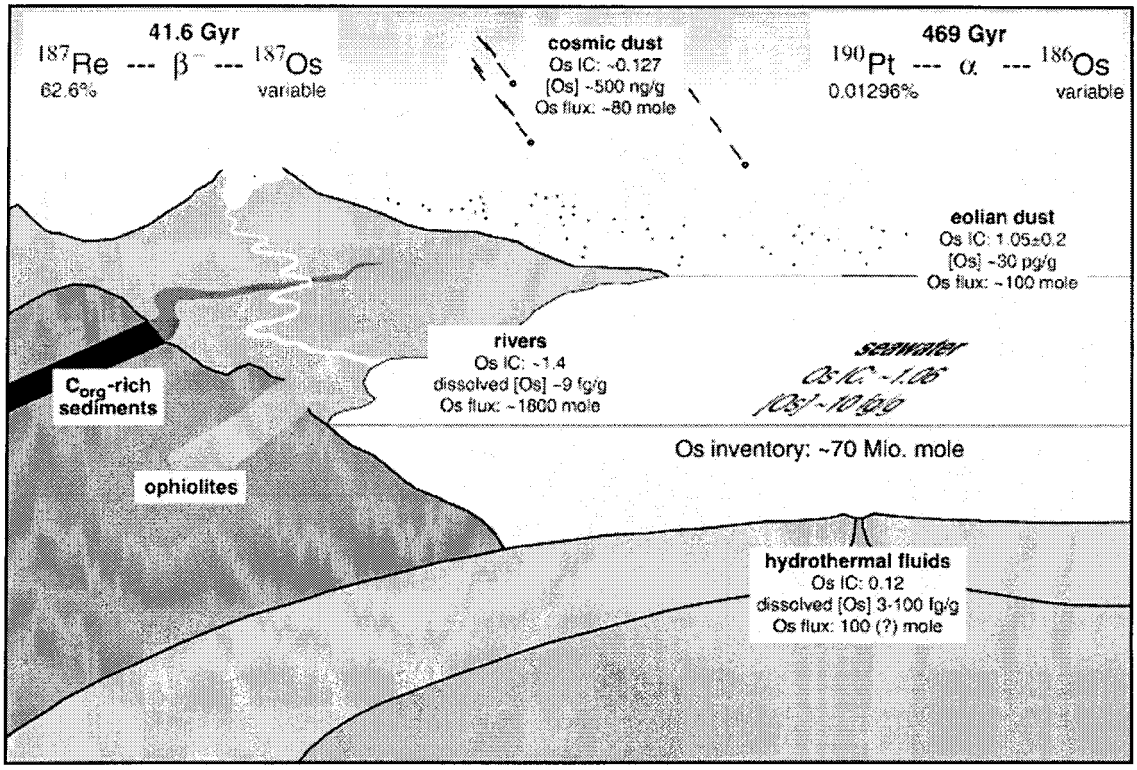

Figure 3: Principaux réservoirs d'osmium à la surface de la Terre, avec leurs compositions isotopiques. (Peucker-Ehrenbrink et Ravizza, 2000)

Plan de la thèse

Le cœur de cette thèse est présenté sous la forme de trois articles en langue anglaise, pour fin de publication dans des revues scientifiques internationales. Les sections de part et d'autre de ces chapitres, telles celle -ci, sont toutefois rédigées en français, conformément aux règles en vigueur concernant les thèses de doctorat à l'Université du Québec à Montréal.

Le premier chapitre concerne une météorite chondritique tombée à St-Robert (Qc) en 1994. Les chondrites ne sont ni plus ni moins que les ancêtres des planètes du système solaire, dont la Terre. Pour comprendre l'évolution terrestre, on se doit d'en saisir l'origine. Ici, l'étude des météorites, fragments résiduels de corps proto-planétaires, se révèle indispensable. Au fil des années, une "pré-histoire terrestre" relativement exhaustive est ainsi ressortie des nombreuses études météoritiques (et astrophysiques) publiées. Beaucoup de

chondrites ordinaires, nommées de la sorte de par leur grande abondance, ont été étudiées pour leur systématique Re-Os, mais peu d'entre elles l'ont été de manière intensive (typiquement moins de 3 analyses par météorite). Le chapitre I présente les résultats de plusieurs analyses Re-Os de fragments rocheux et de phases métalliques de la chondrite de St-Robert. La météorite que nous avions à notre disposition n'avait pas été étudiée en ce qui a trait aux isotopes de longue durée. Afin de pouvoir retirer des informations utiles des analyses Re-Os, il fallait s' assurer qu'aucune perturbation grave n'avait affecté cette chondrite; le système Pb-Pb a permis de le vérifier.

Le second chapitre apporte une nouvelle perspective de l'impact de l'Homme sur le cycle géochimique de l'osmium. Comme on se base nécessairement sur le présent pour décrypter le passé de la planète, cette connaissance est indispensable, puisqu'elle peut perturber les processus naturels (*c.f.* les études de Pb anthropique de l'équipe de Clair Patterson publiées dans les années 60). Des études passées ont avancé l'idée, sans la tester, que les voitures seraient une source de pollution en osmium (par ex. Ravizza et Bothner, 1996). Le chapitre II confirme cette possibilité et en quantifie l'impact environnemental.

Le troisième et dernier chapitre porte sur la géochimie du rhénium-osmium des sédiments de Saanich Inlet (B.C.), un milieu sédimentaire réducteur. Les sédiments anoxiques riches en matière organique, tels ceux de Saanich Inlet, sont réputés pour pouvoir enregistrer la composition isotopique de l'osmium de l'eau de mer contemporaine de leur dépôt (par exemple : Peucker-Ehrinbrink et Ravizza, 2000; Selby et Creaser, 2004). Ces sédiments ont la capacité de concentrer l'osmium directement à partir de l'eau de mer sus - jacente, faisant en sorte que la signature isotopique marine domine celle de l'apport terrigène. Par contre, l'enregistrement de cette signature marine dans certains des environnements réducteurs actuels est équivoque, l'apport détritique terrigène pouvant biaiser la composition isotopique mesurée dans le sédiment (Ravizza et al. 1991). Le fjord de Saanich Inlet est un environnement susceptible d'enregistrer la composition isotopique en osmium de l'océan actuel (Saanich Inlet est souvent présenté comme étant un analogue partiel moderne des dépôts de *black shales*). On a voulu vérifier ici la capacité présumée d'un tel milieu d'enregistrer la composition isotopique de l'osmium marin et, par la même occasion, tenter de comprendre les mécanismes de dépôt du Re et de l'Os, dans un environnement aussi particulier. La possibilité d'une pollution en métaux lourds du fjord a justifié un intérêt

complémentaire pour le plomb accumulé dans les sédiments.

Une conclusion générale, rappelant succinctement les points importants de chacun des trois chapitres, viendra clore cette thèse. Dans les pages annexes, on trouvera ensuite une partie analytique portant sur le calibrage inter-laboratoires de la composition isotopique d'une solution d'Os. Les résultats d'une première ronde analytique y sont discutées.

Ma contribution aux trois articles de cette thèse est naturellement essentielle. J'ai réalisé toutes les séparations chimiques, analyses spectrométriques, interprétations et rédaction des manuscrits; c'est pourquoi je suis premier auteur de chacun des articles. Le premier article est cosigné par le Dr. Régis Doucelance, qui a réalisé le logiciel de correction des données de plomb pour la sensibilité en abondance et participé à une partie des analyses et interprétations du plomb, de même qu'à la rédaction du manuscrit. Les articles formant les chapitres I et II sont cosignés par mon directeur de thèse, le Professeur Clément Gariépy, qui a participé à la rédaction du premier chapitre et inspiré certaines idées du second. Dr. Gariépy est décédé alors que le second manuscrit était en cours d'écriture. J'ai rédigé seul le troisième manuscrit.

Références

Arne, D., Bierlein, F., Morgan, J.W., and Stein, H.J. (2001) Re-Os dating of sulfides associated with gold mineralization in central Victoria, Australia: *Economic Geology*, v. 96, 1455-1459.

Brandon, A.D., R.J. Walker, J.W. Morgan, M.D. Norman, et H.M. Prichard, (1998)Coupled ^{186}Os and ^{187}Os evidence for core-mantle interaction, *Science*, **280**, 1570-1572.

Colodner D., Edmond J., and Boyle E. (1995) Rhenium in the Black Sea; comparison with molybdenum and uranium. *Earth and Planetary Science Letters* 131, 1-15.

Creaser R. A., Papanastassiou D. A., and Wasserburg G. J. (1991) Negative thermal ion mass spectrometry of osmium, rhenium, and iridium. *Geochimica et Cosmochimica Acta* 55, 397-401.

Dickin A. P. (1995) *Radiogenic Isotope Geology*. Cambridge University Press, 490 p.

Göpel C., Manhès G., and Allègre C. J. (1985) U-Pb systematics in iron meteorites: Uniformity of primordial lead. *Geochim. Cosmochim. Acta* 49, 1681-1695.

McSween H. Y. (1999) *Meteorites and their parent planets*. Cambridge University Press.

Levasseur S., Rachold, V., Birck, J. L., and Allègre, C. J (2000) Osmium behavior in estuaries: the Lena River example. *Earth and Planetary Science Letters* 177, 227-235.

Levasseur S., Birck J. L., and Allegre C. J. (1998) Direct measurement of fetomoles of osmium and the $^{187}Os/^{186}Os$ ratio in seawater. *Science* 282; 272-274.

Martin C. E. et al. Osmium isotope geochemistry of a tropical estuary. *Geochimica et Cosmochimica Acta* 65; 3193-3200.

Oxburgh R. (2001) Residence time of osmium in the oceans. Geochem.Geophys.Geosyst. 2, doi:10.1029/2000GC000104..

Peucker-Ehrenbrink B. (2002) Comment on "Residence time of osmium in the oceans". Geochem.Geophys.Geosyst. 3, doi:10.1029/2001GC000297.

Piper D. Z. and Perkins R. B. (2004) A modem vs. Permian black shale - the hydrography, primary productivity, and water-column chemistry of deposition. *Chemical Geology* 206, 177-197.

Ravizza G. (1993) Variations of the $^{187}Os/^{186}Os$ ratio of seawater over the past 28 million years as inferred from metalliferous carbonates. *Earth and Planetary Science Letters* 118; 335-348.

Ravizza G., Turekian K. K., and Hay B. J. (1991) The geochemistry of rhenium and osmium in Recent sediments from the Black Sea. *Geochimica et Cosmochimica Acta* 55; 3741-3752.

Ravizza G. E. and Bothner M. H. (1996) Osmium isotopes and silver as tracers of anthropogenic metals in sediments from Massachusetts and Cape Cod bays. *Geochimica et Cosmochimica Acta* 60; 2753-2763.

Shirey S. B. and Walker R. J. (1998) The Re-Os isotope system in cosmochemistry and high-temperature geochemistry. *Annual Review of Earth and Planetary Sciences* 26, 423-500.

Smoliar M., I, Walker R. J., and Morgan J. W. (1996) Re-Os ages of Group IIA, IIIA, IVA, and IVB iron meteorites. *Science* 271; 1099-1102.

Sturges W.T. and Barrie L.A (1987) Lead 206/207 isotope ratios in the atmosphere of North America as tracers of US and Canadian emissions. *Nature* 329, 144-146.

Tatsumoto M., Knight R.J., and Allègre C. J. Time differences in the formation of meteorites as determined from the ratio of lead-207 to lead-206. Science 180, 1279-1283.

Völkening J., Walczyk T. and Heumann K.G. (1991) Osmium Isotope ratio determinations by negative thermal ionization mass spectrometry. Intl. J..Mass Spectrom. Ion Phys. 105, 147-159.

Woodhouse O. B. et al. (1999) Osmium in seawater; vertical profiles of concentration and isotopic composition in the eastern Pacific Ocean. *Earth and Planetary Science Letters* 173; 223-233.

CHAPITRE I
RADIOGENIC ISOTOPE INVESTIGATION OF THE ST-ROBERT H5 FALL

André Poirier, Régis Doucelance et Clément Gariépy

Publié dans *Meteoritics and Planetary Science* (2004), vol. 39, pages 1983-1994.

I. Abstract

The St-Robert H5 chondrite yields a mineral/whole-rock Pb-Pb age of 4565 ± 23 Ma (2σ, model 1, Isoplot Ex/ v 2.49) comparable to the accepted age of most chondrites. The regression of chondrule data give a similar age of 4566 ± 7 Ma (2σ). These results imply that no major perturbation affected the Pb-Pb systematics of this meteorite's parent body within the first few billion years following its accretion. Re and Os concentrations along with Os isotopic compositions of whole-rock fragments, surface fusion crusts and metal phases are also reported. The whole rock measurements for this ordinary chondrite are characterized by high Re/Os ratio coupled with relatively high $^{187}Os/^{188}Os$ (compared to average ordinary chondrites), that we interpret as a long term Re enrichment. As for most chondrites, no precise geochronological information could be extracted from the Re/Os systematics, although most data plot near the IIIAB reference isochron (Smoliar et al. 1996). From the fusion crust results, we rule out the possibility that atmospheric entry caused the perturbations in the Re-Os system, since melted crust analysis yields amongst the most concordant datapoints. Evidence from metal phases suggests that a very recent process perturbed the isochron, relocating Re from kamacite towards troilite.

Keywords: Pb-Pb, Re-Os, isotope geochemistry, St-Robert H5 chondrite.

I.1. Introduction

Chondrites are materials of foremost interest to the Earth and planetary sciences. They yield abundances of nonvolatile elements comparable to that of the Sun's corona and are the oldest rocks retrieved from within the solar system. Thus, most models of primordial Earth evolution are based on geochemical and isotopic parameters derived from the study of chondrites.

Mass spectrometry developments, studies of extinct radioactivities (e.g. Wasserburg, 1985) and studies of long-lived parent-daughter systems (K-Ar, Rb-Sr, Sm-Nd, Lu-Hf, Re-Os or U-Pb) considerably refined our understanding of early solar system evolution (e.g. McSween, 1999). Within the family of long-lived nuclides, the Re-Os system is singular: both elements are both siderophile and chalcophile, thus mainly reside in the metal and sulfide phases of meteorites.

Applications of the Re-Os system to iron meteorites, pallasites and mesosiderites yielded important results: i) accurate isochron ages; and ii) estimates of the initial composition of the solar system (e.g. Smoliar et al. 1996; Shen et al. 1996; Birck and Allègre, 1998; Chen et al. 2002). However, the initial Os isotopic composition of chondrites and chondrite components should be lower than that of iron meteorites, by a few tenths of a percent, if differentiation of the latter lasted for some 50 Ma after parent-body accretion (e.g. Allègre et al. 1995; Walker et al. 2002).

The precise Re-Os determination of chondrite formation age and initial Os isotopic composition may not be possible: these rocks likely are a mixture of cosmic grains and dust from various sources. Consequently the criteria of uniform initial isotopic composition

required to derive a valid isochron may not be fulfilled (e.g. Shirey and Walker, 1998). Nevertheless, Chen et al. (1998) provided a Re-Os isochron age for the St. Séverin chondrite (LL6) that they interpreted as a melting/crystallisation age. It is remarkable to see that a Re-Os isochron was obtained even though the specimen has reported disturbed U-Pb and Rb-Sr systematics (but Pb-Pb on phosphates is not); within the uncertainty, the initial $^{187}Os/^{188}Os$ ratio encompassed the value determined for iron meteorites. Walker et al. (2002) analysed a broad range of C, E and H chondrites, of different metamorphic types for their Re-Os and $^{187}Os/^{188}Os$ systematics and summarized results from previous studies. They concluded that differences in the Re/Os ratios of C vs. E-H chondrites reflected chemical fractionation processes early in the history of the solar system. In addition, deviations of most chondrites from a 4.56 Ga reference isochron were attributed to post-formation redistribution of Re and/or Os. The elemental redistribution scale was of millimeters to centimeters and due to either one of the following processes: terrestrial weathering, aqueous alteration, or shocks events on the parent body within the past 2 Ga (Walker et al. 2002). With the notable exceptions of Allende and St. Séverin, there are few Re-Os data for individual components of chondrites.

This paper reports Pb-Pb and Re-Os isotopic data obtained on rock fragments, fusion crusts, chondrules and metal phase separates from a single chondrite, the St-Robert H5 fall of 1994. Our goal was twofold: i) assess the age, equilibrium state and and post-accretion history of St-Robert using the Pb-Pb systematics; and ii) elucidate the question concerning the processes responsible for the typical open-system behaviour of the Re-Os system in most ordinary chondrites.

I.2. The St-Robert chondrite

The St-Robert fall (45°58'N; 72°58'W) occurred on June 14, 1994 at ~60 km NE of Montréal. Studies by Wilson, (1994), Brown et al. (1996) and Leya et al. (2001) have concluded that : a) it is a monomict breccia of a H5 ordinary chondrite with S2-S3 shock levels; b) it has a high porosity and a high permeability when compared to most ordinary chondrites; c) the well preserved fusion crust is ~50% more permeable than a freshly cut surface; d) it was launched from deep in its parent body about 7-8 Ma ago, without undergoing further major collision, entered in orbital resonance with Jupiter and then traveled to the Earth; e) the modelled orbit is consistent with an aphelion located within the asteroid belt; and f) the pre-atmospheric mass was between 1 and 2 tons at an entry velocity of ~13 km/s.

The Geological Survey of Canada organized a prompt search for fragments and recovered ~25.4 kg of materials, from arable land environments. A consortium of Quebec universities acquired a series of St-Robert samples. The analysed specimen is that of Université du Québec à Montréal (UQAM); it was stored since acquisition in a glass dessicator under dry nitrogen atmosphere, sitting on a ceramic plate.

Compositionally, the St-Robert meteorite is an unremarkable object, typical of a large group of H chondrites which were produced in a major collision 7 to 8 Ma ago (Leya et al. 2001). However, it is one of a few where the simple post-collision history is well documented, the orbital parameters well-established and the recovery occurred within days after the fall event.

I.3. Analytical techniques

About 10 grams were broken off the UQAM specimen using a tungsten carbide chisel and separated into two aliquots. A ~2.5 g bulk fragment was manually powdered, in an agate mortar and pestle apparatus, and analysed for its major and trace element contents by instrumental neutron activation at the SLOWPOKE laboratory of Ecole Polytechnique de Montréal. Isotopic analyses were carried out on the second aliquot, which was gently crushed between tungsten carbide plates, which we found subsequently, might be problematic for Re contamination, especially for the smallest samples. The St-Robert fall proved to be a quite fragile rock and those plates were used only for a first, rough crushing of the fragment. The more delicate crushing prior to hand-picking was accomplished manually with agate mortar and pestle. Most of the chondrules and metal chuncks were directly retrieve from whole rock pieces under microscope. Whole-rock, fusion crust fragments, mineral grains and chondrules were all hand-picked. An additional ''magnetic fraction" was separated using a small hand magnet covered with plastic film. It clearly contained partially rusted metal grains, demonstrating that some humidity have come into contact with the meteorite, but we cannot say much about the source of that water (although we discard water from the soil where it was recovered, since it would have had affected more the external crust, and it is not the case: see Re-Os results below).

The composition of a few grains of each mineral and chondrule separate was assessed using a scanning electron microscope equipped with an energy-dispersive system. All chemical treatments were carried out in HEPA class 100 laboratories using reagents systematically monitored for their Re, Os and Pb levels.

I.3.1 Pb isotope

All solid aliquots were washed in distilled methanol and dried prior to weighing. They were dissolved in sealed teflon capsules using a concentrated HF-HNO_3 acid mixture, placed on a hot plate for ~1 week, and shaken daily using an ultrasonic bath. After evaporation, the salts were taken up in 0.8N HBr and centrifuged. The residues from centrifugation were systematically examined under the microscope to ascertain that complete digestion occurred (although some fluoride precipitates might remain invisible). Weighted aliquots of the solutions were spiked with a pure ^{206}Pb tracer (NIST-SRM-991), calibrated against the NIST-SRM-981 standard, to obtain Pb concentrations by the isotope dilution technique. Lead was isolated from the matrix using anion exchange chromatographic techniques adapted from Manhès et al. (1980), initially using a three-pass procedure. This yielded total Pb blanks in the range of 55±15 pg. This intensive purification was found to be excessive for ICP-MC-MS measurements and reduced to a two-pass procedure, bringing the blank level to below 40 pg. For consistency with the actual sample measurements, the blank levels were also determined by ICP-MC-MS using the Faraday cages assembly. The measured blank level is clearly higher than that determined by TIMS using similar preparation procedures under the same laboratory conditions (typically 10-20 pg). This can only be explained by an additional source of Pb contamination related to the use of the ICP instrument. Possible causes are : i) the use of additional solvents and carrier gases, for which we did not detect any measurable contribution or, most likely, ii) "memory effects" arising from the introduction system, the sampler cones or the hexapole collision cell. A third possibility may reside in the difficulty of mesuring a blank precisely using Farady cups. When the different sources of uncertainties are propagated, the large variance in blank levels

determined by ICP is the main source of uncertainty, and largely exceeds that of analytical statistics and mass fractionation corrections, especially for radiogenic samples. For error propagation calculations, Pb blank levels of 55±15 pg and 40±10 pg were applied depending on the separation procedure used.

I.3.2 Re-Os isotope

The chemical separation of Re and Os followed the protocol of Birck et al. (1998). After a HF-HBr dissolution stage at ~135°C for 48h in tightly sealed Teflon bombs, 1 ml of concentrated HNO_3, 0.5-1 ml of Cr^{VI} in 4N HNO_3 and 1ml of $Br_{2(l)}$ were added to the solution. Chromium oxide is added to ensure spike-sample equilibration by driving all the Re and Os to their highest oxidation state, whereas bromine is used to trap the volatile OsO_4 so formed. The osmium tetra-oxide is then extracted with the liquid bromine and further purified by micro-distillation. Total procedural Os blanks were always <0.3 pg and negligible. Rhenium was recovered from the remaining aqueous solution. It was first extracted into isoamylic alcohol and then in Milli-Q water. The Re blank levels averaged 30±5 pg for teflon digestion and 20 pg for the Carius Tube digestion process (see below) where no CrO_3 is used. The Re blank represents less than 1% of the total Re content for most samples, with the exception of the smallest troilite and kamacite separates.

Given that potential equilibration problems were reported for digestion techniques other than the Carius Tube (CT) procedure (Shirey and Walker, 1995), two rock fragments and one metal-rich piece were processed using the CT technique for comparison. A Carius Tube containing the sample, spikes and inverse *aqua regia* (3 HNO_3 + 1 HCl) was sealed and

slowly brought to 240°C for at least 24h. After CT opening, the Os and Re recovery procedures were the same as for the HF-HBr digestion processes.

The ^{190}Os spike was gravimetrically calibrated against a solution of a K_2OsCl_6 salt obtained from Electronic Space Products International (Ashland, OR, USA) which was reported to be stoichiometric (Yin et al. 2001). The ^{185}Re spike was gravimetrically calibrated against a standard solution of a zone-refined Re ribbon obtained from Rhenium Alloys Inc. (Elyria, OH, USA), the type of material commonly used as "filament" in TIMS. The external reproducibilities for Re and Os spike concentrations were better than 0.4% (assuming the standard concentrations as known perfectly during reversed isotope dilution).

I.3.3 Mass spectrometry

Pb and Re isotope measurements were carried out using a magnetic sector, multicollector ICP-MS instrument (model IsoProbe from Micromass), using Faraday cup collectors with 10^{11} Ω feedback resitors. The collector relative efficiencies were set to unity and amplifier gains were calibrated daily. All purified samples were dissolved in a 2% HNO_3 solution and aspirated freely through an Aridus desolvating microconcentric nebulizer and swept by the Ar carrier gas into the plasma torch. Between samples, wash solutions of 10% and 2% HNO_3 are alternatively aspirated until the background signal returns to a constant level, as measured with the same acid solvent used for sample introduction. For Pb measurements, this level corresponds to a very stable signal of a 1-2 mV on mass ^{208}Pb, compared to the background noise determined with the flight tube isolation valve closed; for Re measurements, there are no detectable memory effects on Faraday cups.

The Os isotopic measurements were done by thermal ionisation mass spectrometry (TIMS) using a VG Sector 54 instrument operated in negative ion mode.

I.3.3.1 Pb isotope measurements

The purified salts (typically 1-2 ng of Pb) were dissolved in a thallium-bearing HNO_3 2% solution. Data acquisition in static multi-collection consisted of 50 x 4 seconds scans; the raw data were processed off-line, cycle by cycle to correct for on-peak-zero, abundance sensitivity effects (Thirlwall, 2001, 2002), mass fractionation, and blank contribution. Tail corrections were based on the method proposed by Dechamps et al. (2003) for uranium (see also Doucelance et al., 2003). A power law (Russell, 1978) was used for mass fractionation corrections. The $^{203}Tl/^{205}Tl$ ratio of the NIST SRM-997 standard used to correct for mass fractionation was determined empirically: its value ($^{203}Tl/^{205}Tl = 2.3899$, n = 32) was adjusted from repeated analyses of the NIST SRM-981 Pb standard mixed with the same HNO_3+Tl solution, over a period of several months. This value minimises the differences in all three ^{206}Pb-normalised ratios with respect to the accepted values for the SRM-981 standard (Doucelance and Manhès, 2001 *in* Thirlwall, 2002). Repeated analysis of NBS-981 yielded: $^{208}Pb/^{206}Pb = 2.1677 \pm 0.0002$; $^{207}Pb/^{206}Pb = 0.9149 \pm 0.0002$; $^{206}Pb/^{204}Pb = 16.9480 \pm 0.0008$. The Tl isotopic composition is comparable, within error limits, to the value of Thirlwall (2002) but 540 ppm higher than that of IUPAC.

Isotope dilution (spiked with ^{206}Pb) and isotope composition samples were grouped in different batches and analysed on separate analytical sessions in order to minimise memory effects, notably from the desolvating membrane of the nebulizer. Collerson et al. (2002) showed that up to 6% retention of the processed Pb may occur in such introduction devices,

resulting in potential cross-contamination phenomena. In this study, the total amounts of Pb introduced in the instrument were always lower than 2 ng/sample, typically corresponding to an aspiration rate of 1-10 pg Pb/second (with *ca.* 60 µl/min uptake rate). The very low Pb amounts introduced minimizes "memory effects" from the introduction system but, in first approximation, does not reduce the sample-to-sample cross-contamination ratio, because of the approximately similar Pb abundances. However, the in-between sample wash-out procedure (typically 20-40 minutes) becomes considerably more efficient in eliminating small amounts of "memory" Pb rather than very large ones.

I.3.3.2 Re isotope measurements

The purified Re salts were dissolved in a 2% HNO_3 solution doped with tungsten. This approach is analogous to the addition of Tl for on-line mass bias monitoring of Pb isotopic compositions by MC-ICP-MS. Tungsten has stable isotopes in the 180 to 186 mass range. It does not have any isobaric interferences with Re. We used the ratio of $^{186}W/^{184}W$ = 0.927633 (as determined by Lee and Halliday, 1995) to correct the measured $^{187}Re/^{185}Re$ ratio for mass fractionation in ICP-MC-MS instrument. This approach improves the external reproducibility on standard measurements three-fold when compared to the conventional standard-sample bracketing technique (Poirier, 2001). Abundance sensitivity effects are negligible on the measured Re concentrations. Mass 188 was monitored for Osmium potential interferences on Re and W masses.

I.3.3.3 Os isotope measurements

Osmium isotopic compositions and concurrent isotope dilution abundances were determined by negative-TIMS (Creaser et al. 1991; Völkening et al. 1991) using an ion source (collimator), filament block holders, cover slits and filaments dedicated to the analysis of Os. All Os isotopic signals, but ^{184}Os, were collected as trioxides in static multi-collector mode. The oxygen bleeding rate into the source of the mass spectrometer was optimized for each sample (typical resulting pressure: 2-3 x 10^{-7} Torr). Faraday cup efficiencies were set up at unity and the amplifier gains monitored daily. $^{185}Re^{16}O_3$ (mass 233) was systematically monitored for potential interferences on ^{187}Os. Osmium was loaded in HBr on a zone-refined platinum filament and covered with 0.5µl of a freshly prepared barium hydroxide solution. Isotope dilution calculations, oxide contribution and fractionation corrections (normalized to $^{192}Os/^{188}Os$ = 3.08271; Nier, 1937) were performed off-line. In-house standard repeated analysis (corrected to $^{192}Os/^{188}Os$ = 3.08271) gives $^{186}Os/^{188}Os$ = 0.11993 ± 0.00015; $^{187}Os/^{188}Os$ = 0.10704 ± 0.00012; $^{189}Os/^{188}Os$ =1.21951 ± 0.00032 and $^{190}Os/^{188}Os$ = 1.98358 ± 0.00019.

In addition to our in-house standard measurements, analysis of an aliquot of the standard solution LOsTD were performed. This solution (provided by Thomas Meisel, University of Leoben) is now being analyzed by many laboratories as an osmium inter-laboratory mass spectrometry standard. We obtained $^{187}Os/^{188}Os$ = 0.10689±5, (1 S.D, n=5). This value is within error to the mean of all analyses reported by 14 different labs (T. Meisel, pers. comm.).

I.4. Results

I.4.1 Elemental concentrations

Table 1 shows Instrumental Neutron Activation Analysis (INAA) results for major and trace elements in a whole-rock aliquot of St-Robert. When compared to other H chondrites, this meteorite has similar abundance patterns for both lithophile and siderophile/chalcophile elements (Horan et al. 2003).

I.4.2 Lead isotopes

The total Pb abundances and the isotopic data for 17 sub-samples of St-Robert are listed in Table 2. The concentrations range from 4 to 290 ppb and the $^{206}Pb/^{204}Pb$ ratios vary by an order of magnitude (17 to 300) when the acid-washed chondrules are taken into account. The 3 WR fragments and the 2 fusion crusts have ^{204}Pb concentrations (non-radiogenic Pb) in the range of 0.07 to 0.13 ppb, averaging 0.1 ppb. Assuming that these are representative of the entire rock, the initial Pb content of St-Robert is on the same order as the lowest values reported in the literature for H chondrites (e.g. Wasson and Kallemeyn, 1988; Göpel et al. 1994). Thus, sample would be very sensitive to crustal contamination, but show no evidence for it.

Figure 1 llustrates the variations in $^{206}Pb/^{204}Pb$ as a function of the initial Pb content of the sub-samples. The data define two broad arrays. A sub-horizontal array comprising the metal phases, the magnetic fraction and the fusion crusts with a limited spread of $^{206}Pb/^{204}Pb$ values (16.9-20.5): the magnetic fraction is the poorest in ^{204}Pb and troilite the richest. For comparable ^{204}Pb levels, the WR fragments yielded higher $^{206}Pb/^{204}Pb$ ratios (30.0 -32.4). The pyroxene and chondrule fractions yielded the most radiogenic compositions and define a

steep array on Fig. 1. Note that the ^{204}Pb concentrations of the acid-leached chondrules are relative to the total weights before washing; thus their true position on Fig. 1 are left of that illustrated, depending on the amount of Pb removed by the acid treatment (leaches' measured $^{206}Pb/^{204}Pb$ were between 16.1 and 16.9). The radiogenic signatures of the Pb in silicate fractions are clearly related to their content in non-radiogenic ^{204}Pb. The steep array on Fig. 1 thus, likely represents mixing in different proportions, between a radiogenic end-member and unradiogenic component(s) represented by matrix phases such as troilite or troilite±metals.

I.4.3 Pb-Pb isochron ages

Figure 2 shows Pb-Pb isochron diagrams for different sample subsets. The statistical treatments were done with the Isoplot 2.49 software of Ludwig (2001) and all errors are quoted at the ±95% confidence level. All values refer to the "Model 1 Solution" calculation where the analytical errors are the only reason for data-point scatter along a straight line. The choice of Isoplot model calculation will affect the uncertainty of the age, but not the MSWD (Mean Square of Weighted Deviates). The first model was chosen for all calculations to simplify comparison of all the computed ages.

The regression results for all 17 sub-samples are shown on Fig. 2a using data corrected for mass fractionation, blank contribution, and their propagated uncertainties. It yields an age of 4567±23 Ma with a MSWD value of 789. This large scatter indicates that the analysed fractions: i) did not form at the same time and/or same initial Pb isotopic composition. For example, Amelin et al. (2002) reported Pb-Pb ages for calcium-aluminium inclusions (CAI) of CV chondrites which are some 2-3 Ma older than that of CR chondrules. Alternatively, Itoh and Yurimoto (2003) found chondrule fragment embedded in a CAI,

indicating a synchroneous formation for both components; and/or ii) were perturbed by secondary phenomena (i.e. shock metamorphism, aqueous alteration, etc.).

Figure 3b shows the regression results for the six chondrule fractions. The derived age is 4566±7 Ma, with a MSWD value of 12 and a null probability of fit (Ludwig, 2003). Regression of the pyroxene data with the chondrules (not illustrated) does not significantly change these results, suggesting that the pyroxene mineral separates actually are chondrule fragments. Regression of the three acid-washed, and most radiogenic chondrules alone yields an age of 4560±46 Ma (MSWD = 7).

Pb-Pb model ages are calculated assuming that the initial lead value was that of the Canyon Diablo Troilite (CDT, Tatsumoto et al. 1973). By subtracting this primordial lead from the actual sample composition, we get the $^{207}Pb^*/^{206}Pb^*$ ratio, which has age significance. Model age results from the calculations with CDT initial lead are shown in Table 2. Leached chondrules converge to a value of ~4564 Ma at high $^{206}Pb/^{204}Pb$, while unleached fractions give lower values, indicative of unradiogenic Pb from the matrix adhering on their surfaces. Previous studies have demonstrated a tendency for more radiogenic phases to give "correct" Pb-Pb age (e.g. Allegre et al. 1995); this may be rationalized by the fact that these phases contain more Pb that is related to the duration of U-decay (less sensitive to initial lead composition). The whole rocks yield ages up to 4580 Ma, which are higher than the chondrule results. This can be explained by radiogenic terrestrial contamination of the unleached whole-rock.

Although the fit of the regression line to the data is far from perfect, we conclude from the Pb-Pb result on chondrules that no major perturbation affected this meteorite in the

first few billion years of its existence (a very recent thermal event would not be detected from Pb-Pb systematics).

I.4.4 Re-Os systematics

The Re-Os systematics of chondrite bulk samples and components are difficult to interpret. Replicate analysis of whole rocks show significant scatter relative to a 4.56 Ga reference isochron, the assumed age of formation. The reason for such dispersion of chondrite data remains unclear. Recent perturbation of Re has been previously invoked for other chondrite, but the exact cause is still uncertain (Walker et al. 2002; Horan et al. 2003). We examined 10 pieces of St-Robert whole rock and several separated metal-rich components. We also analysed the fusion crust. This was done in order to investigate the possible influence of atmospheric entry fusion on the Re-Os system.

I.4.4.1 Whole rocks

The St-Robert mean Re and Os concentrations calculated from 10 whole-rock fragments are of 82 ± 11 ppb and 841 ± 122 ppb (1 S.D.) respectively and fall within the array defined by most ordinary chondrites (Chen et al. 1998; Walker et al. 2002). The >40% range [(maximum-minimum)/mean] of the Os and Re concentrations of replicate analysis suggests a strong control by the heterogeneously distributed FeNi alloy for both elements. The ranges obtained here are wider than that reported by Horan et al. (2003). The difference may be due to the larger dataset, and greater odds to sample different metal contents among powder splits. The range in Re/Os ratio of the St-Robert fall is also wide (27% controlled by WR-7; 16% when excluding it). Such results show more variability than ordinary chondrites

values of Horan et al. (2003). The ratio of these elements are likely unrelated to the amount of metal sampled in each split (the carrier phases for both Re and Os), this implies either that some disturbance may have variably affected this H5 specimen, or that some technical problem occured. The Carius Tube technique used by Walker et al. (2002) was used on 2 splits of whole rock powder of the St-Robert specimen. These show the same large range of concentrations and Re/Os ratio (deviation of : 16% for [Os], 30% for [Re] and 14% for Re/Os). This confirm that the observed variability in the Re/Os in this specimen is real and that HF-HBr digestion yields results as reliable as CT digestion for ordinary chondrites.

The fact that the $^{187}Os/^{188}Os$ shows a more narrow range of values (5%) indicates that a Re/Os ratio perturbation occurred fairly late in the history of the meteorite. On the other hand, the mean $^{187}Re/^{188}Os$ of 0.4690 is 11% higher than the mean ordinary chondrites (OC) value of Walker et al. (2002). The corresponding mean $^{187}Os/^{188}Os$ being also higher than average OC (1.4% higher) leads us to conclude that the Re enrichment (or Os loss) is due to a long term event. This requires multiple stages of open-system behaviour. Firstly, an early Re/Os fractionation resulted in a higher original bulk rock elemental ratio, secondly a more recent process is needed to explain the scattering observed in the present-day Re/Os ratio (and Os isotope signature).

When plotted on an isochron diagram (Fig. 3), most WR datapoints scatter along the IIIAB regression line (4558 Ma, Smoliar et al. 1996). This indicates that the high Re/Os ratio, relatively to OC average, was most likely acquired very early in the chondrite's history, perhaps during the first 50 Ma (Walker et al. 2002) giving enough time for ^{187}Re to decay and yield the observed high $^{187}Os/^{188}Os$. Mechanisms for the early fractionation of Re from Os extend from high-temperature nebular condensation phenomenon to low-temperature fluid

transport during grade 5 metamorphism on parent body. Determining which one applied here is not possible on the sole basis of Re–Os data, as both mechanisms have the same effect. The second event (or series of) causing the Re/Os scattering is more puzzling. It might in part be related to the shock metamorphism (S2-3 level), although Walker et al. (2002) showed that such events have limited impact. Alteration while in Earth's oxidising atmosphere (post fall alteration) was invoked by most previous studies to rationalize some of the dispersal of Re-Os data. We agree to this hypothesis, Re being very mobile at Earth's surface conditions

On figure 3, we observe that most of our data plot on the hi-Re side of the IIIAB reference isochron; 70% of the whole rock analyses (n=10) fall on the Re-rich side of the Iron reference isochron in this study. Similar observation was done in previous studies (Walker et al. (2002): 58%, n=34,ordinary chondrites; Chen et al. (1998): 75%, n=12 H chondrites). From the two most discordant WR datapoints (WR–4 and –7) and the extremely discordant troilite value, we calculated a secondary isochron age of 248 ± 26 Ma (MSWD = 0.69) which may point to some spatially restricted elemental exchange at that time, perhaps along a fracture.

When theoretical Re/Os is calculated from the $^{187}Os/^{188}Os$ to stay clear of a recent elemental mobilization effect as in Walker et al. (2002) study, we obtain Re/Os mean value of 0.0911 ± 0.0050 (1 s.d.), which is slightly higher (but overlaps within uncertainty) with the 0.0876 ± 0.0052 (1 s.d.) given by Walker et al. (2002). This gives further support to the hypothesis of recent elemental perturbation at the whole rock level of the St-Robert meteorite.

Calcium-aluminium inclusions (CAI) have an important role in the Re-Os budget – being the host phase for PGE-rich opaque assemblages (Blum et al. 1988)- but although some

occurrences were reported, they remain of very low modal abundances in ordinary chondrites. This may be at the origin of some of the observed scatter since both dissolution techniques employed here may not digest completely CAI's. Moreover, a recent study from Meisel et al. (2003) suggests that the HF-HBr dissolution *and* CT procedures are both ineffective for digesting Os of some specific mineral phases of serpentinized peridotite such as spinel. Their results indicate that the HF-HBr has a lower Os yield than CT, which also has a low yield when compared to high pressure asher attacks. Our results do not support such claim for ordinary chondrites, the Os concentrations and Re/Os ratios obtained from CT attacks being indistinguishable from the HF-HBr attacks. Nevertheless, it remains possible that some refractory Re-Os carrying phases were not effectively digested by either technique (although these phases would probably be insensitive to mild secondary effects which would affect sulfides).

I.4.4.2 Fusion crusts

Fusion crusts represent the remainder of the surface melt that occurred during the incandescent stage of meteoroid fall (due to atmospheric drag). Following the fireball is the dark flight, during which the last fused material cools off and the hot surrounding atmosphere oxidizes elemental iron contained within this melt to produce magnetite. This process creates the characteristic black crust that is often seen on Fe-rich meteorites. This rapid hi-temperature oxidation could affect rhenium and osmium concentrations: the volatile nature of these two elements, when in oxide form, might favour a loss. Moreover, the high permeability of this crust (Leya et al. 2001) might facilitate mobility of gases within it (both osmium and rhenium form volatile oxides at high fO_2). The analysis of two fusion crusts gave

results quite comparable to the WR data in Re and Os abundances and Re/Os ratio. They gave low $^{187}Os/^{188}Os$ and $^{187}Re/^{188}Os$ values but are amongst the closest to the IIIAB isochron data; in fact Cr-2 is the most concordant datum (-0.5 delta unit, see Table 3). These results suggest that the surface's extensive melting/volatilization during the atmospheric entry, a dramatic phenomenon for a meteorite, does not affect significantly the Re-Os systematics.

Lets consider in more details what effect the melting process may have on the crust's Re/Os system. By melting, the region is homogenised for both $^{187}Os/^{188}Os$ and $^{187}Re/^{188}Os$ ratios, cancelling any small scale Re/Os differences between mineral phases involved in the melt (with no major Re/Os partitioning in the resulting glassy crust). This should not necessarily render the whole crust homogeneous, because of the initial Re/Os variations throughout the meteorite, and since only negligeable lateral mixing of melt occurs all along the meteorite's surface (as seen from the heterogeneous $^{187}Os/^{188}Os$ and Re/Os of our two analysed crusts). Heteorgeneities will be attenuated by the melting event, and if the phases involved were originally on both sides of the isochron, a resulting mixture of the right proportion could –fortuitously- be located right on the 4.56 billion years isochrone. Hence less scatter around the isochron can be expected for fusion crusts, just as our limited dataset shows. Sampling of larger mass of crust could also help minimize even more the scatter. But then, even if an age computed by regression of such crusts has an acceptable age value (i.e close to 4.56Ga) and a better MSWD, it would only represent a somewhat spurious correlation.

I.4.4.3 Metal phases

Kamacite-rich grains were sampled, along with many small troilite pieces. Pure troilite (FeS) can be sub-sampled because its brittleness helps its breaking loose from the surrounding silicate, although in very small pieces. In contrast, kamacite is ductile and does not separate easily from silicate minerals. The $^{187}Re/^{188}Os$ ratio measured in St-Robert pure sulfide is much higher than any WR results. As in the case of the sulfide phase from St. Severin (Chen et al. 1998), the St-Robert sulfide has a disturbed Re-Os sytematics, and gives a model age of 1.7 billion years. When considered alone, the sulfide might be indicative of the late-stage shock that imparted the S2-S3 level of this meteorite, although we wish to issue a caveat about this datum, because of its low Re sample to blank ratio. The Re and Os concentrations of kamacite-rich fragments are anti-correlated to their silicate content (the smaller piece was pure kamacite), indicating dilution of the siderophile elements by low-HSE silicate phases. The very low $^{187}Re/^{188}Os$ of 2 kamacite-rich fragments indicate a strong disturbance of the rhenium-osmium distributions (Re loss and/or Os uptake). This disturbance must have occurred recently since the $^{187}Os/^{188}Os$ of the perturbed fragments are close to average WR.

Although some Re contamination coming from tungsten carbide plates in not possible to rule out for the troilite data (nor for any other sample), we believe it is very minor, otherwise the small Metal-4 (2.4 mg) would have been contaminated too, and hence would be on the high-Re side of the isochron.

A first possibility for linking the observations from metal phases and troilite is by electrolytic transport (Birck et al. 1998) of some of the Re from kamacite closely followed by troilite uptake due to its chalcophile nature. An isochrone with a slope of near zero can be

fitted through these disturbed metals, indicating the very recent nature of this transport. At standard Earth's surface conditions, Re is more easily mobilized than Os (Jaffe et al. 2002; Palme, 1988 *in* Walker et al. 2002). If we assume that those metal phases started on the IIIAB isochron, and that Os was not mobilized, then the kamacite-rich fragments lost about 700-1000 pg of Re while troilite gained 27 pg of Re to reach its present position. Moreover, Os being an order of magnitude more concentrated than Re in those samples, it might be buffered against such elemental exchange. The fact that whole rock fragments and one metal-rich piece are not as disturbed indicates that the remobilization acted locally, and might have followed only some fractures (St-Robert is a monogenic breccia).

Another possibility to explain the metal results also involves fracture. This other explanation is impact-induced partial melting of the FeNi-FeS system during the collision that liberated the meteorite from its parent body, some 7-8 Ma ago (Leya et al. 2001). With regard to this question, Wilson (1994) reported metal-sulfide relations seen in thin sections of St-Robert that are consistent with a weak level shock (St-Robert is a S2-S3 shock level).

I.5.Conclusions

Pb-Pb results yielded a regression corresponding to an age of 4565 ± 23 Ma while chondrule separates regression corresponds to an age of 4566 ± 7 Ma (2σ). These ages agree with the accepted age of chondrite formation. This indicates that no major perturbation occurred in the early history of the parent body. As for most ordinary chondrites, the St-Robert H5 whole rock data do not form a statistically significant Re-Os internal isochron, although they scatter around the IIIAB reference isochron. As mentioned by Walker et al. (2002), there are few explanations for such perturbed array: heterogeneous initial isotopic

composition, and/or analytical problems, and/or elemental remobilization. The analytical bias was investigated: the Birck et al. (1997) technique did not give Os yields 25% lower than from Carius tube analysis, as implied by the Meisel et al. (2003). Nonetheless, we do acknowledge that both these techniques recently raised some suspicions (Meisel et al. 2003). Apart from analytical bias, which cannot be totally excluded (including Re contamination), some of the scatter seen on the isochron diagram for the St-Robert H5 can be interpreted as the outcome of recent elemental mobilization for the most discordant datapoints, superposed to smaller original heterogeneities not obliterated by grade 5 metamorphism. Metal phases point towards a recent event, as the slope of the fit to the most perturbed data points is close to zero. This event is possibly the 7-8 Ma impact on the H parent body. Fusion crust results show that atmospheric entry did not affect differentially Re and Os. The INAA study points out that the chemistry of major and trace elements of the St-Robert meteorite is quite typical for a H5 ordinary chondrite.

I.Acknowledgements

This paper is dedicated to the memory of Clément Gariépy, who regrettably passed away during the writing of this manuscript. G. Kennedy from Ecole Polytechnique de Montréal is thanked for INAA data. R. Mineau (UQAM) is acknowledged for the SEM analysis. A.P. acknowledges scholarship grants from NATEQ and NSERC. R.D. acknowledges partial PDF support through a Lavoisier grant. J. David (MRNQ) is thanked for his help during the preliminary tests that triggered this project. A.P. and R.D. are grateful to J.-C. Mareschal and P. Schiano for careful reading and comment on the manuscript. This

manuscript greatly benefited from the thorough reviews of R.J. Walker, T. Meisel and an anonymous reviewer.

Table I.1 Whole-rock elemental abundances.

	(wt. %)		(ppm)
Fe	25.0	Sc	7.9
Si	18.4	As	1.8
Mg	13.7	Se	10.6
Ni	1.51	Sb	0.04
Ca	1.22	La	0.30
Al	1.01	Sm	0.19
Na	0.62	Eu	0.09
Cr	0.35	Yb	0.21
Mn	0.24	Re*	0.08
	(ppm)	Os*	0.84
K	724	Ir	0.69
Co	726	Au	0.19
V	73		

* : mean of 10 WR analyses by isotope dilution.

Table I.2 . Pb isotopic results, fractionation and blank corrected, with their propagated errors at the 95% level of confidence.

Sample	Weight (g)	[Pb] (ppb)	$^{206}Pb/^{204}Pb$ ± 2σ	$^{207}Pb/^{204}Pb$ ± 2σ	$^{208}Pb/^{204}Pb$ ± 2σ	$^{207}Pb/^{206}Pb$ ± 2σ	Error correlations $^{204}Pb/^{206}Pb$ vs $^{207}Pb/^{206}Pb$	Error correlations $^{206}Pb/^{204}Pb$ vs $^{207}Pb/^{204}Pb$	$^{207}Pb^*/^{206}Pb^*$ ± 2σ	Model Age (Ma)
WR fragment 1	0.12922	12.89	29.960±0.173	23.321±0.115	48.777±0.153	0.7784±0.0008	0.890	0.996	0.6308±0.0006	4581±1
WR fragment 2	0.13091	7.84	32.402±0.405	24.825±0.266	49.993±0.331	0.7661±0.0016	0.892	0.996	0.6292±0.0011	4577±3
WR fragment 3	0.13364	7.88	30.317±0.322	23.565±0.215	48.390±0266	0.7773±0.0014	0.891	0.996	0.6317±0.0010	4583±2
Fusion crust 1	0.20116	8.17	20.052±0.022	16.796±0.015	39.557±0.014	0.8376±0.0002	0.893	0.995	0.6051±0.0002	4520±1
Fusion crust 2	0.13586	8.13	20.450±0.042	17.084±0.030	39.640±0.023	0.8354±0.0003	0.892	0.995	0.6094±0.0004	4530±1
Troilite	0.00994	197.71	16.891±0.011	15.051±0.015	37.008±0.012	0.8911±0.0004	-0.589	0.927	0.6273±0.0012	4572±3
Kamacite 1	0.11701	14.39	18.448±0.012	15.789±0.010	38.301±0.012	0.8559±0.0001	0.334	0.996	0.6011±0.0003	4511±1
Kamacite 2	0.20433	7.08	18.989±0.010	16.278±0.010	39.186±0.010	0.8572±0.0001	-0.849	0.997	0.6180±0.0004	4551±1
Magn. Fraction	0.26256	4.13	19.927±0.034	16.780±0.025	39.180±0.015	0.8421±0.0002	0.887	0.997	0.6107±0.0004	4534±1
Grey pyroxene 1	0.03683	45.34	82.272±2.189	55.726±1.374	82.245±1.498	0.6773±0.0015	0.884	0.999	0.6227±0.0008	4562±2
Pale pyroxene 2	0.00551	290.55	40.556±0.465	29.528±0.292	56.786±0.383	0.7281±0.0013	0.890	0.997	0.6155±0.0008	4545±2
Chondrule 1	0.01835	96.30	50.175±0.717	35.462±0.448	69.005±0.687	0.7068±0.0014	0.888	0.998	0.6158±0.0008	4546±2
Chondrule 2	0.03931	40.92	85.323±2.588	57.416±1.616	89.094±1.955	0.6729±0.0017	0.885	0.999	0.6199±0.0009	4555±2
Chondrule 3	0.02212	65.47	72.577±2.129	49.604±1.335	85.927±1.861	0.6835±0.0019	0.886	0.999	0.6213±0.0010	4559±2
Chondrule 4*	0.02310	64.19	301.585±23.85	192.217±14.87	279.208±20.26	0.6374±0.0012	0.884	0.999	0.6224±0.0006	4561±1
Chondrule 5*	0.01140	126.74	198.839±30.56	128.704±19.15	206.559±28.45	0.6473±0.0034	0.926	0.999	0.6248±0.0014	4567±3
Chondrule 6*	0.02300	58.91	102.339±7.421	68.306±4.658	115.686±6.817	0.6675±0.0033	0.894	0.999	0.6236±0.0016	4564±4

* Sequential leaching with 0.2N, 3N and 6N HCl. Blank composition is 204 :206 :207 :208 = 1 : 18.20 :15.50 :38.40.

Table I.3 Re-Os isotopic results, fractionation and blank corrected.

Sample	Weight (g)	[Re] (ppb)	[Os] (ppb)	$^{187}Re/^{188}Os$	$^{187}Os/^{188}Os$ ± (2σ)*	Delta
WR 1	0.0522	81.25	817.1	0.47950	0.13350±3	4.5
WR 2	0.0847	67.40	738.4	0.43986	0.12918±2	-7.6
WR 3	0.0534	76.25	786.0	0.46757	0.13014±2	-19.7
WR 4	0.0484	82.94	800.2	0.49954	0.12991±1	-47.3
WR 5	0.0670	74.07	827.2	0.43150	0.12859±1	-6.8
WR 6	0.0544	75.84	770.0	0.47474	0.13116±1	-15.2
WR 7	0.0677	82.86	723.2	0.55227	0.13012±2	-86.7
WR 8	0.0897	100.6	1119.5	0.43314	0.13041±2	10.1
WR 9 CT	0.0729	73.94	840.1	0.42411	0.12834±7	-3.5
WR 10 CT	0.0540	99.94	987.4	0.48814	0.13481±1	10.7
Troilite	0.00187	22.63	81.0	1.35040	0.1345±27	-672.1
Fusion Crust 1	0.0366	76.21	855.9	0.42903	0.12804±3	-10.4
Fusion Crust 2	0.0231	69.39	825.4	0.40506	0.12714±2	-0.5
Metal 1	0.1212	1.91	99.3	0.09277	0.13442±12	318.7
Metal 2	0.0559	38.15	354.4	0.51918	0.13581±30	-3.8
Metal 3 CT	0.0076	74.42	688.9	0.52079	0.13174±4	-45.8
Metal 4	0.0024	56.14	3519.3	0.07691	0.13397±25	326.6

* Error bars refer to the last significant digits. WR = Whole-rock. CT = Carius Tube digestion.

Delta=10000 x $[^{187}Os/^{188}Os_{sample}-(0.09524+0.07887*^{187}Re/^{188}Os_{sample})]$ (Walker et al. 2002).

I.Reference List

Allègre C. J., Manhès G., and Göpel C. (1995) The age of the Earth. *Geochimica et Cosmochimica Acta* 59, 1445-1456.

Amelin Y. Krot, A.N., Hutcheon, I.D. and Ulyanov, A.A. (2002) Lead isotopic ages of chondrules and calcium-aluminum-rich inclusions. *Science* 297, 1678-1683.

Anders E. and Grevesse N. (1989) Abundances of the elements: Meteoritic and solar. *Geochimica et Cosmochimica Acta* 53, 197-214.

Birck J.-L., Roy-Barman M, and Capmas F. (1997) Re-Os Isotopic Measurements at the Femtomole Level in Natural Samples. *Geostandards Newsletter* 20, 19-27.

Birck J. L. and Allègre C. J. (1998) Rhenium-187-osmium-187 in iron meteorites and the strange origin of the Kodaikanal meteorite. *Meteoritics & Planetary Science* 33, 647-653.

Blum J.D., Wasserberg,G.J., Hutcheon I.D., Beckett J.R. and Stolper E.M. (1988) 'Domestic' origin of opaque assemblages in refractory inclusions in meteorites. *Nature* 331, 405-409

Brown, P., Hildebrand, A.R., Green-Daniel,W.E., Page, D., Jacobs, C., Revelle, D. Tagliaferri, E., Wacker, J. and Wetmiller,B. (1996) The fall of the St-Robert Meteorite. *Meteoritics* 31; 4, Pages 502-517, -517.

Chen J. H., Papanastassiou D. A., and Wasserburg G. J. (1998) Re-Os systematics in chondrites and the fractionation of the platinum group elements in the early solar system. *Geochimica et Cosmochimica Acta* 62; 3379-3392.

Chen J. H., Papanastassiou D. A., and Wasserburg G. J. (2002) Re-Os and Pd-Ag systematics in Group IIIAB irons and in pallasites. *Geochimica et Cosmochimica Acta* 66, 3793-3810.

Collerson K. D., Kamber B. S., and Schoenberg R. (2002) Applications of accurate, high-precision Pb isotope ratio measurement by multi-collector ICP-MS. *Chemical Geology* 188, 65-83.

Creaser R. A., Papanastassiou D. A., and Wasserburg G. J. (1991) Negative thermal ion mass spectrometry of osmium, rhenium, and iridium. *Geochimica et Cosmochimica Acta* 55, 397-401.

Deschamps P., Doucelance R., Ghaleb B. and Michelot J.-L. (2003) Further investigations on optimized tall correction and high-precision measurement of Uranium isotopic ratios using Multi-Collector ICP-MS, *Chemical Geology* 201, 141-160.

Doucelance R. and Manhès G. (2001) Reevaluation of precise lead isotope measurements by thermal ionization mass spectrometry : comparison with determinations by plasma source mass spectrometry. *Chemical Geology*, 176, 361-377.

Doucelance R., Escrig S., Moreira M., Gariépy C. and Kurz M.D. (2003) Pb-Sr-He isotope and trace element geochemistry of the Cape Verde Archipelago. *Geochimica et Cosmochimica Acta* 67, 3717-3733.

Göpel C., Manhès G., and Allègre C. J. (1994) U-Pb systematics of phosphates from equilibrated ordinary chondrites. *Earth and Planetary Science Letters* 121, 153-171.

Horan M. F., Walker R.J., Morgan J.W., Grossman J.N. and Rubin A.E. (2003) Highly siderophile elements in chondrites. *Chemical Geology* 196, 5-20.

Itoh S. and Yurimoto H. (2003) Contemporaneous formation of chondrules and refractory inclusions in the early Solar System. *Nature* 423, 728-731.

Jaffe L.A, Peucker-Ehrenbrink B. and Petsch S.T. (2002) Mobility of rhenium, platinum group elements and organic carbon during black shale weathering. *Earth and Planetary Science Letters* 198, 339-353.

Kallemeyn G.W., Rubin A.E., Wang D. and Wasson J.T. (1989) Ordinary Chondrites: Bulk compositions, classification, lithophile-element fractionations, and composition-petrographic type relationships. *Geochimica et Cosmochimica Acta* 53, 2747-2767.

Leya, I., Wieler, R., Aggrey, K., Herzog, G.F., Schnabel, C., Metzler, K., Hildebrand, A.R., Bouchard, M., Jull, A.-J.T., Andrews, H.R., Wang, M.S., Ferko, T.E., Lipschutz, M.E., Wacker, J.F., Neumann, S., and Michel, R. (1996) Exposure history of the St-Robert (H5) fall. *Meteoritics and Planetary Science* 36; 11, 1479-1494.

Ludwig K. R. (2001) Isoplot /Ex 2.49, A Geochronological Toolkit for Microsoft Excel. [Special Publication No.1a.]. Berkeley, CA, USA, Berkeley Geochronology Center.

Lee D.C and Halliday A. N. (1995) Precise determination of the isotopic compositions and atomic weights of molybdenum, tellurium, tin and tungsten using ICP magnetic sector multiple collector mass spectrometry. *International Journal Mass Spectrometry and Ion Processes* 146/147, 35-46.

Manhès G., Allègre C.J., Dupré B. and Hamelin B.(1980) Lead isotope study of basicultrabasic layered complexes: speculation about the age of the Earth and primitive mantle characteristics. *Earth and Planetary Science Letters* 47, 370-382.

McSween H.Y. (1999) *Meteorites and their parent planets*. 2nd edition. Cambridge Univ. Press.

Meisel T., Reisberg L., Moser J., Carignan J., Melcher F. and Bruegmann G. (2003) Re-Os systematics of UB-N, a serpentinized peridotite reference material. *Chemical Geology* 201, 161-179.

Nier A.O. (1937) The isotopic constitution of osmium. *Physical Review* 52, 885.

Palme H. and Jones A. (2003) In *Meteorites, Comets, and Planets* (ed. A.M.Davis). Vol. 1. Chap. 3, pp. 41-61. Elsevier-Pergamon, Oxford.

Russell A. D. Papanastassiou, D.A.and Tomborello T.A. (1978) Ca isotope fractionation on the Earth and other solar system materials. Papanastassiou, D. A. and Tomborello T.A. *Geochimica et Cosmochimica Acta* 42, 1075-1090.

Shen J. J., Papanastassiou D. A., and Wasserburg G. J. (1996) Precise Re-Os determinations and systematics of iron meteorites. *Geochimica et Cosmochimica Acta* 60; 15, Pages 2887-2900, -2900.

Shirey S. B. and Walker R. J. (1995), Carius tube digestion for low-blank rhenium-osmium analysis. *Analytical Chemistry* 67, 2136-2141..

Shirey S. B. and Walker R. J. (1998) The Re-Os isotope system in cosmochemistry and high-temperature geochemistry. *Annual Review of Earth and Planetary Sciences* 26, 423-500.

Smoliar M., Walker R. J., and Morgan J. W. (1996) Re-Os ages of Group IIA, IIIA, IVA, and IVB iron meteorites. *Science* 271; 5252, Pages 1099-1102, -1102.

Tatsumoto M., Knight R.J., and Allègre C. J. (1973) Time differences in the formation of meteorites as determined from the ratio of lead-207 to lead-206. *Science* 180, 1279-1283.

Tera F. and Carlson R. W. (1999) Assessment of the Ph-Ph and U-Pb chronometry of the early solar system. *Geochimica et Cosmochimica Acta* 63, 1877-1889.

Thirlwall M. (2001) Inappropriate tail corrections can cause large inaccuracy in isotope ratio determination by MC-ICP-MS. *Journal of Analytical Atomic Spectrometry* 16, 1121-1125.

Thirlwall M. F. (2002) Multicollector ICP-MS analysis of Pb isotopes using a (207)pb-(204)pb double spike demonstrates up to 400 ppm/amu systematic errors in Tl-normalization. *Chemical Geology* 184, 255-279.

Völkening J. and Walczyk T.and Heumann K.G. (1991) Osmium Isotope ratio determinations by negative thermal ionization mass spectrometry. *International Journal of Mass Spectrometry and Ion Physics* 105, 147-159.

Walker R. J.; Horan, M.F. Morgan, J.W., Becker, H.; Grossman, J.N. and Rubin, A.E. (2002) Comparative Re-187-Os-187 systematics of chondrites: Implications regarding early solar system processes. *Geochimica et Cosmochimica Acta* 66, 4187-4201.

Wasserburg G.J. (1985) In *Protostars and Planets,* edited by. Black D.C. and Matthews M.S. Univ. Arizona Press. pp. 703-737.

Wasson J. T. and Kallemeyn G. W. (1988) Composition of chondrites. *Phil.Trans. R.Soc. Lond.* A325, 535-544.

Yin Q.Z., Jacobsen S.B., Lee C.-T., McDonough W.F., Rudnick R.L. and Horn I.. (2001) A gravimetric K_2OsCl_6 standard; application to precise and accurate Os spike calibration. *Geochimica et Cosmochimica Acta* 65; 13, 2113-2127.

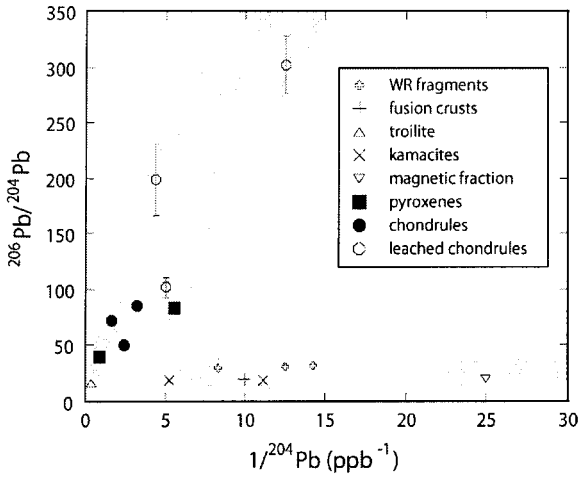

Figure I. 1. $1/^{204}Pb$ vs $^{206}Pb/^{204}Pb$ diagram indicating two main trends for the dataset: a first one controlled by U decay, and another by common (initial) lead content.

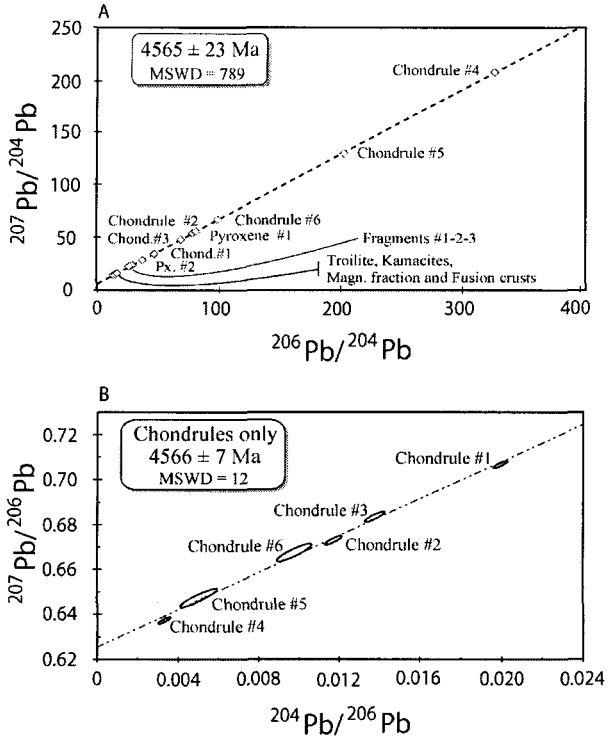

Figure I. 2 Pb-Pb isotope results for St-Robert H5 chondrite presented in isochron diagrams. Errors are given at 2σ confidence interval. Datapoints are blank and fractionation corrected. A. Internal Pb-Pb isochron (see table 2 for data). Comprised in the error envelope of the regression is the primordial lead value from Tatsumoto et al. (1973) with $^{207}Pb/^{204}Pb$=9.307 and $^{206}Pb/^{204}Pb$=10.294. B. Diagram of $^{207}Pb/^{206}Pb$ vs $^{204}Pb/^{206}Pb$ for the chondrule separates only. Ages computed with Isoplot /Ex v 2.49 (Ludwig K. R. 2001).

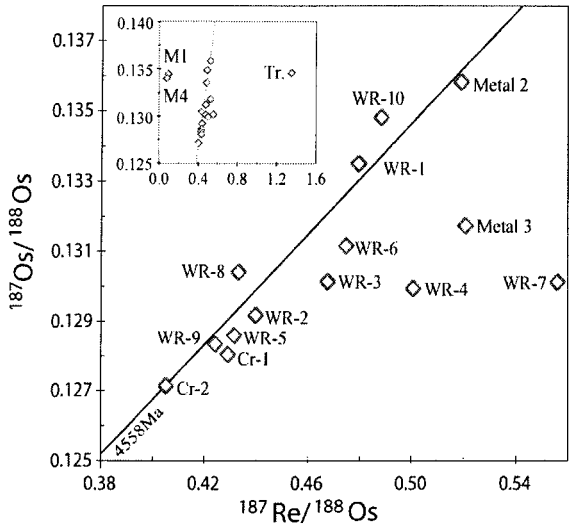

Figure I. 3 Re-Os data shown in an isochron diagram. The 4558 Ma line is a reference isochron from the IIIAB iron meteorite (Smoliar et al. 1996) WR: ''whole rock'' fragment, Tr. : Troilite pure separate, M : metal-rich fragment.

CHAPITRE II
ISOTOPIC SIGNATURE AND IMPACT OF CAR CATALYSTS ON THE ANTHROPOGENIC OSMIUM BUDGET

André Poirier et Clément Gariépy

Publié dans *Environmental Science and Technology* (2005); vol. *39*(12); pages 4431-4434.

Abstract

Higher osmium concentrations and lower $^{187}Os/^{188}Os$ ratios in sediments from urban areas have been linked to anthropogenic osmium sources and automobile catalytic converters that use platinum group metals (PGM) are a potential source for this Os pollution. We present the first direct Os concentrations and isotopic measurements of catalytic converters for major automobile brands in order to test the assumption that car catalysts release Os with a distinct signature in the environment. The analysis of 4 new catalytic converters yield similar low $^{187}Os/^{188}Os$ ratios (0.1-0.2), suggesting a similar source for the PGM. The Os concentrations measured are in the ppt range (6-228 ppt). From our results, the osmium contribution of the car catalysts to the environment through *attrition* (wearing and grinding down of the catalyst by friction) is predicted to be low; < 0.2 pg Os/m^2/year in highly urbanized environment. We show that Os loss from catalysts as volatile OsO_4 is important at car catalyst operating temperatures. Moreover, we estimate that car catalysts may be responsible for up to ~120 pg Os/m^2 deposited per year in urban areas, and that part of it may be exported to sedimentary sinks. Car catalytic converters are thus an important anthropogenic osmium source in densely populated areas. The NIST car catalyst standard (SRM-2557, made from recycled catalysts) yields higher concentrations (up to 721 ppt Os) and a more radiogenic isotopic composition (~0.38), perhaps indicative of Os contamination during its preparation.

Keywords: urban pollution, catalytic converter, osmium, $^{187}Os/^{188}Os$, isotope geochemistry.

Introduction

The accumulation of heavy metals in the sedimentary record was greatly enhanced by the onset of the industrial era. In most urban environments, recent sediments contain metal concentrations orders of magnitude higher than pre-industrial levels. Metals with naturally variable isotopic compositions (e.g., Pb) allow a better understanding of the impact of pollution in sedimentary environments, by enabling tracing of sources –either natural or man-made. Osmium, a member of the platinum group metals (along with Pt, Pd, Rh, Ru and Ir), is also enriched in urban shallow sedimentary records despite its rather limited industrial use (*1-5*). Osmium also has a wide range of isotopic compositions in nature because the ^{187}Os isotope varies in relative abundance in different lithologies of diverse geological ages. This is attributable to the fact that part of the ^{187}Os comes from the radioactive decay of ^{187}Re ($T_{1/2}$ ~ 42 billion years). The present-day $^{187}Os/^{188}Os$ of a rock is controlled by its Re/Os ratio and its geological age. The variablity in Re/Os is due to the different geochemical behaviour of the two elements; Os is more enriched in ultramafic rocks, whereas Re is preferentially enriched in more differentiated lithologies.

Some of the most important sources for platinum group metals (PGM) are ore bodies from magmatic ultramafic intrusions of mantle origin, which were contaminated with minor amounts of (relatively radiogenic) continental osmium during emplacement. Consequently, commercial PGM from these deposits have $^{187}Os/^{188}Os$ isotopic signatures of *ca.* 0.15-0.20; e.g., Bushveld Complex (*6*). Sediments derived from continental crust, although heterogeneous in nature, have a higher average $^{187}Os/^{188}Os$ of ~ 1.0 due to long term Re enrichment of the crust (*7*). The large differences in Os isotopic signatures between these two sources allow the

anthropogenic and natural components in a given sedimentary basin to be distinguished and quantified.

Urban sewage sludge contains high concentrations of osmium and is suspected to be a major contributor of anthropogenic Os to shallow urban sediments (*2,3,5*). Sources of Os in this sludge, and ultimately in sediments, were attributed to the biomedical and industrial uses of this PGM; OsO_4 is a lipid stain used to enhance cell structures for optical and electron microscopy (*1,4,5*). Automobile catalytic converters have been mentioned as another possible contributor of anthropogenic Os to recent sediments (*2,5*). Esser and Turekian (*1*) mentioned catalytic converters as a Pd source but discarded it for Os because it is not directly employed in the automobile emission control industry. Automobile catalytic converters (hereafter termed catalysts) use Pd, Pt, and Rh to decrease the conversion temperature of carbon monoxide, nitrous oxides and unburned hydrocarbons to less noxious exhaust fumes. In a converter, these metals are coated (using a washcoat) on to a honeycomb-structure that provides a high surface/volume ratio that is typically composed of cordierite (due to its excellent thermal properties). These devices are known to lose a fair amount of their noble metals by attrition during normal use (*8*). Although osmium is not directly employed in car catalysts, the strong association between the PGM means that osmium impurities can persist even among refined PGM. Thus, a significant level of Os impurity could be present among the other PGM in the catalysts and contribute to the anthropogenic input of Os to the urban environment.

An estimate of how much osmium could theoretically be introduced into urban environments by attrition every year can be obtained from the equation used for platinum release (equation 1):

Equation 1 :
$$Os_{attrition} = Pt_{attrition} \times \Sigma_{cars} \times \mathrm{K}m \times \left(\frac{Os}{Pt}\right)_{catalyst}$$

Where $Pt_{attrition}$ is the amount of platinum delivered through attrition by recent monolithic catalyst -20 to 136ng Pt/km (*8*)-, Σ_{cars} is the quantity of currently catalyst-equipped cars (*ca.* 500 million) and Km is the average annual mileage per car (15

000 km per years; *9*). The Os/Pt ratio of catalytic converters is unknown, but estimating an impurity of a few ppm of osmium in the bulk PGM yields values of several grams of Os released worldwide every year (mostly in urban environments). Because the $^{187}Os/^{188}Os$ ratio of industrial osmium is so distinct from the average natural input, this human contribution could have a major impact on the Os isotopic signature in sedimentary records from densely populated areas. Moreover, because osmium oxide is a volatile species (OsO_4 becomes gaseous at 110°C) at the catalyst's operating temperature of several hundred degrees, loss of Os as OsO_4 could be even more significant than for the other non-volatile PGM.

In this paper, we directly analyze catalysts of selected major brands of passenger vehicles, and we also evaluate the volatility-related loss of osmium from these devices. To our knowledge, this study is the first to try to quantify the impact of the automobile industry on the anthropogenic Os budget.

Experimental section

Three new monolithic (honeycomb) catalysts were acquired from automobiles from representing different major automobile companies (DaimlerChrysler Neon, Ford Motor Company F-150 and Toyota Corolla) in order to measure their Os content. The honeycomb catalytic structures were removed from their metallic casings using a new saw blade for each casing to avoid contamination between the different catalysts. The inner portion of the catalysts was then crushed using an alumina mortar and pestle. The Chrysler and Toyota pipes contained only one monolithic structure whereas the Ford F-150 contained 2 successive monolithic structures within the pipe (a small close-coupled catalyst with a rapid operation time and a larger underfloor catalyst); all 4 catalysts were analyzed. The monolithic technology has been in use in North America since the early 1980's. The limitation of this study resides in the samples' representativeness, although the chosen car models are amongst the best sellers; the

relative and absolute quantities of the PGM used by different companies on different vehicle models are most probably variable.

A monolithic catalyst standard (NBS-2557), obtained from the National Institute of Standard and Technology (NIST) was also analysed. This standard, made from a used catalyst, was obtained because: 1- it is a more representative sample, because it is an aliquot from a ~135 kg batch of crushed and homogenized (< 74μm) recycled used monolithic catalysts (recycled by Inco, ltd. and subsequently shipped to NIST); and 2- it can be used to test whether volatile osmium is lost as OsO_4. If volatile loss of Os is significant, there should be a depletion in the Os concentration of the used catalyst standard compared to new catalysts.

The chemical separation and purification of osmium was accomplished in a class 100 laboratory using the procedure developed by Birck et al. (*10*); following dissolution in an HF-HBr acid mixture, Cr^{VI} and $Br_{2(l)}$ are added to the solution (chromium oxide to ensure spike-sample homogeneity by driving Os to its highest oxidation state, and liquid bromine allowing extraction of the oxidized osmium). Os concentrations were obtained by the isotope dilution technique, using a ^{190}Os spike calibrated against a K_2OsCl_6 stochiometric standard (*11*). The concentrations and isotopic compositions reported in Table 1 were acquired by negative thermal ionization mass spectrometry (NTIMS) on a VG Sector 54 (*12,13*). This instrument is equipped with 7 faraday cages, a Daly ion counter, a Channeltron electron multiplier used for small negative ion beams and an O_2-bleeding valve. Faraday cups efficiencies are set up at unity whereas relative Faraday amplifier gains are monitored daily. We measured all isotopes (except 184) as oxides and monitored $^{185}Re^{16}O_3$ for potential Re interference on $^{187}Os^{16}O_3$ beam. The osmium samples are loaded on a platinum filament and covered with 0.5 μl of freshly prepared barium hydroxide solution. The oxygen bleeding rate into the mass spectrometer source is optimized for each sample. Spike-sample unmixing, oxide contributions and fractionation corrections (normalized to $^{192}Os/^{188}Os = 3.08271$; (*14*) were performed off-line.

During the course of this study, full-procedure blanks (n=2) yielded 0.12 and 0.20 pg of total osmium with $^{187}Os/^{188}Os$ ratios of 0.16 and 0.22, respectively. Osmium K_2OsCl_6 standard measurements yielded means of $^{187}Os/^{188}Os$ = 0.1067±2 (standard deviation from the mean, Channeltron measurements, n = 8, for 10 to 200 pg of loaded osmium) and $^{187}Os/^{188}Os$ = 0.1070±1 (standard deviation from the mean, Faraday static multi-collector measurements, n = 15, for >100 pg of loaded osmium). Analysis of an aliquot of the standard solution LOsTD (provided by Thomas Meisel, University of Leoben) yielded a $^{187}Os/^{188}Os$ ratio of 0.10689±5, (1 S.D, n=5). This value is in agreement with the mean of all analyses reported by 14 different labs (T. Meisel, pers. comm.). This solution is now being analysed by many laboratories with the intention of making it an inter-laboratory mass spectrometry standard for osmium.

The Teflon bomb dissolution technique used here for the catalysts has been shown to be inefficient (60-65% dissolution) for samples containing very insoluble or refractory phases such as spinel (*15*). However, the PGM in car catalysts (and associated osmium) are found in the thin washcoat layer (<1 mm thick on the surface of the alumina substrate) that renders the noble metals more accessible for chemical reactions, including dissolution by acids. Moreover, in a worst case scenario of only a 60% Os yield, the released osmium calculated here would be a minimum and the conclusions from this study would then be even more significant.

Results and discussion

New catalysts

The new catalysts were examined for major elements on a Hitachi S-2300 scanning electron microscope at the Université du Québec à Montréal. X-ray spectra indicated that the catalysts consisted of similar alumino-silicate substrates covered by a rare-earth based washcoat of variable but typical compositions: 40 to 60% Ce ± La ± Ba for all catalysts. The PGM in the washcoats were always below the detection limit of the instrument.

The new catalysts yielded osmium isotopic signatures between 0.16 and 0.19 (Table 1, fig.1), consistent with those obtained from ultramafic PGM ore deposits such as found in the Bushveld Complex (*6*). However, their Os concentrations (6-228 ppt) were lower than the theoritical estimates (ppb range). These results are indicative of an efficient fractionation of the different PGM during the purification processes. Replicates of the Os isotopic ratios differ by up to 10% and exceed the overall analytical uncertainty. This may reflect heterogeneities in the monolithic catalyst, linked to variable proportions of the components used, and subsequently sampled by us (for example: the PGM washcoat and MgO used to make the synthetic cordierite substrate probably have different but unradiogenic $^{187}Os/^{188}Os$ ratios).

Table II. 1: Os content (pg/g) and isotopic composition of new catalytic converters and used catalytic converter standard from NIST. Analytical uncertainty on $^{187}Os/^{188}Os$ ratios is presented at the 96% confidence level.

Sample	Size (g)	ppt Os	$^{187}Os/^{188}Os$
Chrysler Neon	1.6287	227	0.191±3
replicate	1.2068	228	0.172±1
Ford F-150 small	2.5360	20	0.186±1
Ford F-150 big	2.9052	176	0.158±1
Toyota	6.1163	6	0.162±1
replicate	7.7162	8	0.174±1
Heated Chrysler -1 *	1.0708	55	0.168±1
Heated Chrysler -2 *	2.0277	12	0.164±2
SRM-2557	3.8868	721	0.379±1
replicate	4.3845	631	0.389±1

* heated at 400°C for 330 hours

The Os/Pt ratio for equation 1 can now be directly calculated using the above Os concentrations and 0.15% platinum in the catalysts (16), yielding Os/Pt ratios between 10^{-9} and 10^{-7}. Addition of these values to equation 1 yields a maximum of 0.2 gram of Os released by attrition per year for the total number of cars. However, prior to 1980 catalytic converters were of the pellet-type and used more PGM and were more affected by attrition, so they could have contributed more PGM to the anthropogenic input. In addition, it is likely that Pt refining procedures have improved through time, and that early catalysts would have had poorer separation of Os from other PGM. This effect could be critical in discussing the older used NISTcatalysts standard below.

Used catalysts standard

The analysis of the SRM-2557 used car catalysts standard shows a higher Os concentration (600-700 ppt) with relatively radiogenic $^{187}Os/^{188}Os$ ratios (0.38; Table 1, Figure 1). Thus the loss of Os through volatilization cannot be evaluated because the concentration of osmium in the used NIST standard exceeds that of the new catalysts. The results for the NIST standard may reflect: 1) car-related contamination (kerogen is a rich and radiogenic source of osmium (*17*), so perhaps refined gasoline still has traces of osmium in it); 2) contamination by the crusher at Inco, Ltd. facilities by ores previously crushed using the same equipment; 3) The PGM material of the recycled catalysts used to produce SRM-2557 was derived from a more radiogenic ore deposit; e.g. $^{187}Os/^{188}Os$ ratios of the Sudbury PGM ore body are as high as those measured in SRM-2557 (*18*); and 4) possibly earlier catalysts were more Os-rich because of inferior purification of the PGM used (see previous section).

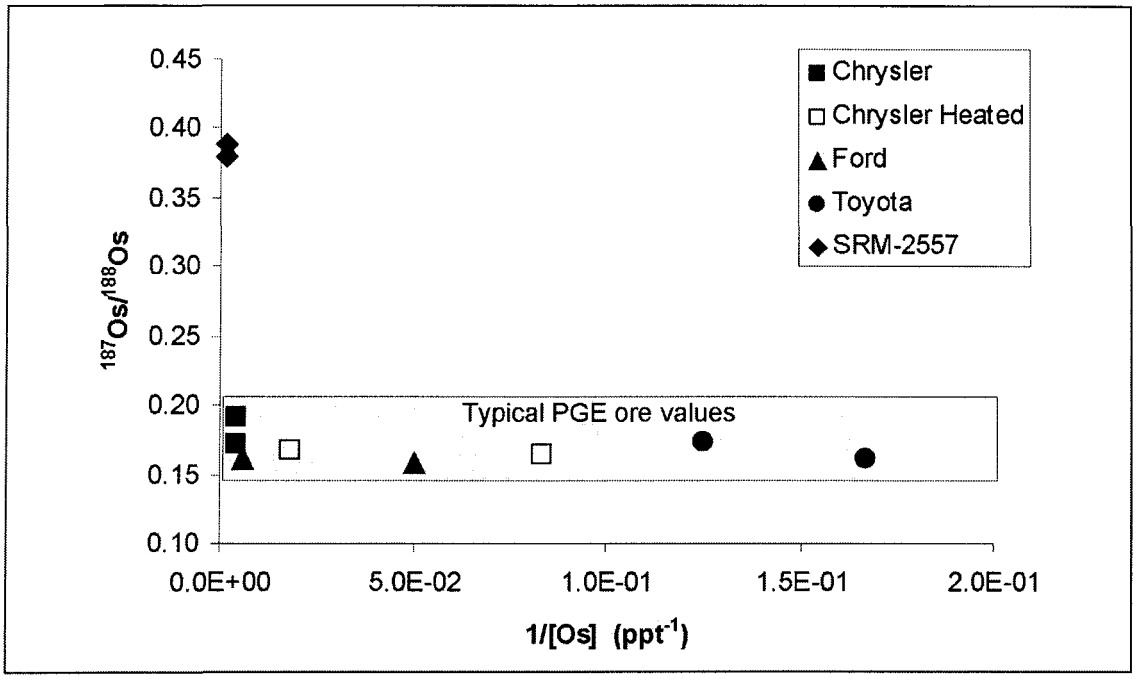

Figure II. 1. Inverse of osmium content and isotopic signature of new car catalysts, heated catalysts and catalysts standard SRM-2557.

Assessment of osmium volatility

Since the physical conditions in catalysts are effective in promoting the oxidation of osmium into its gaseous form, we suspected that osmium volatility played a major role in the loss of Os from catalysts. A simple experiment was done in order to validate this hypothesis. A piece of Chrysler Neon catalyst was heated in an oven for 330 hours, roughly equivalent to a year of use for an hour a day, at 400°C which is about the lowest temperature at which the catalyst activity is significant (the *light-off* temperature). We recognize that limitations in this experimentation lie in the gas phase composition (air) which is not the same as automobile exhaust gas, 0.5 vol.% O_2; (*19*)- and in the fact that there is (almost) no gas flow in our experiment while many liters of exhaust gasses per second pass through the catalyst of an exhaust pipe. In any case, the results (Table 1) show a 75% to 95% depletion in osmium due to heating at 400°C. We believe that this loss is due to the oxidation of Os (combined

with ambient oxygen or from the washcoat's CeO) to form OsO_4, followed by evaporation and loss. Compared to the new Chrysler catalysts, the heated catalysts have isotopic compositions that fall within a narrower range. This favors our hypothesis of binary (or multiple) mixing for the un-heated catalyst replicates in that the PGM-rich coating (designed to facilitate oxidation and volatilization) has a slightly higher $^{187}Os/^{188}Os$ ratio than the more chemically refractory endmember (conceivably the cordierite substrate). Because this is a relatively low temperature experiment, catalysts may reach 1100°C in some conditions (*16*), we expect that most of the osmium would be lost from catalysts upon normal automobile use, since the kinetics of the oxidation/volatilisation would be enhanced.

Assessment of catalysts' environmental impact

The above results allow us to calculate an estimate of the quantity of osmium released in North America. Sixteen million new cars are sold yearly in North America (obtained by adding up the 2002 values published in the annual reports of all major automobile manufacturers). We assume that each is equipped with an approximately 1 kg monolithic catalyst which contains between 6 and 228 ppt Os (respectively our lowest and highest measured values for new catalysts) and 100% osmium loss by evaporation in the tetraoxide species. The choice of 100% loss was made in order to calculate an upper limit on the Os release from car catalysts. We obtain a range of 0.1 to 3.6 g of Os during the running lives of these cars. If we further assume that Os is lost on the first year (fast degassing yielding a maximum value, an assumption supported by our results from the heated catalyst), we can evaluate how much osmium will be distributed on the North American continent every year, assuming a constant renewal rate of the automobile pool. Using the area of entire USA, and the first 1000 km of southern Canada (comprising almost the entire Canadian population and cars), yields concentrations of 0.006 to 0.234 picograms of Os per square meter per year. These low amounts suggest that new catalysts are not a significant source of

anthropogenic osmium on the continental scale (for comparison, when using a mean continental denudation rate of 10 m/My (20), which translates into 10 g/m^2/yr using d = 2.7 g/cc, we calculate a natural input from continental erosion of ~ 810 pg Os/ m^2/yr, using 30 ppt Os for eroding material).

If calculations are carried out for a densely populated area such as New York City, the values become more significant. We approximate the yearly amount of new car sales by applying the same population/car sales ratio of North America (300M/16M) to NYC (population of 8 million) and obtain 427100 new cars in circulation per year. Keeping the 1 kg monolithic converter and the Os concentrations measured in this study, with 770 km^2 for NYC area, we obtain 3 to 126 pg Os/m^2/yr (attrition only yields a maximum of 0.2 pg Os/m^2/yr). Bearing in mind that the osmium content of average eroding continental crust is on the order of 800 pg/m^2/yr (the denudation rate in low topography is much lower, so this can be as low as a few pg Os/m^2/yr in some areas), and that in the North Pacific, natural transported continental dust in the atmosphere deposits about 1 pg Os/m^2/yr (21), osmium derived from catalysts would then have significant impact on the environment near urban centers.

The residence time of OsO_4 in the atmosphere is not known, but the high reactivity of this strongly oxidizing molecule tends to suggest that it is very short, being reduced on the first particle it collides with (*22*). Osmium is then most probably reduced to non-volatile dioxide or metal form that can be subsequently mobilized by weathering and deposited into sediments.

The above estimates are based on a 100% volatility of the Os contained within catalyst material and are thus a maximum value. However they provide an order of magnitude for emissions from cars catalysts and show how significant the impact of the automobile industry can be on the osmium geochemical cycle. We believe that automobile catalytic converters are strong candidates to account for the higher Os concentrations coupled with lower $^{187}Os/^{188}Os$ ratios encountered in urban sedimentary records.

Acknowledgement

This paper in dedicated to the memory of Clément Gariépy, who regrettably passed away during the writing of this manuscript. Thanks are due to R. Mineau for the microprobe analysis. AP acknowledges scholarship grants from NATEQ and NSERC. Thanks are also due to Rive-Sud Chrysler for their new catalyst donation. Discussions with A. Beaulieu, J. David, C. Hillaire-Marcel and R.K. Stevenson helped to improve the manuscript. This study benefited from the reviews of G. Helz, G. Riedel and an anonymous reviewer.

Literature Cited

1. Esser B. K. and Turekian K. K. (1993) The osmium isotopic composition of the continental crust. *Geochim. Cosmochim. Acta* **57**, 3093-3104.

2. Ravizza G. E. and Bothner M. H. (1996) Osmium isotopes and silver as tracers of anthropogenic metals in sediments from Massachusetts and Cape Cod bays. *Geochim. Cosmochim. Acta* **60;** 2753-2763.

3. Williams G., Marcantonio F., and Turekian K. K. (1997) The behavior of natural and anthropogenic osmium in Long Island Sound, an urban estuary in the Eastern U.S. *Earth Planet. Sci. Lett* **148;** 341-347.

4. Helz G.R.; Adelson J.M.; Miller C.V.; Cornwell J.C.; Hill J.M.; Horan, M. F.; Walker, R. J. (2000) Osmium Isotopes Demonstrate Distal Transport of contaminated Sediments in Cheasapeake Bay. *Environ. Sci. Technol.* **34**, 2528-2534.

5. Rauch S., Hemond H.F., and Peucker-Ehrenbrink B. (2004) Recent Changes in Platinum Group Element Concentrations and Osmium Isotopic Composition in Sediments from an Urban Lake. *Environ. Sci. Technol* **38**, 396-402.

6. McCandless T. and Ruiz J. (1991) Osmium isotopes and crustal sources for platinum-group mineralization in the Bushveld Complex, South Africa. *Geology* **19**, 1225-1228.

7. Peucker-Ehrenbrink B. and Jahn B. M. (2001) Rhenium-osmium isotope systematics and platinum group element concentrations: Loess and the upper continental crust. *Geochemistry Geophysics Geosystems* **2**, art-2001GC000172.

8. Merget R. and Rosner G. (2001) Evaluation of the health risk of platinum group metals emitted from automotive catalytic converters. *The Science of total Environment* **270;** 165-173.

9. Barbante C.; Veysseyre A.; Ferrari C.; Van de Velde K.; Morel C.; Capodaglio G.; Cescon P.; Scarponi G.; and Boutron C. (2001) Greenland Snow Evidence of Large Scale Atmospheric Contamination for Platinum, Palladium, and Rhodium. *Environ. Sci. Technol* **. 35**, 835-839.

10. Birck J.-L., Roy-Barman M, and Capmas F (1998) Re-Os Isotopic Measurements at the Femtomole Level in Natural Samples. *Geostandard Newsletter* **20**, 19-27.

11. Yin, Q. Z.; Jacobsen, S. B.; Lee, C. T.; McDonough, W. F.; Rudnick, R. L.; Horn, I. (2001) A gravimetric K_2OsCl_6 standard; application to precise and accurate Os spike calibration. *Geochim. Cosmochim. Acta* **65;** 2113-2127.

12. Creaser R. A., Papanastassiou D. A., and Wasserburg G. J. (1991) Negative thermal ion mass spectrometry of osmium, rhenium, and iridium. *Geochim. Cosmochim. Acta* **55**, 397-401.

13. Völkening J., Walczyk T. and Heumann K.G. (1991) Osmium Isotope ratio determinations by negative thermal ionization mass spectrometry. Intl. J. Mass Spectrom. Ion Phys. **105**, 147-159.

14. Nier A.O. (1937) The isotopic constitution of osmium. *Physical Review* **52**, 885.

15. Meisel, T.; Reisberg, L.; Moser, J.; Carignan, J.; Melcher, F.; Bruegmann, G. (2003) Re-Os systematics of UB-N, a serpentinized peridotite reference material. *Chem. Geol.* **201**, 161-179.

16. Farrauto R. and Heck R. (1999) Catalytic converters: state of the art and perspectives. *Catalysis Today* **51**, 351-360.

17. Ripley, E. M.; Park, Y. R.; Lambert, D. D.; Frick, L. R. (2001) Re-Os isotopic variations in carbonaceous pelites hosting the Duluth Complex; implications for metamorphic and metasomatic processes associated with mafic magma chambers. *Geochim. Cosmochim. Acta* **65;** 2965-2978.

18. Cohen, A. S.; Burnham, O. M.; Hawkesworth, C. J.; Lightfoot, P. C. (2000) Pre-emplacement Re-Os ages from ultramafic inclusions in the sublayer of the Sudbury igneous complex, Ontario. *Chem Geol.* **165;** 37-46.

19. Heck R and Farrauto R. (2001) Automobile exhaust catalysts. *Applied Catalysis* **221**, 443-457.

20. Stanford, S. D., Ashley, G. M., Russell, E.W.B., and Brenner, G. J. (2002), Rates and patterns of late Cenozoic denudation in the northernmost Atlantic Coastal Plain and Piedmont : Geological Society of America Bulletin 114, 1422-1437 .

21. Williams, G.A. and Turekian, K.K. (2002) Atmospheric supply of osmium to the oceans, Geochimica Cosmochimica Acta, v. 66 n. 21, 3789-3791.

22. Smith I. C., Carson B. L., and Ferguson T.L. (1974) Osmium: An Appraisal of Environmental Exposure. Environ. Health Perspectives 8, 201-213.

CHAPITRE III

Re-Os and Pb isotope systematics in reduced fjord sediments from Saanich Inlet (Western Canada)

André Poirier

III. Abstract

Re-Os and Pb-Pb isotopic analysis of reduced varved sediments cored in the deeper basin of Saanich Inlet (B.C.) are presented. From core top to 61 cm downcore, spanning approximately the last 100 years of sedimentation, $^{187}Os/^{188}Os$ ratio and Os concentration respectively decrease from ~0.9 to ~0.8, and increase from 55 to 60 ppt, whereas Re concentration decrease from 4000 to 2800 ppt. Re correlates with C_{org} (R^2=0.6) throughout the entire section, whereas Os follows Re and C_{org} trends only below 8 cm down-core, suggesting a decoupling of a Re- and Os-geochemistry during burial and/or very early diagenesis. No systematic compositional differences are observed between varves or seasonal layers. ^{204}Pb-normalized lead isotope ratios increase from sediment surface down to 7 cm down-core, then decrease steadily to pre-industrial levels at ~ 50 cm downcore. This pattern illustrates the contamination from leaded gasoline until the recent past. The measured Pb isotopic ratios point primarily toward gasoline related atmospheric lead from the USA.

The osmium isotopic values measured are significantly lower than those of modern seawater-Os (1.06; Levasseur et al. 1998). In comparison with other anoxic environments, the osmium content of Saanich Inlet sediments is low, suggesting prominent inputs from unradiogenic, detrital and/or dissolved sources. Ultramafic lithologies in the watershed of the Fraser River are suspected to contribute to sedimentary inputs as well as to the input of dissolved unradiogenic osmium in the water of Saanich Inlet. The presence of some unradiogenic Os from anthropogenic contamination cannot be discounted near the core top, but since deeper, pre-anthropogenic levels also yielded unradiogenic Os results, one is led to conclude that the overall low $^{187}Os/^{188}Os$ ratios result from natural geochemical processes. Thus, the bulk sediment of Saanich Inlet does not appear to record $^{187}Os/^{188}Os$ composition of the marine end-member of the only slightly below normal salinity, fjord water. The low

seawater-derived Os content of the sediment, coupled with unradiogenic Os inputs from local sources, explain the overall low isotopic values observed. As a consequence, such near-shore anoxic sediments are unlikely to record changes in the past ocean Os isotopic composition.

Keywords: Re-Os isotopes, Pb isotopes, anoxic sediments, Saanich Inlet.

III. Introduction

The $^{187}Os/^{188}Os$ ratio of seawater corresponds to a weighted average of all the osmium that enters the ocean. Present-day seawater was recently shown to have a uniform osmium isotopic composition, with a $^{187}Os/^{188}Os$ ratio of ~1.06 (Sharma et al. 1997; Levasseur et al. 1998, Woodhouse et al. 1999). This value is the end result of a mixture of both radiogenic sources (continental) and unradiogenic sources (mainly from seafloor alteration and meteorites/cosmic dust dissolution). Table 1 summarizes the typical isotopic compositions, concentrations and fluxes of the major reservoirs that affect seawater composition. The difference in isotopic composition of these sources is due to long-term rhenium enrichment of the continental crust (^{187}Re decays to ^{187}Os with a half-life of 42 Ga). The fluxes of some of these sources are still being debated.

The evolution of seawater Os isotopic composition through time provides information about past tectono-climatic changes (Peucker-Ehrinbrink et al. 1995; Cohen et al. 1999; Singh et al. 1999). Several sedimentary lithologies appear to record the osmium hydrogeneous (seawater-derived) signature, but for periods older than the ocean floor (*ca.* 180 Ma), black shale is the lithology that seems most promising (Ravizza and Turekian, 1989; Cohen et al. 1999; Singh et al. 1999; Selby and Creaser, 2003). Although no perfect contemporary analogue for black shale deposition environment exists (e.g., Piper and Perkins, 2004), sedimentary basins that serve as partial analogues are available for study. Of those basins, some were investigated for their osmium content and isotopic composition. Modern ultra-organic-rich marine sediments (10-60% organic matter) have been shown by Ravizza and Turekian (1992) to successfully record the present-day seawater $^{187}Os/^{188}Os$ ratio (with 100-200 ppt Os). The anoxic sediments off the coast of Peru (Koide et al. 1991),

although highly enriched in Os (up to 12 ppb), has a $^{187}Os/^{188}Os$ ratio close to the mantle value (~0.12), a composition that is not explained by the authors. The Black Sea, considered as a classic "type euxinic" basin and perhaps one of the best black shale analogues, was studied by Ravizza et al. (1991). They reported up to 685 ppt Os concentrations and indicated a large contribution from local terrigeneous osmium, with a lower than seawater $^{187}Os/^{188}Os$ ratio. This basin is strongly influenced by riverine input (salinity of ~18-22), which prevents the recording of a seawater signature.

This led us to examine Os geochemistry in reduced organic-rich sediments from a setting closer to normal marine salinity conditions at Saanich Inlet (western Canada).

Table III. 1: Typical values of major sources of osmium for the ocean.

Source	$^{187}Os/^{188}Os$	Osmium concentration (g Os/g)	Flux to ocean (kg/yr)
Seawater	~1.06	~10 x 10^{-15}	
Continental crust			
-black shale	1 to >10	10^{-11} to 10^{-8}	
-ophiolite	0.1-0.2	up to 10^{-9}	
-aeolian dust	1.0±0.2	~30 x 10^{-12}	
-average rivers	~1.4	~9 x 10^{-15}	>350
Ocean crust			
-hydrothermal alteration	0.1-0.4	<100 x 10^{-15}	20-30
Meteorite			~15
-ordinary chondrite	~0.12	850 x 10^{-9}	
-iron meteorite	~0.12	>10^{-6}	
Anthropogenic	~0.1-0.2		

Saanich Inlet is a seasonally anoxic fjord on Vancouver Island, British-Columbia. It has been previously mentioned as a possible partial modern analogue of a black shale depositional environment (Bornhold et al. 1996). The osmium content of sediment in Saanich Inlet was reported at 0.89 ppb Os (Koide et al. 1991). Corresponding to a concentration ~30 times more enriched in Os than sediments coming from the erosion of the average continental crust, this reported osmium content led us to believe that the anoxic conditions at the bottom of this basin fostered concentration of seawater Os. No Os isotopic composition was reported by Koide et al. (1991) for Saanich Inlet.

In fine, the main objective of this study was to ascertain the capability of sediments such as those from Saanich Inlet to record the present-day seawater $^{187}Os/^{188}Os$ ratio. We examined the effect of terrigeneous inputs by comparing disctinct seasonal layers of the varves (different seasons). We also estimated burial fluxes of rhenium and osmium in the deepest part of the basin –with abundant H_2S. Calvert et al. (2001) reported large peaks of lead enrichment (almost tenfold) in the shallower part of ODP core 1033C raised from this basin, which they suspected to be metal contamination from an unknown source. Pb isotopes from freeze-core 1034A are also reported here, this element being an excellent tracer of recent heavy metal pollution.

Local geology and hydrography

Saanich Inlet is located on southern Vancouver Island, which belongs to the Insular belt subdivision of the Canadian Cordillera. This belt is interpreted as being the end product of several collisions between the main North American continent and some exotic crusts brought to the area by plate tectonics. The terrane comprising most of Vancouver Island is called Wrangellia; it was created by volcanic eruptions (arc-related) along with sedimentary cycles and intrusions that date back to the Late Devonian. Basement rocks that can be found around Saanich Inlet include limestones, cherts, basaltic and calc-alkaline volcanics, granitic and gabbroic intrusives, along with gneisses. Tholeiitic intrusion-hosted Ni-Cu and PGE showings are known on southern Vancouver Island (Geofile 2000-2: PGE Mineral Occurences in B.C.; B.C. Ministry of Energy and Mines). The Saanich Inlet fjord was shaped during the Fraser glaciation, which occurred between 29,000 and 10,000 years ago (Blais-Stevens et al. 2001). This last glaciation deposited large quantities of till on Vancouver Island. This till was later partially remobilised by mecanical erosion. More information about the geology of the area can be found in Monger (1994).

Saanich Inlet is characterized by a stratified surface water layers, high primary productivity, and a shallow sill that restricts bottom water circulation resulting in a deep anoxic water layer containing hydrogen sulfide, except during periodic deep water ventilation events (Blais- Stevens et al. 2001). Because of the low oxygen content of bottom water, the deeper part of the basin is almost free of bioturbation. Bottom sediments consist of organic-rich varved layers occuring in dark terrigeneous and light diatom-rich pairs. Sedimentation

rates range from 0.4 to 3 cm/year, with the highest values observed in the less compacted, shallower sedimentary sections (Gucluer and Gross, 1964; Matsumoto and Wong, 1977).

This fjord is caracterized by high sedimentation rates and organic content. Its bottom water is only slightly diluted by river water (S=31). It is O_2-free and contains H_2S throughout most of the year, minimizing mixing of the sedimentary record by benthic organisms (Blais-Stevens et al. 2001). Varved sediments are deposited in this basin as pale summer diatom-rich layers and dark winter layers that are more terrigeneous-rich.

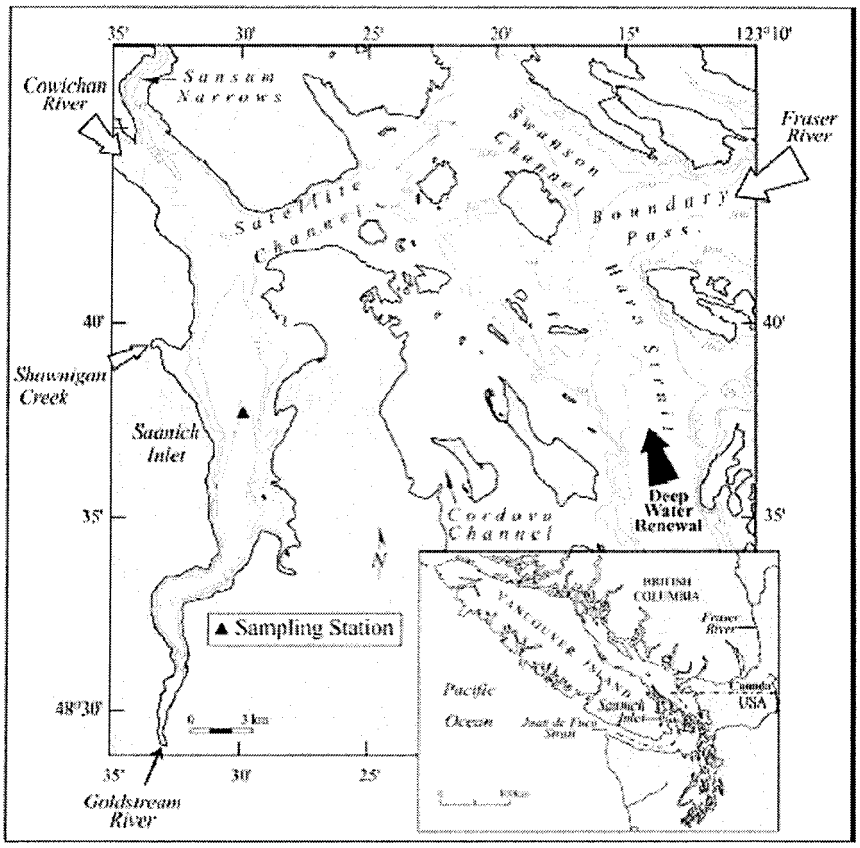

Figure III. 1 :Saanich Inlet's location and bathymetry, and major water inputs to the inlet (modified from Gargett et al. 2003)

Fresh water (and detritic sediments) comes mainly from the Fraser River in July, the Cowichan River during the winter months, and a very minor component from Shawnigan Creek, the Goldstream River and other minor rivers in its immediate watershed. Rain is also a freshwater contributor to this inlet. Strong tidal currents control the mixing of waters flowing

from the Fraser River and the Juan de Fuca Strait to Saanich Inlet. Sedimentary detritus (brought as a suspended load) is preferentially deposited near the sill, with less of it flowing further into the inlet (Gucluer and Gross, 1964).

Many occurences of molybdenite, gold, and base metals were reported from the Cowichan River region (including past base metal mines that operated in the 1900s). The Fraser River and its tributaries flow through the 238,000 km^2 that pass through the Canadian Cordillera and, as such, encounter numerous lithologies. This river also flows through Greater Vancouver (pop. ~1.7 million), with the associated potential urban contamination. Millions of tonnes of sediment are dredged annually from the bottom of Fraser River to make the passage between New Westminster and the Georgia Strait accessible to deep-sea vessels (Thompson, 1981). This activity undoubtedly has the effect of resuspending both sediments and contaminants at the same time. The Goldtream River, and especially the Fraser River, are historically known for the gold rush of the late 1850s, during which thousands of prospectors came to mine placer gold. Many kilograms of platinum group elements were retrieved from the Fraser's placers, including osmium and iridium alloy, called osmiridium (O'Neill and Gunning, 1934).

III. Methodology

This study reports results from freeze-core 1034A, sampled by S. Calvert's team in 1999 (S.K. Juniper, pers. comm.), and which comes from the same location as hole 1034 of ODP Leg 169S, at a water depth of 200 m. Freeze-cores keep the water-rich top sediments stratigraphically intact. Following the retrieval of the core, sediments were stored in a freezer, at –20°C. Our samples were taken from the top section of the Holocene Unit I of Bornhold et al. (1998). These varved sediments consist of olive-gray and diatomaceous muds with silt grade quartz, feldspar, mica and clay, as well as diatom and some rare plant debris.

The core was partially thawed and varves of both colors (seasons) were sub-sampled and oven-dried at 50°C. Some of the sediments were weighted before and after heating to dryness; water contents of *ca.* 65-70% wgt. were calculated. These numbers are lower than the 85-93% reported by Matsumoto and Wong (1977). Sublimation in the freezer may account for such discrepancies. Dried sediments were then ground in a zirconium mortar and

pestle apparatus. We calculated the sedimentation rate by counting the varves (assuming one pale/dark doublet per year) and obtained a rate of 0.7 cm/year in the lower part of the core, a value that is mentioned in the previously cited literature. In the top centimeters of the core (7-8 cm), varves were not as sharply defined as in the lower section. The age attribution discussed below is calculated along with this rate, but should only be regarded as a rough estimate since the exact number of years encompassed in the top of the core is uncertain. Thus, we get an estimated age of ~100 years for the analysed core (61 cm).

Through the ODP Gulf Coast Repository, we obtained a core section from hole 1033C from the 1998 *Ocean Drilling Project* Leg 169S in Saanich Inlet for comparison purposes (14-30 cm). Since approximately 1.5 m of sediment are missing from the top of 1033C core (Blais-Stevens et al. 2001), these sediments pre-date anthropogenic contamination. The location of hole 1033C is more to the south of the basin, where sediments are more organic-rich because of lower detritic input. The varved sediments were disturbed during shipment, so on arrival in Montreal, it was not possible to identify any more varves.

Chemical procedures and mass spectrometry

The Saanich Inlet sediments are characterized by a very high sedimentation rate, and should therefore have minimal meteoritic input (a phenomenon of high relevance to Os systematics since meteoritic dust can be of up to several ppm Os). Since we wanted to see the detritic impact on the osmium isotopic composition, at first, we did not attempt leach procedures to extract the hydrogeneous phase. Adding to the fact that some leach procedures were shown to dissolve non-hydrogeneous Os (Peuker-Ehrenbrink et al. 1995, Pegram and Turekian, 1999), the high Os content reported by Koide et al. (1991) led us to believe that most of it would be hydrogeneous in origin. In order to obtain the Re concentration, Os concentration and isotopic composition, between 0.5 and 1g of weighted sample were spiked with ^{185}Re and ^{190}Os enriched solutions prior to dissolution in HF-HBr in a Teflon™ bomb at 145°C for 24 hours. Liquid bromine was used in the elemental separations to first extract Os; then isoamylic alcohol was used to separate Re from the remaining aqueous solution. Following the procedure of Birck et al. (1998), spike-sample homogenization was done by adding excess Cr^{IV} to the solution and boiling it for 4-5 hours. Os is then purified by micro-distillation prior to being loaded on a platinum filament with barium hydroxide. The osmium

isotopic composition and concentration were obtained by negative thermal ionization mass spectrometry (NTIMS) on a VG Sector 54 equipped with an O_2-bleeding valve. Measurements were either taken in peak-jumping mode on a Channeltron electron multiplier or on Faraday cups using static multi-collection. Repeated standard measurements yielded $^{187}Os/^{188}Os = 0.10671 \pm 0.00023$ (2σ, n=8, on the Channeltron, for <100 pg Os) and 0.10704 ± 0.00012 (2σ, n=15, Faraday cups) for a K_2OsCl_6 standard from Jonhson Matthey. We also analysed the LOsTD standard solution distributed by T. Meisel (University of Leoben) and obtained $^{187}Os/^{188}Os = 0.10689 \pm 0.00005$ (2σ, n=5, Faraday cups).

Rhenium concentrations were acquired on a multi-collector ICP-MS (Micromass IsoProbe). The Re recovered from chemistry was dissolved in 2% HNO_3 doped with tungsten and pumped in free-aspiration mode through an Aridus desolvating membrane. The W–doping technique allows on-line monitoring of the mass bias to apply to spiked Re samples and allows a external reproducibility of better than ±0.2% to be obtained on the measured $^{187}Re/^{185}Re$. Pb isotope compositions were also acquired on the IsoProbe, with the mass bias corrected using the thallium doping technique, and normalising the Tl isotopic value by repeated analysis of the NBS-981 standard.

Selby and Creaser (2003) reported a protocol that they present as capable of digesting specifically Re-Os from organic matter (the hydrogenous fraction) in black shales, using an H_2SO_4-CrO_3 attack in Carius tube apparatus (240°C + high pressure). We used this reagent on an aliquot of Saanich Inlet sediments in a low pressure Teflon bomb (at 145°C), which should be less aggressive than a Carius tube, ideally leaving any non-hydrogenous phase intact. An aliquot of level 61 cm yielded 77 ppt Os and a $^{187}Os/^{188}Os$ ratio of 0.57 (see Table 1). This value is less radiogenic than another aliquot from the same sample processed with the HF-HBr dissolution step. The low ratio of this analysis cannot be attributed to a stratigraphic level of low $^{187}Os/^{188}Os$ hydrogenous osmium, since the aliquot from the same level using the regular procedure gave a more radiogenic result (an unradiogenic value of hydrogenous origin would have been recorded by two aliquots from the same varve). We suspect the procedure might have digested some of the Os from a detritic unradiogenic grain that was accidentally introduced into the sub-sample. A H_2SO_4-CrO_3 solution was used by Ravizza et al. (1991) to leach recent Black Sea sediment samples. These authors pointed out that such a leach solution was capable of partially digesting many mineral phases (not only

hydrogeneous). Since it also seemed capable of digesting more than the hydrogeneous phases of our sediments, we stopped using this technique.

Total carbon (C_{tot}) was obtained using a Carlo-Erba Elemental Analyser. Inorganic carbon was obtained using the coulometry technique, and C_{org} was estimated from (C_{tot} - C_{inorg}).

III. Results

Bulk sediment concentrations of Re, Os, $C_{org,}$ and C_{inorg}, along with isotopic ratio measurements of Os and Pb from 1034A freeze-core and additional data from hole 1034 of ODP Leg 169S are reported in table 2.

Carbon

Organic carbon increases in the core, from 2.2% at 61 cm to 2.5% at the surface. Inorganic carbon ranges from 500 to 1450 ppm in the core, increasing irregularly with depth. Two different sections can be distinguished based on C_{inorg} contents: a first one from the sediment-water interface down to *ca.* 35 cm with approximately 600 ppm of inorganic C and, below that, a second section with significantly higher content.

Lead isotopes

For core 1034A, we observed a shift to more radiogenic isotope compositions from core bottom up to *ca.* 10 cm, then values close to the ones found for the deeper samples near core top (Table 1, Fig. 2). This observation is true for the three 204-normalised lead isotopic ratios. The two analyses performed on the pre-anthropogenic levels of ODP core 1033C yielded compositions more radiogenic than those from 1034A core bottom.

Table III. 2: Elemental concentrations of Re, Os, Corg, Cinorg and N, and isotopic composition in Os and Pb

Sample depth (cm)	Re (ppt)	Os (ppt)	$^{187}Os/^{188}Os$ ± 2σ	$^{187}Re/^{188}Os$	$^{206}Pb/^{204}Pb$ ± 2σ	$^{207}Pb/^{204}Pb$ ± 2σ	$^{208}Pb/^{204}Pb$ ± 2σ	C_{org} (%)	C_{inorg} (ppm)
1.2	3570	51.9	0.874±0.046	361	18.350±0.004	15.610±0.005	38.201±0.015	2.35	600
3.2	3560	55.7	0.768±0.011	335				2.67	600
5.0	11030	55.0	0.807±0.020	1053	18.536±0.003	15.635±0.003	38.434±0.011	2.24	638
8.5	3470	55.6	0.939±0.018	328				2.31	555
11.5	3110	265	0.256±0.003	62				2.23	598
16.5	3950	55.5	0.945±0.007	374	18.522±0.005	15.623±0.005	38.372±0.014	2.66	757
21.5	4090	77.0	0.742±0.009	279				2.56	617
29.5	3090	66.7	0.630±0.020	243				2.43	543
33.5	8670	64.8	0.886±0.005	702	18.405±0.005	15.622±0.005	38.241±0.015	2.47	790
-duplicate	3560	55.2	0.899±0.035	339					
37.5	2900	59.8	0.865±0.013	254				2.07	734
45.5	3160	58.7	0.839±0.011	283				2.39	1431
47.0	2840	55.6	0.955±0.011	268				2.38	1034
51.5	2730	57.7	0.870±0.011	248	18.297±0.003	15.623±0.004	38.184±0.012	2.19	973
57.0	3040	64.2	0.899±0.008	249				2.42	1022
61.0	2560	60.4	0.873±0.005	222	18.296±0.003	15.614±0.003	38.182±0.013	2.15	798
61.0 Leach		77.8	0.574±0.005						
ODP 1033-I	4110	68.7	0.868±0.007	314	18.402±0.004	15.622±0.006	38.254±0.014		
ODP 1033-II	4540	61.8	0.931±0.007	386	18.366±0.003	15.612±0.004	38.212±0.008		

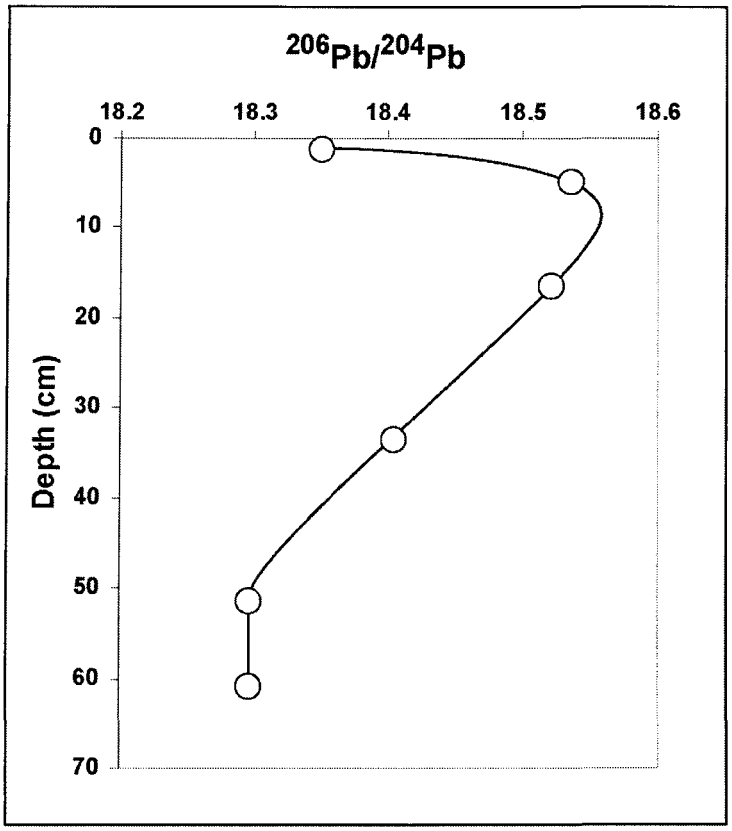

Figure III. 2: Pb isotopic composition in Saanich Inlet shallow sediments. Errors are smaller than symbols.

Rhenium

The rhenium content ranges from 2,500 to 11,000 ppt in shallow sediments in Saanich Inlet (Fig. 3). This corresponds to 55 times the Re concentration of average eroding continental crust (198 ppt, Peucker-Ehrenbrink and Jahn, 2001). We noted a general decrease in rhenium content, from ~3600 ppt at core top to 2600 ppt at 61 cm, as well as two excursions to higher values. A duplicate analysis of level 33.5 cm (Table 1) suggests that these higher values are probably due to small scale sediment lateral heterogeneities, as the replicate follows the main trend. Sediment heterogeneity seems significant at the sample size used (approx. 1g). Such high enrichment in Re is not realistically explained by blank problems. Such outliers, with very high Re content, may be attributed to some Re-rich detritic

grains and Os-poor phase since neither osmium content nor $^{187}Os/^{188}Os$ are affected (see below). Laminae of different seasons do not seem to have systematically distinct Re content. When the two outliers are excluded, Re content correlates with C_{org} with a R^2 of 0.6.

Re analyses from ODP core 1033C yielded about 30-40% more Re than the average value in core 1034A.

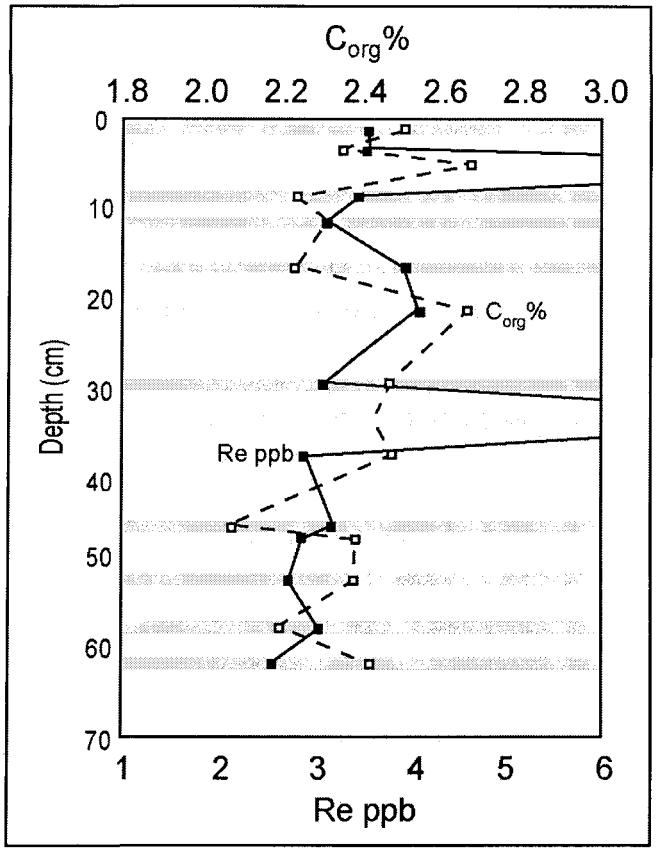

Figure III. 3: Re and organic carbon contents in Saanich Inlet. The dark bands indicate samples from terrigeneous-rich levels, pale bands samples from diatom-rich levels.

Osmium

Osmium concentrations in core 1034A are low compared to what was expected, given the anoxic nature of the basin (most data show 50-65 ppt –Fig 4-, compared to somewhat more Os-rich Black Sea sediments; Ravizza et al. 1991). Our results are also much lower than the result of the previous study of Koide et al. (1991) of 890 ppt Os. Our osmium

concentrations correspond to about twice the average eroding continental crust (31 ppt, Peucker-Ehrenbrink and Jahn, 2001).

The osmium content increases with depth from about 50 ppt at core top to 62 ppt at 61 cm down core, with a high Os-excursion near 20 cm from core top. Two trends can be identified: the first, from 61 cm to 26 cm below core-top, where Os and Re content patterns follow each other (R^2=0.7) and the second, in the overlying section, where the two elements are decoupled (Fig. 4). This is discussed below. In the top section of the core, osmium seems decoupled from the C_{org}, Os concentration, and gets lower as C_{org} increases (Fig. 5a). Below 20 cm, Os does follow the overall trend of organic C (R^2 = 0.4).

Measured values of the $^{187}Os/^{188}Os$ ratio range from 0.259 to 0.955 (Fig. 5), all of which are significantly lower than the value of the modern ocean osmium (1.06; Levasseur et al. 1998). The ODP 1033 core has similar Os concentrations and $^{187}Os/^{188}Os$ results (Table 1). One sample clearly stands out from the main trend (11.5 cm below core-top). It has a higher Os content (265 ppt) with a much lower isotopic composition (0.256). Such a high amount of osmium cannot be related to any blank problem, and is most probably related to sediment heterogeneity at the given sample size, as mentioned previously for Re. We noted that, for the same osmium content (55-56 ppt), five levels have isotopic ratios that range from 0.76 to 0.96.

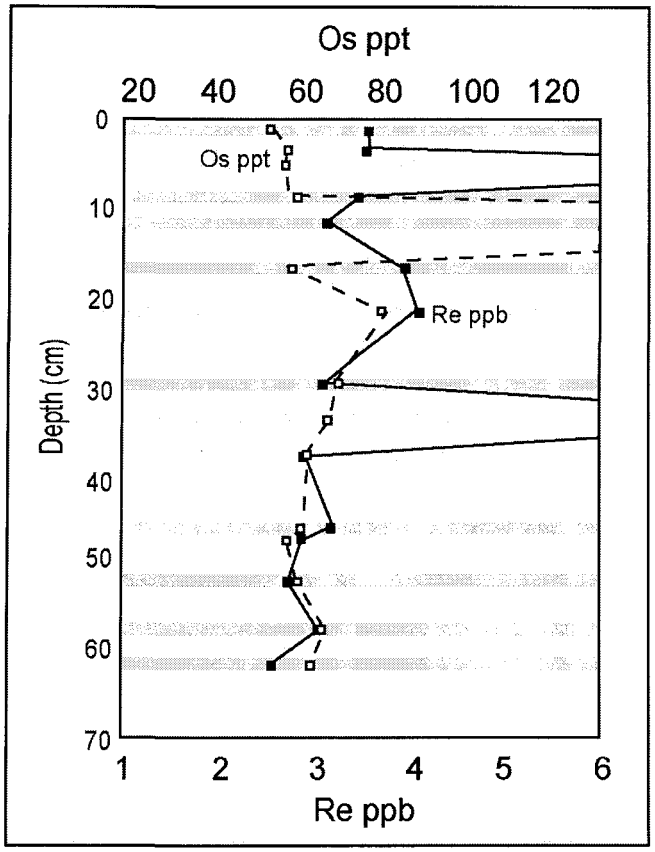

Figure III. 4: Comparative Re and Os content variations according to depth in Saanich Inlet surface varves. The dark bands indicate samples from terrigeneous-rich levels, pale bands samples from diatom-rich levels.

The osmium concentrations of core 1034A on which we are reporting are low compared to what was expected, given the anoxic nature of the basin and the value reported by Koide et al. (1991). Since results in hole 1033C show similar osmium concentrations and $^{187}Os/^{188}Os$ ratios as in hole 1034A, either we have a systematic bias (such as a severe incomplete spike-sample equilibrium) or, as we suspect, the Koide et al. value of 0.89 ppb may be due to ultramafic contamination, as is the case for the outlier value observed here at 11.5 cm below core-top. The fact that the Os content at deep levels correlates with both Re and organic C is in favor of the authenticity of our measured Os values (fig III.5).

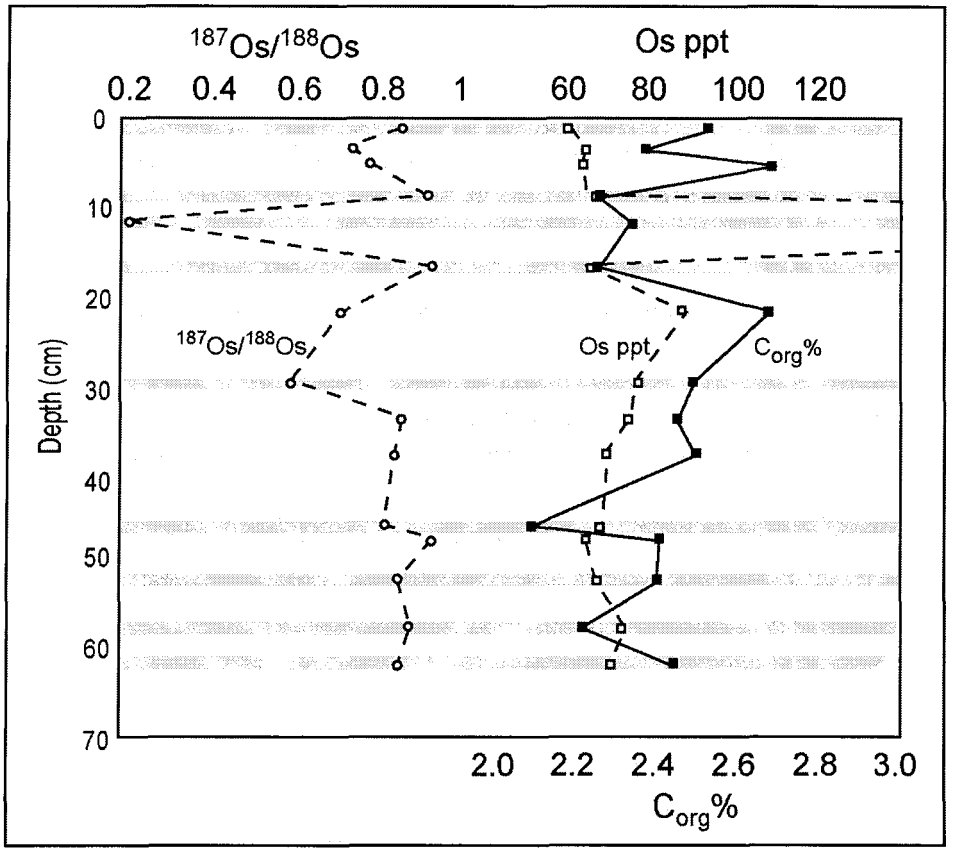

Figure III. 5: Os and organic carbon content and Os isotopic composition in Saanich Inlet core 1034A. The dark bands indicate samples from terrigeneous-rich levels, pale bands samples from diatom-rich levels.

III. Discussion

Carbon

McQuoid et al. (2001) explain the Holocene monotonic rise of organic C in Saanich Inlet recent sediments as the result of a steady increase in primary production. A similar increase in organic carbon is also seen here. It could be due to the same process, although a loss of C_{org} from anaerobic organic matter degradation during early diagenesis, as depth increased, cannot be discarded.

The sharp inorganic carbon content change at mid-core(Table III.2) -roughly 50-60 yrs ago-, could respond to a change in the sedimentary flux of $CaCO_3$ at that level. At the beginning of the 20th century, two limestone quarries were operating on the east (Tod Inlet)

and the west shores (Bamberton). Limestone from Tod Inlet was exhausted in 1921, but the Bamberton quarry operated until 1957 (161,638 tons of rock was quarried at Bamberton that in 1957).This end date approximately corresponds to the observed decrease in C_{inorg}. Some of the inorganic carbon may also come from mollusc shell fragments (Gucluer and Gross, 1964).

Lead isotopes

The shift in Pb isotopic composition observed in the 1034A freeze-core can be best explained by the change in atmospheric aerosol Pb composition ultimately deposited in Saanich Inlet. The use of tetraethyl-lead ($Pb(C_2H_5)_4$) as an anti-knocking agent in gasoline in North America between 1930 and the early 1980s is most probably the cause of the isotopic shifts. This was by far the biggest lead input to the environment (which, for the USA, peaked at over 270,000 metric tons of leaded gasoline used annually in the early 1970s; Nriagu, 1990). When observed in $^{208}Pb/^{204}Pb$ vs $^{206}Pb/^{207}Pb$ isotopic space (Fig. 6), the data progress towards compositions typical of American atmospheric aerosols (Sturges and Barries, 1987) before returning to background values (as in pre-industrial sediments from core 1033C).

The geographical proximity of Saanich Inlet to the USA border and the enormous size of that country's automobile pool explains why this fjord is more strongly affected by American, rather than Canadian, atmospheric pollution. We interpret the upper decrease in isotopic values as reflecting the ban on tetraethyl-lead additives; Figure 2 is remarkably similar to the historical trend in lead consumption in the USA (Fig.1, Nriagu, 1990). Francois (1988) pointed to the Bamberton quarry as a Pb source to explain the enrichment he observed in some sediment samples; but we do not have the isotopic composition of this limestone to compare with our dataset. Moreover, the lead isotopic composition pattern does not coincide with the inorganic carbon profile in this core.

The Trail Pb-Zn smelter (southern B.C., with a $^{206}Pb/^{207}Pb \sim 1.07$; Godwin and Sinclair, 1982) does not seem to be contributing to the lead input of Saanich Inlet. A similar conclusion was reached from Pb isotope results of lichen from southern Vancouver Island (Simonetti et al. 2003). Of all the epiphytic lichens from Vancouver Island used in Simonetti's work (n=8), only one had a composition similar to that seen in contaminated sediments Saanich Inlet (i.e., similar to that of USA aerosols); the rest had a Canadian aerosol

composition (that can also be interpreted as a southern Asian composition; Simonetti et al. 2003). This discrepancy is likely due to the fact that these lichens were sampled between 1995 and 1997 from young tree branches (likely <5 years; Simonetti et al. 2003), many years after the addition to Pb to gasoline had stopped (the residence time of atmospheric lead is in number of days).

The lead composition of the deepest levels analysed is likely representative of the natural composition of Pb brought to the inlet mainly by rivers and through deposition of natural aerosols. It is a weighted average of the composition of all these (uncharacterized) sources. Pre-automobile Pb pollution (coal burning, smelting, etc.) cannot be totally ruled out. Calvert et al. (2001) reported a variable Pb enrichment for the top section of core 1034A from ODP leg 169S. This is a pre-anthropogenic sedimentary section, so man-made lead contamination does not apply to their data. This varying Pb content may be indicative of a change in the Pb source(s) through time. This might also explain our variable pre-anthropogenic 1033C core results, which are isotopically different from the deepest levels of the 1034A freeze-core.

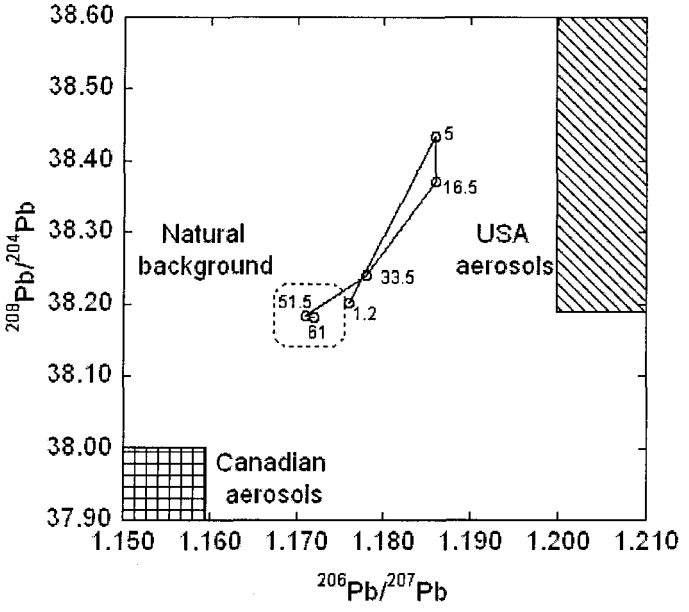

Figure III. 6: Pb isotopic composition of Saanich Inlet's surface sediments. Aerosol boxes from Graney et al. (1995). The boundaries of the 'Natural background' box are not constraint. The numbers next to the datapoints indicate depth (cm) from core 1034A.

Rhenium

Three main sources contribute to the burial of a trace metal: 1) a purely terrigeneous fraction, already within the mineral lattice of the accumulating material (part of which may exchange with water prior to deposition); 2) a hydrogenous phase that can be adsorbed/exchanged onto settling particles and 3) a post-depositional diagenetic fraction. The terrigeneous fraction content depends upon source rocks and relative weathering impacts on them. Re being rather mobile under Earth surface conditions, a significant fraction is brought from solid to solution by chemical erosion. Average eroding crust, as approximated by loess, has about 198 pg Re/g (Peucker-Ehrinbrink and Jahn, 2001). Rhenium contents in Saanich Inlet's surficial sediments are much higher than this value, suggesting that only a small amount of sedimentary Re is of terrigeneous origin here. In the absence of precise data on Re exchanges between settling particles and dissolved Re, one may only hypothesize that the diagenetic fraction is likely dominant here due to the Eh-sensitivity of Re.

Indeed, accumulation from diffusion, through the sediment-water interface, of reducing sediments is known to be important for Re burial. Crusius et al. (1996) reported trap sediments of crustal abundance values for Re in some H_2S-bearing basins, indicating that the enrichment of Re seen in these basins occurs below the sediment-water interface. This is also an observation from Mo data (François, 1988). For Saanich Inlet, Crusius et al. (1996) calculated a depth of Re reduction of approximately 1 cm below the sediment-water interface. The fact that the Re enrichment is not synchronous with the sediment deposition explains the lack of correlation with seasonal layers. One may suspect that organic matter has the effect of allowing a higher Re diagenetic enrichment at the sediment-water interface because of enhanced reducing conditions due to organic matter degradation. Crusius et al. (1996) shows that maximum Re enrichment in Saanich Inlet occurred in a no O_2, no H_2S zone (sub-oxic, 80-160 m depth) where the Re content rises to more than 40 ppb.

Osmium

Figures 4 and 5 show that Os concentrations correlate with both Re and C_{org} in the deeper part of the studied core. This suggests a close relationship in the burial of these elements. The decoupling of Os and both Re and C_{org} in the upper 8 cm suggests that 1) part of the osmium enters the sedimentary record through diffusion in the pore water, and 2) Os may be reduced and enriched deeper in the sediment than Re. This is consistent with dissolved osmium being found in the chemical complexes that precipitates with slow kinetics (Levasseur et al. 1998), thus precipitation occurs at greater depths from pore water. As above, no systematic differences between laminae of different seasons are seen. This suggests that a large fraction of the Os enrichment of such sediments is delayed with respect to their depositional age.

Measured values of the $^{187}Os/^{188}Os$ ratio range from 0.259 to 0.955 (Fig. 5, Table 1), all of which are significantly lower than the isotopic composition of the modern ocean ($^{187}Os/^{188}Os$ of 1.06). Since our data do not allow the hydrogenous Os fraction to be distinguished from the detrital fraction, these values reflect in part terrigenous Os isotopic signature; the local geology of the watershed includes mafic-ultramafic rocks that should have low Os isotopic compositions. If terrigenous fractions were more important, one would then expect a difference in $^{187}Os/^{188}Os$ ratios between cores 1034A and 1033C, since the latter

was raised farther from the sill and has been shown to contain lesser detrital fractions (Blais-Stevens et al. 2001). No such difference is observed. Additionally, the 2nd and 3rd most radiogenic data from core 1034A were obtained from dark terrigeneous-rich layers (Fig. 4). From those observations, unradiogenic detrital components apparently have a low impact on the measured osmium composition of these sediments.

When plotting the $^{187}Os/^{188}Os$ ratio against $1/[^{188}Os]$, a linear relationship (R^2=0.8) essentially controlled by the most unradiogenic point is seen (fig. 7). The simplest explanation for the observed distribution would involve a mixing of two end-members. The first end-member, Os-poor and with high $^{187}Os/^{188}Os$ ratio, would represent seawater-derived osmium. The second end-member, unradiogenic and Os-rich, can have multiple origins, either in solid and/or dissolved forms. Its only specific feature is a low isotopic composition. The scatter from a pure binary mixing would account for seasonally and spatially variable mixings of these end-members.

The unradiogenic end-member that dilutes the seawater-derived osmium can have the same three origins mentioned in the rhenium section : i) solid terrigeneous, ii) adsorbed by settling particles, and iii) post-depositional, diagenetically taken up (i.e., by diffusion of dissolved Os below the sediment-water interface). There are many possible sources for each of these, which we describe next.

Terrigeneous osmium input will necessarily vary through time in both quantity and quality (i.e., $^{187}Os/^{188}Os$ ratio) since the major rivers (Fig. 1) that contribute to the sediments buried in Saanich Inlet have seasonally changing water fluxes. The diversity of the lithologies encompassed within the watersheds of these rivers would have a bearing on both the Os content and isotopic composition.

Aerosols might also be a contributing factor to the solid phase. On such a local scale, aerosols may be variable in their Os content and isotopic composition reflecting the diversity of local outcrops.

Most of the non seawater-derived dissolved Os that is buried in Saanich Inlet deposits will be brought in by rivers. Dissolved Os may be incorporated into the sedimentary record via two different pathways: 1) syn-depositional, adsorbed dissolved osmium on settling particles and 2) post-depositional, dissolved Os that diffused through the water-sediment interface and reduced/precipitated at some depth in the sedimentary record. These cannot be

distinguished from one another from our dataset. Because it shares its geological origin (the watershed) with the terrigeneous fraction, the total dissolved Os of Saanich Inlet water will also certainly vary through time in both its concentration and isotopic composition. Deciphering every discrete source that contributes to osmium in the inlet is not possible from our bulk sediment data. The distribution and partitioning of dissolved and particulate osmium from the water of this fjord and its rivers would be interesting to investigate in future studies.

Several unradiogenic osmium sources can be cited to explain the low $^{187}Os/^{188}Os$ values of Saanich Inlet sediments:

1- an anthropogenic contribution (osmium is usually mined from ultramafic rocks of low $^{187}Os/^{188}Os$, i.e. ~ 0.2);

2- aerosol sources;

3- local unradiogenic inputs from rivers.

It is not possible to discriminate between these sources on the basis of osmium isotopes, but they can be at least examined

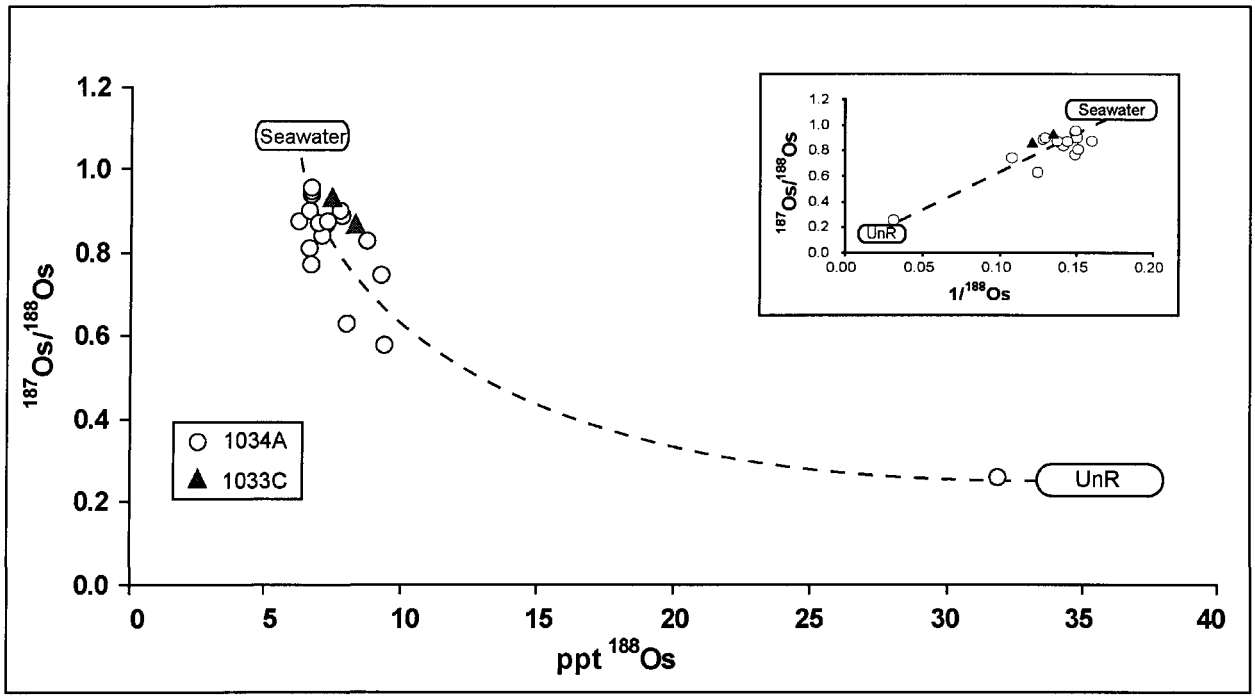

Figure III. 7: Reciprocal of Os content vs $^{187}Os/^{188}Os$ of Saanich Inlet sediments. A simple binary mixture would show a linear array in this diagram. Unradiogenic (UnR) and seawater fields indicate isotopic compositions.

Anthropogenic Os contamination in Saanich Inlet might come from the neighbouring Vancouver City metropolitan area, from aerosols and/or in dissolved/suspended form. Some aerosols may come from the US, as lead isotopes have shown. Where osmium is concerned, we have no way of discriminating between American and Canadian aerosols. Aerosols may contain osmium from various sources, either natural (continental dust) or anthropogenic (for example, from medical incinerators, Williams and Turekian, 2002). Since the pre-anthropogenic levels of ODP core 1033C show similar Os content and isotopic composition as the more recent sediment of freeze-core 1034A, we believe a natural cause explains our dataset. As such, we do not intend to consider the possibility of anthropogenic contamination further.

The contribution of natural aerosols is difficult to assess since we have no idea of its osmium content or its isotope signature (studies from other locations do not present quantitative constraints for us: aerosols are of local importance, see Williams and Turekian, 2002). Average loess has a more radiogenic mean isotopic composition than seawater (Peucker-Ehrinbrink and Ravizza, 2000) and, as such, would not explain our results. Some arc related volcanic unradiogenic input (Alves et al. 2002) could also be involved -from the Cascade- to explain some of our data. It does not A continuous input is unlikely

The last possibility considered to explain the results concerns the dissolved unradiogenic osmium from river waters. Unfortunately, representative measurements are missing, but the geological context of their watersheds provides a clue as to the possible isotopic composition of dissolved riverine Os. It is known, for instance, that osmiridium and platinum nuggets from ultramafic origin occur on the bottom of the Fraser River (as placers, O'Neil and Gunning, 1934). One can thus infer that ultramafic rocks in the watershed could give a low $^{187}Os/^{188}Os$ ratio to the Fraser River water. Riverine osmium thus seems the best source of unradiogenic Os to the inlet sediments.

Re and Os burial fluxes

The non-terrigeneous fraction of Re and Os buried in the sediments can be estimated as follows. The detrital fraction is calculated following eq.1 from Ravizza and Turekian (1992):

Equation 1: Detritus % = (100%-$CaCO_3$%-Organic Matter%-Opal%)

where $CaCO_3\%$ = C_{inorg} x 8.33, Organic Matter% = C_{org} x 2.5 (organic matter being approximated as CH_2O, all dry weight %). Carbonate and organic carbon values, along with estimates of opal content are taken from the literature (19 to 36% depending on the season; Gross et al. 1964; Calvert et al. 2001). Final calculation offers a range from 57 and 75% detritus. These values are consistent with Al% concentrations of 5-6 % reported by Calvert et al. (2001) at the coring site, compared with 9% in pure terrigeneous sediments.

Estimates of the Re hydrogenous fluxes are calculated as follows. We subtracted the terrigeneous input from the sediment, using the average Re content of eroding continental crust (198 ppt, Peucker-Ehrinbrink and Jahn, 2001). Re being significantly enriched in the study sediments, the Re content of the detritus does not weigh much on the Re-budget. Using the measured Re/C_{org} ratios, one can estimate a sedimentary Re-uptake ranging from 100 to 150 ng Re per gram of organic carbon buried. McQuoid et al. (2001) report burial fluxes of 10-11 mg TOC/cm^2.yr for shallow sediments of core ODP 1034B. This converts to 1 to 1.5 ng Re/cm^2.yr burial rates in the deep anoxic Saanich Inlet (ignoring two rhenium outliers from the data base). The study by Crusius et al. (1996) shows that the suboxic portion of this basin contains sediments with more Re than measured here. To estimate the total burial flux of Re in the fjord correctly, one would thus need a better knowledge its redox properties, spatially and temporarily, from "a rhenium perspective".

The same calculation made for osmium yields a flux of ~16 pg/cm^2/year of hydrogenous osmium in the sediments of the deep part of the basin. Since the diagenetic enrichment factor of Os is lower than that for Re, the setting of the osmium concentration for the detrital end-member greatly influences the calculated flux. Using the average eroding continental crust value of 31 ppt, one may estimate the hydrogenous fraction to represent between 55 and 77% of total osmium in the sediment, excluding the major outlier (fig. 6).

Such hydrogenous osmium fluxes are within ranges calculated for other anoxic basins (Ravizza and Turekian, 1992; Ravizza et al. 1991). Considering that most of the sediment Os carries an unradiogenic signature, one is led to conclude that either unradiogenic dissolved osmium is abundant in Saanich Inlet water, or that the average eroding crust composition used above is not appropriate for this basin.

Consequence for a future Re-Os isochron

In much older black shales, mismatches between the $^{187}Os/^{188}Os$ ratio of the sediment record and that of the contemporaneous ocean were discussed by Ravizza et al. (1991). They result in systematic errors for both the radiometric ages and estimates of initial isotopic compositions, depending on the Os "contamination" of the hydrogeneous Os fraction during deposition by an Os source that can be more or less radiogenic than seawater. The mean present-day $^{187}Os/^{188}Os$ ratio recorded for Saanich Inlet sediments (~0.68) is 35% lower than that of seawater Os. We can calculate the future isotopic composition of every sedimentary level using the radioactive decay equation, and then regress an isochron through the new dataset (keeping present-day uncertainties in the data). Doing this yields an age that is within uncertainty of the time used in the calculations (i.e., regression of 494 ± 10 Ma for T = 500 Ma injected). This is noteworthy, considering that a regression of the present-day data gives a non-zero age. The initial value from the 494 Ma regression yields values of 0.75 ± 0.15 for all data, and 0.88 ± 0.08 when the two most unradiogenic values are excluded. So, if Saanich Inlet matures as a closed system, it might be possible to date it correctly (i.e.,. agreeing with paleontological data), but the problem lies in the initial ratio of this isochron. The 1.06 composition of present-day seawater is not achieved with any subset of our dataset; as such, any interpretation based on the initial value of such an isochron would be misleading.

III. Conclusions

Shallow sediments from Saanich Inlet have recorded the rise and fall in the use of leaded gasoline by automobiles (*ca.* 1930-1980). The Pb isotope signatures of these sediments point to a predominance of contamination from the US. This is not surprising considering the proximity of southern Vancouver Island from the United States and the enormous amount of gasoline burnt there annually over the last century.

The Re and Os contents of Saanich Inlet varves seem to be related to the organic matter content. Rhenium data agree with a shallow reduction depth in the sediments (~1cm, Crusius et al. 1996). Osmium in the deep part of this fjord seems to be characterized by a deeper reduction depth than Re, which would limit the diagenetic enrichment of the most shallow sediments. There is no systematic difference in the Re-Os for laminae of different seasons (and terrigeneous content), indicating the limited importance of terrigeneous input for these two elements.

Saanich Inlet's sediments have an $^{187}Os/^{188}Os$ ratio that is significantly lower than the modern ocean. This can be accounted for by the addition of natural local unradiogenic osmium. The low osmium content (50-60 ppt) of this material means it is more easily contaminated by any unradiogenic osmium. Anthropogenic osmium (of low $^{187}Os/^{188}Os$) is rejected as a possible source since pre-anthropogenic sediments from ODP core 1033C have a similar low isotopic signature. As such, to explain our data, we cite natural sources of unradiogenic osmium brought to the inlet by riverine input and the associated sedimentary load derived in part from erosion of mafic-ultramafic lithologies.

The Saanich Inlet sediments have a low hydrogeneous-Os enrichment (16 pg $Os/cm^2/year$), but a good rate of Re burial (1 to 1.5 ng $Re/cm^2/yr$). Given this, a future 'bulk rock' Re-Os isochron dating of the Saanich Inlet lithified sediments would be feasible (the Re radioactive decay would be sufficient within a few million years), but the regression would yield an incorrect initial value, and, as such, would be misleading for the study of paleo-changes.

III. Acknowledgements

Thanks go to S.K. Juniper for supplying the sediments from freeze-core 1034A, and to TAMU ODP for the sediments from hole 1033C. Freeze-core 1034A was raised by S. Calvert. AP is very grateful to C. Hillaire-Marcel for his constructive comments on earlier versions of the manuscript.

References

Alves S., Schiano P. , Capmas F, Allègre C.J., (2002) Osmium isotope binary mixing arrays in arc volcanism. Earth and Planetary Science Letters 198; 355-369.

Birck, J.-L., Roy-Barman, M, and Capmas, F. (1998). Re-Os Isotopic Measurements at the Femtomole Level in Natural Samples. Geostandards Newsletter 20: 19-27.

Blais, S.A., Bornhold, B.D., Kemp-Alan, E.S., Dean, J.M., and Vaan, A.A. (2001). Overview of late Quaternary stratigraphy in Saanich Inlet, British Columbia; results of Ocean Drilling Program Leg 169S. Marine Geology 174: 3-26.

Bornhold, B.D., Firth J, Fox P.J., Baldauf J., and Francis T. (1996) OCEAN DRILLING PROGRAM, LEG 169S SCIENTIFIC PROSPECTUS, SAANICH INLET. ODP Publications Ocean Drilling Program, Texas A&M University.

Calvert, S.E., Pedersen, T.F., and Karlin, R.E. (2001). Geochemical and isotopic evidence for post-glacial palaeoceanographic changes in Saanich Inlet, British Columbia. Marine Geology 174; 287-305.

Cohen, A.S., Coe, A.L., Bartlett, J.M., and Hawkesworth, C.J. (1999) Precise Re-Os ages of organic-rich mudrocks and the Os isotope composition of Jurassic seawater. Earth and Planetary Science Letters 167; 159-173.

Creaser, R.A., Papanastassiou, D.A., and Wasserburg, G.J. (1991). Negative thermal ion mass spectrometry of osmium, rhenium, and iridium. Geochimica et Cosmochimica Acta 55: 397-401.

Crusius, J., Calvert, S.E., Pedersen, T., and Sage, D. (1996) Rhenium and molybdenum enrichments in sediments as indicators of oxic, suboxic and sulfidic conditions of deposition. Earth and Planetary Science Letters 145; 65-78.

Deschamps, P., Doucelance, R., Ghaleb, B., and Michelot, J.-L. (2003) Further investigations on optimized tall correction and high-precision measurement of Uranium isotopic ratios using Multi-Collector ICP-MS, Chem. geol. Chemical Geology 201, 141-160. 2003.

Francois, R. (1988) A study on the regulation of the concentrations of some trace metals (Rb, Sr, Zn, Pb, Cu, V, Cr, Ni, Mn and Mo) in Saanich Inlet sediments, British Columbia, Canada. Marine Geology 83: 285-308.

Gargett, A.E., Stucchi, D., and Whitney, F. (2003) Physical processes associated with high primary production in Saanich Inlet, British Columbia. Estuarine Coastal and Shelf Science 56: 1141-1156.

Godwin, C.I. and Sinclair, A.J. (1982) Average lead isotope growth curves for shale-hosted zinc-lead deposits, Canadian Cordillera. Economic Geology 77: 675-690.

Graney, J.R.; Halliday, A.N.; Keeler, G.J.; Nriagu, J.O.; Robbins, J.A.; Norton, S.A. (1995) Isotopic Record of Lead Pollution in Lake-Sediments from the Northeastern United-States. Geochimica et Cosmochimica Acta 59 : 1715-1728.

Gucluer, S.M. and Gross, M.G. (1964). Recent marine sediments in Saanich Inlet, a stagnant marine basin. Limnology and Oceanography 9: 359-376.

Koide, M., Goldberg, E.D., Niemeyer, S., Gerlach, D., Hodge, V., Bertine, K., and Padova, A. (1991). Osmium in marine sediments. Geochimica et Cosmochimica Acta 55: 1641-1648.

Levasseur, S., Rachold, V., Birck, J.L., and Allegre, C.J. (2000). Osmium behavior in estuaries: the Lena River example. Earth and Planetary Science Letters 177: 227-235.

Levasseur, S., Birck, J.L., and Allegre, C.J. (1998). Direct measurement of fetomoles of osmium and the $^{187}Os/^{186}Os$ ratio in seawater. Science 282: 272-274.

Manhès, G., Allegre, C.J., Dupré, B., and Hamelin, B. (1980) Lead isotope study of basicultrabasic layered complexes: speculation about the age of the Earth and primitive mantle characteristics. Earth and Planetary Science Letters 47, 370-382.

Matsumoto, E. and Wong, C.S. 1977. Heavy metal sedimentation in Saanich Inlet measured with ^{210}Pb technique. Journal of Geophysical Research 82; 5477-5482.

McQuoid, M.R., Whiticar, M.J., Calvert,S.E., and Pedersen,T.F. (2001) A post-glacial isotope record of primary production and accumulation in the organic sediments of Saanich Inlet, ODP Leg 169S. Marine Geology 174; 273-286.

Meisel, T., Reisberg, L., Moser, J., Carignan, J., Melcher ,F., and Bruegmann, G. (2003). Re-Os systematics of UB-N, a serpentinized peridotite reference material. Chemical Geology 201: 161-179.

Monger, J.W.H. (1994) Geology and Geological Hazards of the Vancouver Region, Southwestern British Columbia. Geological Survey of Canada, Natural Resources Canada.

Morford, J.L. and Emerson, S. (1999) The geochemistry of redox sensitive trace metals in sediments. Geochimica et Cosmochimica Acta 63; 1735-1750.

Nier, A.O. (1937). The isotopic constitution of osmium. Physical Review 52: 885.

Nriagu, J.O. (1990). The rise and fall of leaded gasoline. The Science of total Environment 92: 13-28.

O'Neill, J.J. and Gunning, H.C. (1934) Platinum and Allied Metal Deposits of Canada. Economic Geology Series. [No. 13], -165 p.. Geological Survey of Canada.

Oxburgh,R. (2001) Residence time of osmium in the oceans. Geochem. Geophys. Geosyst. 2, doi:10.1029/2000GC000104.

Pegram, W.J. and Turekian, K.K. (1999) The osmium isotopic composition change of Cenozoic sea water as inferred from a deep-sea core corrected for meteoritic contributions. Geochimica et Cosmochimica Acta 63, 4053-4058.

Peucker-Ehrenbrink, B. and Ravizza, G. (2000). The marine osmium isotope record. Terra Nova 12: 205-219.

Peucker-Ehrenbrink, B. and Hannigan, R.E. (2000). Effects of black shale weathering on the mobility of rhenium and platinum group elements. Geology 28: 475-478.

Peucker-Ehrenbrink, B. and Jahn, B.M. (2001). Rhenium-osmium isotope systematics and platinum group element concentrations: Loess and the upper continental crust. Geochemistry Geophysics Geosystems 2.

Peucker-Ehrenbrink, B. (2002) Comment on "Residence time of osmium in the oceans". Geochem.Geophys.Geosyst. 3, doi:10.1029/2001GC000297.

Peucker, E.B., Ravizza, G., and Hofmann, A.W. (1995) The marine (super 187) Os/ (super 186) Os record of the past 80 million years. Earth and Planetary Science Letters 130; 155-167.

Piper, D.Z. and Perkins, R.B. (2004). A modem vs. Permian black shale - the hydrography, primary productivity, and water-column chemistry of deposition. Chemical Geology 206: 177-197.

Ravizza, G. and Turekian, K.K. (1992) Application of the ^{187}Re-^{187}Os geochronometry system to black shale. Geochimica et Cosmochimica Acta 53, 3257-3262.

Ravizza, G., Turekian, K.K., and Hay, B.J. (1991). The geochemistry of rhenium and osmium in Recent sediments from the Black Sea. Geochimica et Cosmochimica Acta 55; 3741-3752.

Ravizza, G. and Turekian, K.K. (1992). The osmium isotopic composition of organic-rich marine sediments. Earth and Planetary Science Letters 110; 1-6.

Selby, David and Creaser, Robert A. (2003). Re-Os geochronology of organic rich sediments: an evaluation of organic matter analysis methods. Chemical Geology 200: 225-240.

Sharma, M. and Wasserburg, G.J. (1999) Osmium in the rivers. Geochimica et Cosmochimica Acta 61; 5411-5416.

Simonetti, A., Gariepy, C., and Carignan, J. (2003). Tracing sources of atmospheric pollution in Western Canada using the Pb isotopic composition and heavy metal abundances of epiphytic lichens. Atmospheric Environment 37: 2853-2865.

Singh, S.K., Trivedi, J.R., and Krishnaswami, S. (1999). Re-Os isotope systematics in black shales from the Lesser Himalaya; their chronology and role in the $^{187}Os/^{188}Os$ evolution of seawater. Geochimica et Cosmochimica Acta 63: 2381-2392.

Sturges, W.T. and Barrie, L.A (1987). Lead 206/207 isotope ratios in the atmosphere of North America as tracers of US and Canadian emissions. Nature 329: 144-146.

Thompson, R.E. (1981). Oceanography of the British Columbia Coast. Can. Spec. Publ. Fish. Aquat. Sci. ed.

Williams, G.A. and Turekian, K.K. (2002). Atmospheric supply of osmium to the oceans. Geochimica et Cosmochimica Acta 66: 3789-3791.

Woodhouse, O.B., Ravizza, G., Falkner, K.K., Statham, P.J., and Peucker, E.B. (1999). Osmium in seawater; vertical profiles of concentration and isotopic composition in the eastern Pacific Ocean. Earth and Planetary Science Letters 173; 223-233.

CONCLUSIONS GÉNÉRALES ET PERSPECTIVES

Ce manuscrit regroupe les résultats de trois études portant sur des thèmes géologiques distincts choisis parmi une foule d'autres qui auraient pu être abordés par la méthode Re-Os. L'objectif était donc de faire progresser l'état des connaissances de la géochimie Re-Os autant dans des domaines d'intérêt général, comme la pollution en métaux lourds en zone urbaine, que dans ceux plus académiques, par exemple via l'étude d'une météorite. En résumant ici, en français, les résultats de ces travaux rédigés en anglais aux fins de publication, on vise également à identifier certaines pistes de recherche envisageables pour le futur, d'abord pour chacun des domaines traités dans le mémoire, puis de manière plus globale, en ce qui a trait à la géochimie du couple Re-Os.

Dans le premier chapitre, publié sous le titre «Radiogenic Isotope Investigation of the St-Robert H5 Fall», le système isotopique Pb-Pb appliqué aux chondrules tend à démontrer que la météorite étudiée a eu une histoire précoce "typique", livrant un âge "classique" de 4.56 milliards d'années. Les données Re-Os des fragments de "roche totale" (RT), bien que situées autour d'une isochrone de 4.56 Ga, ne permettent pas d'établir une droite de régression pour obtenir un âge radiométrique digne de confiance. Cette constatation est fréquente dans les études Re-Os portant sur les chondrites et pourrait en partie être due aux différences de composition initiale des phases minérales constituantes des chondrites. Des phases métalliques de type kamacite-taenite donnent des résultats très équivoques, étant parfois dans le lot des données RT, d'autres montrant une perte importante et récente de Re. Une donnée sur un sulfure de fer (troïlite) suggère un enrichissement récent en Re, laissant croire à un échange de Re entre les phases métalliques. Des résultats surprenants viennent des croûtes de fusion; celles-ci ayant été générées lors de l'entrée atmosphérique du météore, par échauffement, jusqu'à volatilisation de la surface du spécimen. Les deux fragments de croûte analysés sont parmi les données les plus concordantes de l'ensemble de celles-ci; l'une des croûtes analysée livre même le résultat le plus près de l'isochrone de référence de 4.56 Ma. Il semble donc, à première vue, que la fusion/volatilisation dans l'atmosphère terrestre n'ait pas perturbé le système Re-Os de cette chondrite. Ces données ont été interprétées comme l'effet

d'une homogénéisation locale des phases, par fusion, donnant, par hasard, des valeurs proches de l'isochrone. Certaines questions non traitées ici demeurent: comment se comportent les phases silicatées pures (incluant les chondrules) en ce qui a trait au couple Re-Os? Y a-t-il une part de perturbation du jeu de données Re-Os attribuable à l'exposition à l'atmosphère terrestre, malgré la récupération rapide de ce spécimen? (l'effet d'une telle perturbation post-récupération sera approfondie dans mon stage post-doctorale à venir).

Le second chapitre, portant le titre «Isotopic Signature and Impact of Car Catalyst on the Anthropogenic Osmium budget», montre que les pots catalytiques des voitures contiennent bel et bien de l'osmium en quantité non négligeable. Cet osmium se retrouve là par simple contamination des platine, palladium et rhodium utilisés dans ces pièces automobiles. Ces trois éléments du groupe du platine (EPG) ont pour fonction de catalyser les réactions chimiques permettant de réduire la quantité de produits nocifs en sortie de pot d'échappement des véhicules. L'osmium n'est donc pas employé comme substance catalytique dans ces pièces, mais, appartenant au groupe du platine, il se retrouve en forte concentration dans les minerais du groupe. La séparation et la purification industrielles sont efficaces, mais incomplètes; il demeure ainsi dans les EPG un peu d'osmium résiduel dans les pots catalytiques. La composition isotopique non-radiogénique de l'osmium mesuré dans les catalyseurs confirme l'idée que l'osmium provient de gisements de platinoïdes (de signature isotopique typiquement mantellique). Les poussières de bord de route sont connues pour accumuler des EGP: un enrichissement attribué à la désagrégation des pots catalytiques, laissant sortir des particules riches en platinoïdes avec les gaz d'échappement automobile. Les concentrations relativement faibles en Os du matériel catalytique laissent prévoir un faible enrichissement en Os des bords de route par ce phénomène. Par contre, sous l'effet de la grande volatilité de l'osmium oxydé, soit sous la forme chimique favorisée par les fortes températures d'opération du pot catalytique, celui-ci passe sous la forme OsO_4 gazeuse à 110°C. Rappelons à ce sujet que les pots catalytiques atteignent des températures supérieures à 400°C. On est ainsi porté à croire que l'osmium pourrait être émis des pots catalytiques de façon préférentielle par rapport aux autres platinoïdes considérablement moins volatils. Une simulation des conditions d'opération d'un catalyseur automobile a permis de vérifier cette hypothèse: de 85 à 95% de l'osmium présent au départ dans le catalyseur fut perdu par dégazage. Un bilan global simplifié permet de prévoir que ce mécanisme émettrait

annuellement dans l'environnement urbain plusieurs picogrammes d'osmium par mètre carré. Cet osmium déposé à la surface des sols urbains est aisément mobilisable. Il constitue donc une nouvelle source d'osmium non radiogénique susceptible de contaminer les milieux sédimentaires. La phase suivante de cette étude consisterait ainsi à vérifier directement la quantité d'osmium relâchée en sortie des pots d'échappement automobiles et de retracer l'itinéraire de cet osmium dans l'environnement, d'abord sous forme OsO_4 gazeuse (et toxique!) et, ensuite, sous forme plus inerte réduite.

Le dernier chapitre porte sur les sédiments récents de Saanich Inlet, un fjord anoxique, en profondeur, de l'ouest du Canada. Les sédiments réducteurs du fjord ont la particularité de concentrer certains métaux dissous dans l'eau océanique sus-jacente. Ici, le but de l'étude était de vérifier la capacité de tels sédiments à concentrer l'osmium marin et à en enregistrer la composition isotopique. Les sédiments échantillonnés, représentant près de 100 ans de sédimentation récente, présentent de faibles teneurs en osmium (50-60 ppt) et une composition isotopique plus basse ($^{187}Os/^{188}Os$ = 0.8-0.95) que celle de l'eau de mer actuelle (1.06). La possibilité d'une contamination en Os d'origine anthropique des sédiments ne pouvant être écartée, on a eu recours aux isotopes du plomb afin de déceler l'ampleur éventuelle d'une telle contamination. Le signal d'entrée du Pb anthropique automobile dans la séquence sédimentaire est très visible (avec une diminution attendue en surface). On note cependant que les contaminations en Pb et éventuellement en Os sont découplées l'une de l'autre. On relève néanmoins que les sédiments les plus anciens analysés, donc d'âge "pré-contamination anthropique", présentent une composition isotopique en Os plus faible que celle de l'océan, suggérant donc une cause naturelle à l'origine de la signature isotopique de l'Os du fjord. La fraction marine d'osmium estimée dans ces sédiments est relativement faible (moins de 80% du total). Le rapport $^{187}Os/^{188}Os$ enregistré dans le sédiment paraît donc fortement influencé par une source non radiogénique. Deux sources de contamination peuvent rendre compte des données: 1) un apport terrigène qui rendrait compte du fait que la géologie locale et régionale des sources sédimentaires comporte nombres d'affleurements mafiques à ultramafiques; 2) un apport dissous fluviatile, particulièrement en provenance de la rivière Fraser connue pour les placers de platinoïdes de son lit. Ces concentrations d'osmium de composition isotopique typiquement non-radiogénique indiquent que l'on retrouves des roches ultramafiques dans le bassin versant de la Fraser. Sur la seule base de la

présente étude, il est donc impossible de trancher en ce qui a trait aux sources d'osmium à faible composition isotopique. Des analyses de l'eau du fjord et de ces tributaires pourraient permettre d'apporter une réponse univoque à ce sujet.

Enfin, un aspect encore problématique persiste pour ce qui concerne la géochimie Re-Os. Il concerne les approches analytiques. Certaines ambiguïtés des nombreux protocoles analytiques utilisés actuellement devront être levées. Pour cela, on devra comparer entre eux les divers protocoles (voir Appendice I de la présente thèse) et les tester sur différents matériaux géologiques (voir, par exemple, Meisel et al. 2003). Il est en effet possible que certains problèmes dits géologiques ne soient en fait que le résultat de biais analytiques (liés par exemple à la persistance de phases insolubles comprenant un partie significative de l'osmium des échantillons). ...De nombreuses années de travail sont donc garanties aux géochimistes isotopiques!

BIBLIOGRAPHIE GÉNÉRALE

Allègre C.J., Manhès G. & Göpel C. (1995) The age of the Earth. *Geochimica et Cosmochimica Acta* 59, 1445-1456.

Amelin Y., Krot A.N., Hutcheon I.D. & Ulyanov A.A. (2002) Lead isotopic ages of chondrules and calcium-aluminum-rich inclusions. *Science* 297, 1678-1683

Anders E. & Grevesse N. (1989) Abundances of the elements: Meteoritic and solar. *Geochimica et Cosmochimica Acta* 53, 197-214.

Barbante C., Veysseyre A., Ferrari C., Van de Velde K., Morel C., Capodaglio G., Cescon P., Scarponi G. & Boutron C. (2001) Greenland Snow Evidence of Large Scale Atmospheric Contamination for Platinum, Palladium, and Rhodium. *Environmental Science and Technology* 35, 835-839

Birck J.-L., Roy-Barman M & Capmas F. (1998) Re-Os Isotopic Measurements at the Femtomole Level in Natural Samples. *Geostandards Newsletter* 20, 19-27

Birck J.L. & Allegre C.J. (1998) Rhenium-187-osmium-187 in iron meteorites and the strange origin of the Kodaikanal meteorite. *Meteoritics & Planetary Science* 33, 647-653

Blais S.A., Bornhold B.D., Kemp-Alan E.S., Dean J.M. & Vaan A.A. (2001) Overview of late Quaternary stratigraphy in Saanich Inlet, British Columbia; results of Ocean Drilling Program Leg 169S. *Marine Geology* 174, 3-26

Blum J.D., Wasserberg G.J., Hutcheon I.D., Beckett J.R. & Stolper E.M. (1988) 'Domestic' origin of opaque assemblages in refractory inclusions in meteorites. *Nature* 331, 405-409

Bornhold B.D., Firth J, Fox P.J., Baldauf J. & Francis T. (1996) Ocean Drilling Program, Leg 169S Scientific Prospectus, Saanich Inlet. ODP Publications Ocean Drilling Program, Texas A&M University.

Brown P., Hildebrand A.R., Green-Daniel W.E., Page D., Jacobs C., Revelle D., Tagliaferri E., Wacker J. & Wetmiller B. (1996) The fall of the St-Robert Meteorite. *Meteoritics* 31; 502-517.

Calvert S.E., Pedersen T.F. & Karlin R.E. (2001) Geochemical and isotopic evidence for post-glacial palaeoceanographic changes in Saanich Inlet, British Columbia. *Marine Geology* 174; 287-305.

Chen J.H., Papanastassiou D.A. & Wasserburg G.J. (1998) Re-Os systematics in chondrites and the fractionation of the platinum group elements in the early solar system. *Geochimica et Cosmochimica Acta* 62, 3379-3392

Chen J.H., Papanastassiou D.A. & Wasserburg G.J. (2002) Re-Os and Pd-Ag systematics in Group IIIAB irons and in pallasites. *Geochimica et Cosmochimica Acta* 66, 3793-3810

Cohen A.S., Burnham O.M., Hawkesworth C.J. & Lightfoot P.C. (2000) Pre-emplacement Re-Os ages from ultramafic inclusions in the sublayer of the Sudbury igneous complex, Ontario. *Chemical Geology* 165; 37-46.

Cohen A.S., Coe A.L., Bartlett J.M. & Hawkesworth C.J. (1999) Precise Re-Os ages of organic-rich mudrocks and the Os isotope composition of Jurassic seawater. *Earth and Planetary Science Letters* 167; 159-173.

Collerson K.D., Kamber B.S. & Schoenberg R. (2002) Applications of accurate, high-precision Pb isotope ratio measurement by multi-collector ICP-MS. *Chemical Geology* 188, 65-83

Colodner D., Edmond J. & Boyle E. (1995) Rhenium in the Black Sea; comparison with molybdenum and uranium. *Earth and Planetary Science Letters* 131, 1-15

Creaser R.A., Papanastassiou D.A. & Wasserburg G.J. (1991) Negative thermal ion mass spectrometry of osmium, rhenium, and iridium. *Geochimica et Cosmochimica Acta* 55, 397-401

Crusius J., Calvert S.E., Pedersen T. & Sage D. (1996) Rhenium and molybdenum enrichments in sediments as indicators of oxic, suboxic and sulfidic conditions of deposition. *Earth and Planetary Science Letters* 145; 65-78.

Deschamps P., Doucelance R., Ghaleb B. & Michelot J.-L. (2003) Further investigations on optimized tall correction and high-precision measurement of Uranium isotopic ratios using Multi-Collector ICP-MS, *Chemical Geology* 201, 141-160.

Dickin A.P. (1995) *Radiogenic Isotope Geology*. Cambridge University Press.

Doucelance R. & Manhès G. (2001) Reevaluation of precise lead isotope measurements by thermal ionization mass spectrometry: comparison with determinations by plasma source mass spectrometry. *Chemical Geology* 176, 361-377

Doucelance R., Escrig S., Moreira M., Gariépy C. & Kurz M.D. (2003) Pb-Sr-He isotope ans trace element geochemistry of hte Cape Verde Archipelago. *Geochim.Cosmochim.Acta* 67, 3717-3733.

Esser B.K. & Turekian K.K. (1993) Anthropogenic osmium in coastal deposits. *Environmental Science and Technology,* 27; 2719-2724.

Farrauto R. & Heck R. (1999) Catalytic converters: state of the art and perspectives. *Catalysis Today* 51, 351-360.

Francois R. (1988) A study on the regulation of the concentrations of some trace metals (Rb, Sr, Zn, Pb, Cu, V, Cr, Ni, Mn and Mo) in Saanich Inlet sediments, British Columbia, Canada. *Marine Geology* 83, 285-308.

Gargett A.E., Stucchi D. & Whitney F. (2003) Physical processes associated with high primary production in Saanich Inlet, British Columbia. *Estuarine Coastal and Shelf Science* 56, 1141-1156.

Godwin C.I. & Sinclair A.J. (1982) Average lead isotope growth curves for shale-hosted zinc-lead deposits, Canadian Cordillera. *Economic Geology* 77, 675-690.

Göpel C., Manhés G. & Allegre C.J. (1985) U-Pb systematics in iron meteorites: Uniformity of primordial lead. *Geochim.Cosmochim.Acta* 49, 1681-1695.

Göpel C., Manhés G. & Allegre C.J. (1994) U-Pb systematics of phosphates from equilibrated ordinary chondrites. Earth and Planetary Science Letters 121, 153-171.

Graney J.R., Halliday A.N., Keeler G.J., Nriagu J.O., Robbins J.A. & Norton S.A. (1995) Isotopic Record of Lead Pollution in Lake-Sediments from the Northeastern United-States. *Geochimica et Cosmochimica Acta* 59, 1715-1728.

Gucluer S.M. & Gross M.G. (1964) Recent marine sediments in Saanich Inlet, a stagnant marine basin. *Limnology and Oceanography* 9, 359-376.

Harry Y.McSween (1999) *Meteorites and their parent planets*, 2nd ed. edn. Cambridge Univ. Press.

Heck R & Farrauto R. (2001) Automobile exhaust catalysts. *Applied Catalysis* 221, 443-457.

Helz G.R., Adelson J.M., Miller C.V., Cornwell J.C., Hill J.M., Horan M.F. & Walker R.J. (2000) Osmium Isotopes Demonstrate Distal Transport of contaminated Sediments in Cheasapeake Bay. *Environmental Science and Technology* 34, 2528-2534.

Horan M.F., Walker R.J., Morgan J.W., Grossman J.N. & Rubin A.E. (2003) Highly siderophile elements in chondrites. *Chemical Geology* 196, 5-20.

Itoh S. & Yurimoto H. (2003) Contemporaneous formation of chondrules and refractory inclusions in the early Solar System. *Nature* 423, 728-731.

Jaffe L.A, Peucker-Ehrenbrink B. & Petsch S.T. Mobility of rhenium, platinum group elements and organic carbon during black shale weathering. *Earth and Planetary Science Letters* 198, 339-353. 2002.

Kallemeyn G.W., Rubin A.E., Wang D. & Wasson J.T. (1989) Ordinary Chondrites: Bulk compositions, classification, lithophile-element fractionations, and composition-petrographic type relationships. *Geochimica et Cosmochimica Acta* 53, 2747-2767.

Koide M., Goldberg E.D., Niemeyer S., Gerlach D., Hodge V., Bertine K. & Padova A. (1991) Osmium in marine sediments. *Geochimica et Cosmochimica Acta* 55, 1641-1648

Lee D.C & Halliday A.N. (1995) Precise determination of the isotopic compositions and atomic weights of molybdenum, tellurium, tin and tungsten using ICP magnetic sector multiple collector mass spectrometry. *International Journal Mass Spectrometry and Ion Processes* 146/147, 35-46.

Levasseur S., Birck J.L. & Allegre C.J. (1998) Direct measurement of femtomoles of osmium and the Os-187/Os-186 ratio in seawater. *Science* 282, 272-274.

Levasseur S., Rachold V., Birck J.L. & Allegre C.J. (2000) Osmium behavior in estuaries: the Lena River example. *Earth and Planetary Science Letters* 177, 227-235.

Leya I., Wieler R., Aggrey K., Herzog G.F., Schnabel C., Metzler K., Hildebrand A.R., Bouchard M., Jull A.-J.T., Andrews H.R., Wang M.S., Ferko T.E., Lipschutz M.E., Wacker J.F., Neumann S. & Michel R. (2001) Exposure history of the St-Robert (H5) fall. *Meteoritics and Planetary Science* 36; 1479-1494.

Ludwig K.R. (2001) Isoplot /Ex 2.49, A Geochronological Toolkit for Microsoft Excel. [Special Publication No.1a.]. Berkeley, CA, USA, Berkeley Geochronology Center.

Manhès G., Allegre C.J., Dupré B. & Hamelin B. (1980) Lead isotope study of basic-ultrabasic layered complexes: speculation about the age of the Earth and primitive mantle characteristics. *Earth and Planetary Science Letters 47, 370-382.*

Martin C.E., Peucker E.B., Brunskill G. & Szymczak R. (2001) Osmium isotope geochemistry of a tropical estuary. *Geochimica et Cosmochimica Acta* 65; 3193-3200.

Matsumoto E. & Wong C.S. (1977) Heavy metal sedimentation in Saanich Inlet measured with (super 210) Pb technique. *Journal of Geophysical Research* 82; 5477-5482.

McCandless T. & Ruiz J. (1991) Osmium isotopes and crustal sources for platinum-group mineralization in the Bushveld Complex, South Africa. *Geology* 19, 1225-1228.

McQuoid M.R., Whiticar M.J., Calvert S.E. & Pedersen T.F. (2001) A post-glacial isotope record of primary production and accumulation in the organic sediments of Saanich Inlet, ODP Leg 169S. *Marine Geology* 174 ; 273-286.

McSween H.Y. (1999) *Meteorites and their parent planets.* Cambridge University Press.

Meisel T., Reisberg L., Moser J., Carignan J., Melcher F. & Bruegmann G. (2003) Re-Os systematics of UB-N, a serpentinized peridotite reference material. *Chemical Geology* 201, 161-179.

Merget R. & Rosner G. (2001) Evaluation of the health risk of platinum group metals emitted from automotive catalytic converters. *The Science of total Environment* 270; 165-173.

Monger J.W.H. (1994) *Geology and Geological Hazards of the Vancouver Region, Southwestern British Columbia.* Geological Survey of Canada, Natural Ressources Canada.

Morford J.L. & Emerson S. (1999) The geochemistry of redox sensitive trace metals in sediments. *Geochimica et Cosmochimica Acta* 63; 1735-1750.

Nier A.O. (1937) The isotopic constitution of osmium. *Physical Review* 52, 885.

Nriagu J.O. (1990) The rise and fall of leaded gasoline. *The Science of total Environment* 92, 13-28.

O'Neil J.J. & Gunning H.C. (1934) Platinum and Allied Metal Deposits of Canada. Economic Geology Series. [No. 13], -165 p. Geological Survey of Canada.

Oxburgh R. (2001) Residence time of osmium in the oceans. *Geochem.Geophys.Geosyst.* 2, doi:10.1029/2000GC000104.

Palme H. & Jones A. (2003) Solar system abundances of the elements. In: *Meteorites, Comets, and Planets* (ed A.M.Davis), pp. 41-61. Elsevier-Pergamon, Oxford.

Patterson C. (1956) Age of Meteorites and the Earth. *Geochimica et Cosmochimica Acta* 10, 230-237.

Pegram W.J. & Turekian K.K. The osmium isotopic composition change of Cenozoic sea water as inferred from a deep-sea core corrected for meteoritic contributions. *Geochimica et Cosmochimica Acta* 63; 4053-4058.

Peucker-Ehrenbrink B., Ravizza G. & Hofmann A.W. (1995) The marine $^{187}Os/^{186}Os$ record of the past 80 million years. *Earth and Planetary Science Letters* 130; 155-167.

Peucker-Ehrenbrink B. & Ravizza G. (2000) The marine osmium isotope record. *Terra Nova* 12, 205-219.

Peucker-Ehrenbrink B. & Hannigan R.E. (2000) Effects of black shale weathering on the mobility of rhenium and platinum group elements. *Geology* 28, 475-478.

Peucker-Ehrenbrink B. & Jahn B.M. (2001) Rhenium-osmium isotope systematics and platinum group element concentrations: Loess and the upper continental crust. *Geochemistry Geophysics Geosystems* 2, art-2001GC000172.

Peucker-Ehrenbrink B. (2002) Comment on "Residence time of osmium in the oceans". *Geochem.Geophys.Geosyst.* 3, doi:10.1029/2001GC000297.

Piper D.Z. & Perkins R.B. (2004) A modem vs. Permian black shale - the hydrography, primary productivity, and water-column chemistry of deposition. *Chemical Geology* 206, 177-197.

Rauch S., Hemond H.F. & Peucker-Ehrenbrink B. (2004) Recent Changes in Platinum Group Element Concentrations and Osmium Isotopic Composition in Sediments from an Urban Lake. *Environmental Science and Technology* 38, 396-402.

Ravizza G. & Turekian K.K. (1989) Application of the ^{187}Re-^{187}Os geochronometry system to black shale . *Geochimica et Cosmochimica Acta* 53, 3257-3262.

Ravizza G., Turekian K.K. & Hay B.J. (1991) The geochemistry of rhenium and osmium in Recent sediments from the Black Sea. *Geochimica et Cosmochimica Acta* 55; 3741-3752.

Ravizza G. & Turekian K.K. (1992) The osmium isotopic composition of organic-rich marine sediments. *Earth and Planetary Science Letters* 110; 1-6.

Ravizza G.E. & Bothner M.H. (1996) Osmium isotopes and silver as tracers of anthropogenic metals in sediments from Massachusetts and Cape Cod bays. *Geochimica et Cosmochimica Acta* 60; 15, 2753-2763.

Ripley E.M., Park Y.R., Lambert D.D. & Frick L.R. (2001) Re-Os isotopic variations in carbonaceous pelites hosting the Duluth Complex; implications for metamorphic and metasomatic processes associated with mafic magma chambers. *Geochimica et Cosmochimica Acta* 65; 2965-2978.

Russell A.D., Papanastassiou D.A. & Tomborello T.A. (1978) Ca isotope fractionation on the Earth and other solar system materials. *Geochimica et Cosmochimica Acta* 42, 1075-1090.

Selby David & Creaser Robert A. (2003) Re-Os geochronology of organic rich sediments: an evaluation of organic matter analysis methods. *Chemical Geology* 200, 225-240.

Sharma M. & Wasserburg G.J. (1999) Osmium in the rivers. *Geochimica et Cosmochimica Acta* 61; 5411-5416.

Shirey S.B. & Walker R.J. (1995) Carius tube digestion for low-blank rhenium-osmium analysis. Analytical Chemistry 67, 2136-2141.

Shirey S.B. & Walker R.J. (1998) The Re-Os isotope system in cosmochemistry and high-temperature geochemistry. *Annual Review of Earth and Planetary Sciences* 26, 423-500.

Simonetti A., Gariepy C. & Carignan J. (2003) Tracing sources of atmospheric pollution in Western Canada using the Pb isotopic composition and heavy metal abundances of epiphytic lichens. *Atmospheric Environment* 37, 2853-2865.

Singh S.K., Trivedi J.R. & Krishnaswami S. (1999) Re-Os isotope systematics in black shales from the Lesser Himalaya; their chronology and role in the $^{187}Os/^{188}Os$ evolution of seawater. *Geochimica et Cosmochimica Acta* 63, 2381-2392.

Smith I.C., Carson B.L. & Ferguson T.L. (1974) Osmium: An Appraisal of Environmental Exposure. *Environmental Health Perspectives* 8, 201-213.

Smoliar M., Walker R.J. & Morgan J.W. (1996) Re-Os ages of Group IIA, IIIA, IVA, and IVB iron meteorites. *Science* 271; 1099-1102.

Sturges W.T. & Barrie L.A (1987) Lead 206/207 isotope ratios in the atmosphere of North America as tracers of US and Canadian emissions. *Nature* 329, 144-146.

Tatsumoto M., Knight R.J. & Allegre C.J. (1973) Time differences in the formation of meteorites as determined from the ratio of lead-207 to lead-206. Science 180, 1279-1283.

Tera F. & Carlson R.W. (1999) Assessment of the Pb-Pb and U-Pb chronometry of the early solar system. *Geochimica et Cosmochimica Acta* 63, 1877-1889.

Thirlwall M. (2001) Inappropriate tail corrections can cause large inaccuracy in isotope ratio determination by MC-ICP-MS. *Journal of Analytical Atomic Spectrometry* 16, 1121-1125.

Thirlwall M.F. (2002) Multicollector ICP-MS analysis of Pb isotopes using a (207)pb-(204)pb double spike demonstrates up to 400 ppm/amu systematic errors in Tl-normalization. *Chemical Geology* 184, 255-279.

Thompson R.E. (1981) *Oceanography of the British Columbia Coast*, Can. Spec. Publ. Fish. Aquat. Sci. edn.

Völkening J. & Walczyk T.and Heumann K.G. (1991) Osmium Isotope ratio determinations by negative thermal ionization mass spectrometry. *Intl.J.Mass Spectrom.Ion Phys.* 105, 147-159

Walker R.J., Horan M.F., Morgan J.W., Becker H., Grossman J.N. & Rubin A.E. (2002) Comparative ^{187}Re-^{187}Os systematics of chondrites: Implications regarding early solar system processes. *Geochimica et Cosmochimica Acta* 66, 4187-4201.

Wasserburg G.J. (1985) Short-lived nuclei in the early solar-system. In: *Protostars and Planets* (ed D.C.Black and M.S.Matthews), pp. 703-737. Univ. Arizona Press.

Wasson J.T. & Kallemeyn G.W. (1988) Composition of chondrites. Phil.Trans.R.Soc.Lond. A325, 535-544.

Williams G.A. & Turekian K.K. (2002) Atmospheric supply of osmium to the oceans. *Geochimica et Cosmochimica Acta* 66, 3789-3791.

Woodhouse O.B., Ravizza G., Falkner K.K., Statham P.J. & Peucker E.B. (1999) Osmium in seawater; vertical profiles of concentration and isotopic composition in the eastern Pacific Ocean. *Earth and Planetary Science Letters* 173; 223-233.

Yin Q.Z., Jacobsen S.B., Lee C.T., McDonough W.F., Rudnick R.L. & Horn I. (2001) A gravimetric K (sub 2) OsCl (sub 6) standard; application to precise and accurate Os spike calibration. *Geochimica et Cosmochimica Acta* 65; 13, 2113-2127.

APPENDICE I
LA SOLUTION D'OSMIUM LOSTD

Cette section présente les résultats qui ont été obtenus pour l'analyse d'une solution d'osmium fabriquée et distribuée par le Dr. Thomas Meisel (Université de Leoben, Autriche). Le but de la fabrication de cette solution est d'en faire un étalon pour l'inter-calibrage des laboratoires où l'on produit des analyses isotopiques d'osmium. Comme les protocoles analytiques des différents laboratoires n'ont pas la même efficacité pour tous les types d'échantillons, il vaut mieux débuter l'inter-calibrage par une solution pure ne nécessitant pas de séparation/purification chimique. Le projet en est à ces débuts; la solution ne possède pas encore de valeur certifiée. Cette section rapporte les résultats d'une dizaine de laboratoires (dont le GEOTOP), ce qui nous permet de les comparer au niveau de l'analyse spectrométrique d'osmium.

La solution LOsTD

Il s'agit d'une solution de HCl 10% comportant 10^{-3} g $Os/g_{solution}$ (soit 1000 ppm). Cette solution est fortement concentrée et ne nécessite pas de purification préalable à l'analyse spectrométrique, contrairement à la plupart des échantillons géologiques. Aucune donnée à propos des abondances isotopiques en osmium de cette solution n'était transmise aux laboratoires participants.

Les appareils analytiques

Les laboratoires ayant participé à cette première ronde analytique utilisent des spectromètres de masse de technologies différentes. Ces différences étant à même d'influencer les résultats obtenus, nous passeront rapidement en revue les caractéristiques distinguant les spectromètres 1) à source thermique en mode d'ions négatifs (NTIMS), 2) à source plasma et quadripôle (ICP-MS) et 3) à source plasma, secteur magnétique et multi-collecteur (MC-ICP-MS).

Les NTIMS sont les appareils les plus sensibles quant à l'analyse d'osmium ; les rendements à l'ionisation pouvant atteindre 20%, contrairement à quelques % pour les sources ICP. Toutefois, la solution LOsTD fournie comportant suffisamment d'osmium pour

être bien mesurée par tous les appareils, ceci ne devrait pas induire de différences significatives dans les résultats. L'ionisation par NTIMS se fait sur filament de platine, sur lequel on dépose la solution LOsTD et qu'on recouvre ensuite d'un activateur. L'un des isotopes mineurs du platine (^{190}Os, 0.0122% du Pt, période de décroissance de ~450 Ga, Shirey et Walker, 1998) possède un noyau instable et produit, par désintégration radioactive alpha, du ^{186}Os radiogénique. Cette source de contamination est éliminée par le dégazage dans l'air du filament, juste avant de l'utiliser. Ce chauffage en présence d'oxygène permet l'oxydation de l'osmium, sous forme OsO_4, présent dans le filament -dont le ^{186}Os radiogénique- et la volatilisation de l'osmium sous cette forme chimique (le OsO_4 boue à 110 degrés). Un dégazage inadéquat laisserait du ^{186}Os provenant du Pt du filament, et celui-ci serait combiné avec l'osmium de l'échantillon, altérant le rapport ^{186}Os/^{188}Os mesuré.

C'est au niveau de la partie analyseur que l'on retrouve une distinction technologique susceptible d'introduire des différences importantes dans les résultats. Le rôle de l'analyseur d'un spectromètre de masse est de séparer les divers isotopes les uns des autres. Le NTIMS et le MC-ICP-MS sont équipés d'électro-aimants (aussi nommé secteur magnétique), alors que les ICP-MS disposent d'un quadripôle. Un quadripôle permet le passage d'un seul isotope à la fois, obligeant l'utilisateur à mesurer en *peak jumping* pour obtenir des rapports d'abondances isotopiques. Le plasma étant instable, les signaux le sont aussi et cela constitue une limitation à la précision qu'il est possible d'atteindre par la mesure en mono-collection. Une mesure simultanée des divers isotopes remédie à ce problème. Le secteur magnétique permet cette multi-collection, les ions passant dans un champs magnétique sont séparés les uns des autres, et tous les isotopes d'osmium sont mesurables simultanément (de même que certaines interférences isobariques potentielles).

Un second avantage de l'électro-aimant sur le quadripôle, en ce qui concerne la mesure de compositions isotopiques, est le plateau au sommet des pics générés; les pics de quadripôle ayant un sommet arrondi (voir figure A.1). Il est difficiles de mesurer exactement au même endroit l'intensité de deux pics dont les sommets sont ronds, induisant du bruit dans les signaux enregistrés. De plus, ce plateau admet la possibilité d'une légère fluctuation des paramètres critiques au positionnement des pics (champs magnétiques, haute tension, etc.) au cours de l'analyse sans compromettre la précision.

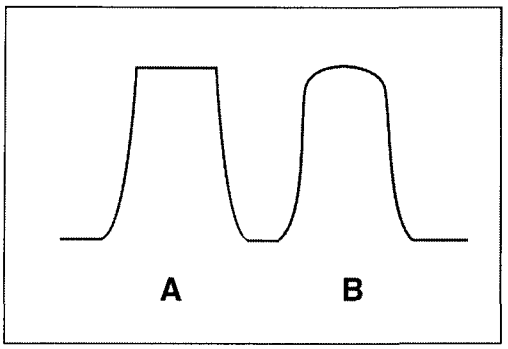

Figure A. 1: A- Pic à sommet plat d'un secteur magnétique, **B-** Pic rond typique d'un quadripôle

Un autre facteur peut influencer les résultats des deux types d'instruments à source plasma : l'utilisation d'une membrane de désolvation. Ces systèmes permettent typiquement d'amplifier les signaux mesurés par un ordre de grandeur, ce qui rend leur utilisation extrêmement répandue. En contrepartie, on doit diluer la solution LOsTD afin de ne pas saturer les amplificateurs des détecteurs, augmentant par le fait même la possibilité d'une contamination par les échantillons précédents. En effet, ces membranes sont connues pour retenir longtemps plusieurs éléments chimiques ("effet mémoire") et ce, malgré des lavages intensifs entre les échantillons. Nous ignorons si ces membranes ont servit aux laboratoires impliqués dans cette ronde analytique.

Tous ces appareils doivent tenir compte de l'interférence isobarique à la masse 187, provenant du Re. On peut aisément surveiller cette possibilité à la masse 185 (l'autre isotope de rhénium).

Les 5 analyses que nous avons fournies au Dr. Meisel pour cette première ronde analytique ont été obtenues par thermo-ionisation en mode d'ions négatifs sur le Sector 54, en multi-collection statique, avec 60 cycles d'acquisition par analyse pour 5-6 ng d'osmium sur le filament. La moyenne de nos données est affichée avec une incertitude de un écart-type. Dans les diagrammes de cette annexe, l'UQAM est le laboratoire numéro 7.

Résultats et discussions

Nous avons analyser la solution LOsTD en la traitant comme une inconnue. Les résultats de ces analyses sont présentés aux figures A.2 à A.6, soit une figure par rapport

isotopique mesuré (nous ne pré0sentons pas les rapports $^{192}Os/^{188}Os$ -de normalisation- et $^{184}Os/^{188}Os$ -que peu de laboratoires mesurent).

Nous avons reporté la reproductibilité externe comme intervalle d'erreur pour nos données, c'est-à-dire l'écart-type de la moyenne de nos analyses. Nous ignorons si c'est le cas pour les autres laboratoires. Notons que les laboratoires 2 et 11 de même que 9 et 10 sont en fait les mêmes laboratoires, qui semblent avoir envoyé deux jeux de données. Le disposition des laboratoires en abscisse est fonction des données $^{187}Os/^{188}Os$ croissantes (voir fig. A.3). Comme les détails analytiques de chaque laboratoire ne sont pas connus pour cette ronde d'analyse anonyme, nous ne pouvons pas faire une analyse exhaustive de ces différences. Par conséquent, nous présentons simplement les résultats afin de montrer notre position, en commentant brièvement chaque diagramme.

La figure A.2 présente les rapports $^{186}Os/^{188}Os$ obtenus pour la solution LOsTD. Les différences des données ne peuvent être expliquées par un dégazage imparfait du filament, puisque les points les plus élevés sont des données obtenues par source plasma. La seule donnée NTIMS qui ne soit pas comprise dans l'intervalle d'erreur de la moyenne (laboratoire #3), est bien en dessous de la moyenne. Nous remarquons que ce laboratoire présente des résultats significativement différents des moyennes pour les rapports $^{189}Os/^{188}Os$ et $^{190}Os/^{188}Os$ aussi, ce qui nous permet de suspecter un problème important au niveau analytique ou de dépouillement des données pour celui-ci.

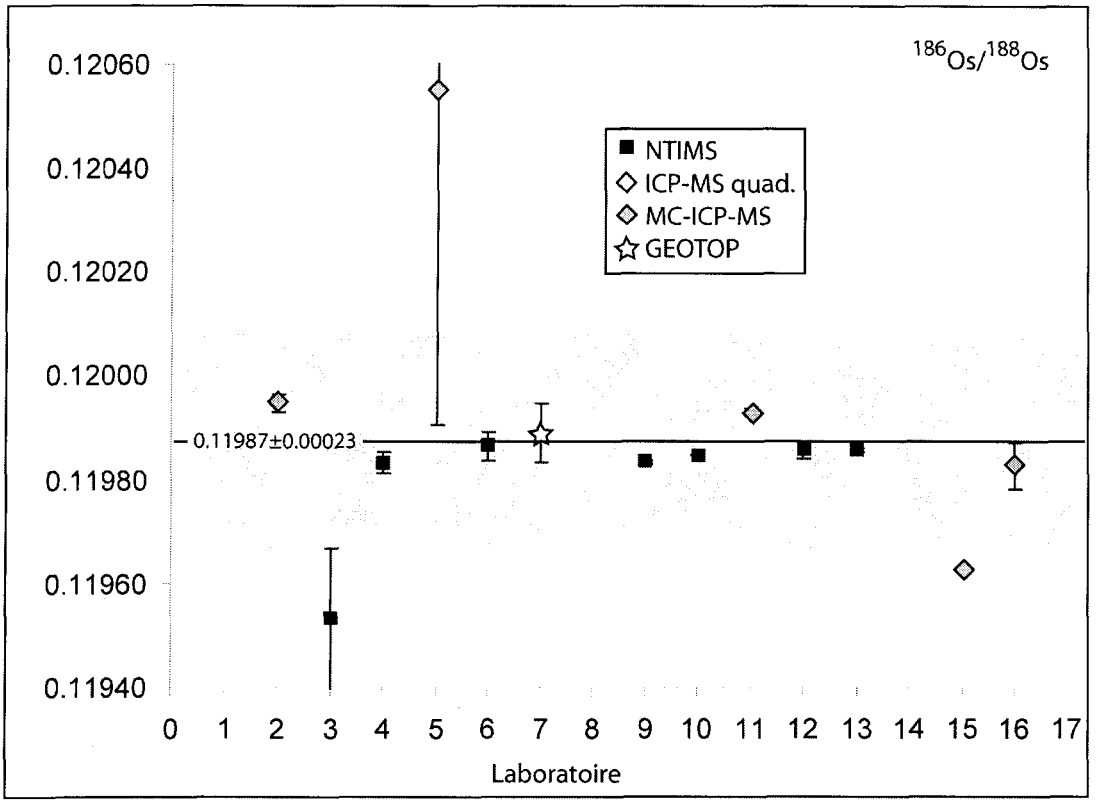

Figure A. 2 Rapports isotopiques $^{186}Os/^{188}Os$ produits par différents laboratoires sur la solution d'osmium LOsTD (valeurs fournies par Dr. T. Meisel). La valeur de la moyenne(±1 écart-type) est indiquée sur la droite horizontale.

La figure A.3 présente les résultats pour la valeur $^{187}Os/^{188}Os$, qui est le rapport le plus intéressant pour la plupart des études Re-Os. On constate que les précisions affichées sont beaucoup plus grandes pour les laboratoires 1 et 14, qui sont des spectromètres ICP avec quadripôle. Notons que ces deux laboratoires n'ont pas présenté de valeurs pour les autres rapports isotopiques.

Les valeurs plus élevées des MC-ICP-MS peuvent s'expliquer par l'utilisation (hypothétique) d'une membrane de désolvatation. La solution LOsTD est peu radiogénique (elle est de composition sub-chondritique), et une solution diluée pourrait facilement être contaminée par un résidu d'osmium crustal radiogénique dans cette membrane. Pour les valeurs TIMS, une interférence isobarique en Re qui serait mal corrigée pourrait induire

certaines différences de cette base de données (des filaments de Re étant souvent utilisés dans ce types d'appareil pour les analyses de Rb-Sr, Sm-Nd et U-Pb).

Nous constatons que le laboratoire 2 n'est pas reproductible avec lui-même (seconde valeur au #11); comme les autres rapports isotopiques sont reproductibles pour ce laboratoire, on peut imaginer un effet mémoire tel que mentionné plus haut, ou encore à une sur-correction d'interférence en 185 (qui ne serait pas du Re) pour la valeur la pus faible.

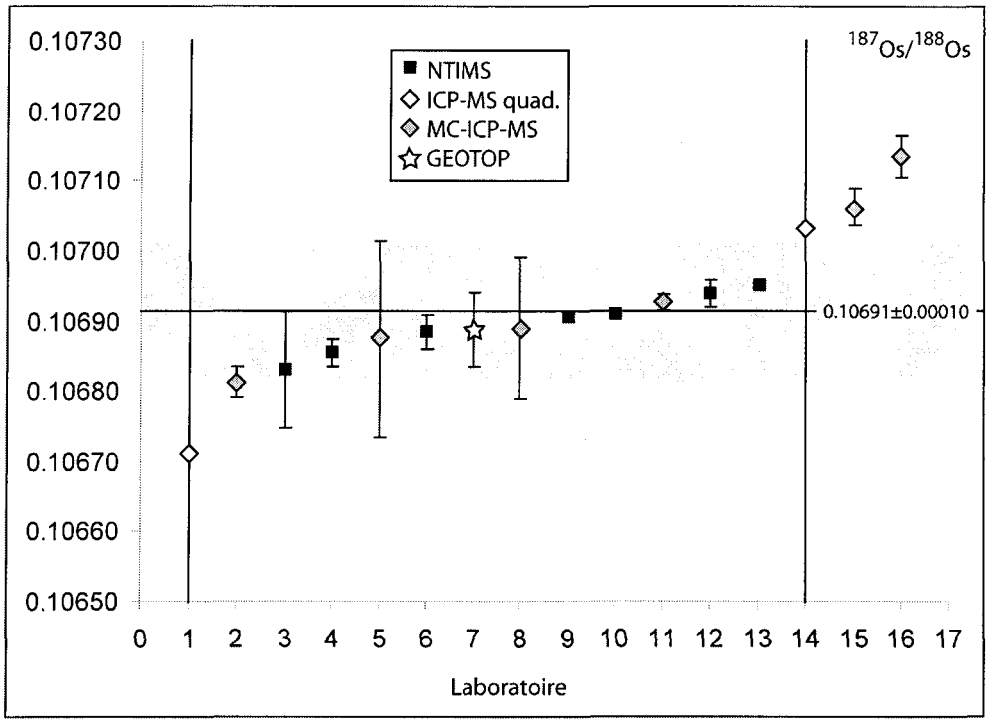

Figure A. 3 Rapports isotopiques $^{187}Os/^{188}Os$ produits par différents laboratoires sur la solution d'osmium LOsTD (valeurs fournies par Dr. T. Meisel). La valeur de la moyenne (±1 écart-type) est indiquée sur la droite horizontale.

Les résultats des rapports naturellement invariables $^{189}Os/^{188}Os$ et $^{190}Os/^{188}Os$ (Fig. A.4 et A.5) semblent relativement homogènes d'un laboratoire à l'autre, mis à part pour les laboratoires 3 et 15 (déjà mentionnés ci-haut comme discordants). On constate toutefois un plus grand éparpillement pour les données en $^{189}Os/^{188}Os$. Pour la figure A.4, en ne tenant pas

compte des deux points aux valeurs les plus faibles, la moyenne devient 1.21965, et se rapproche de la majorité des données.

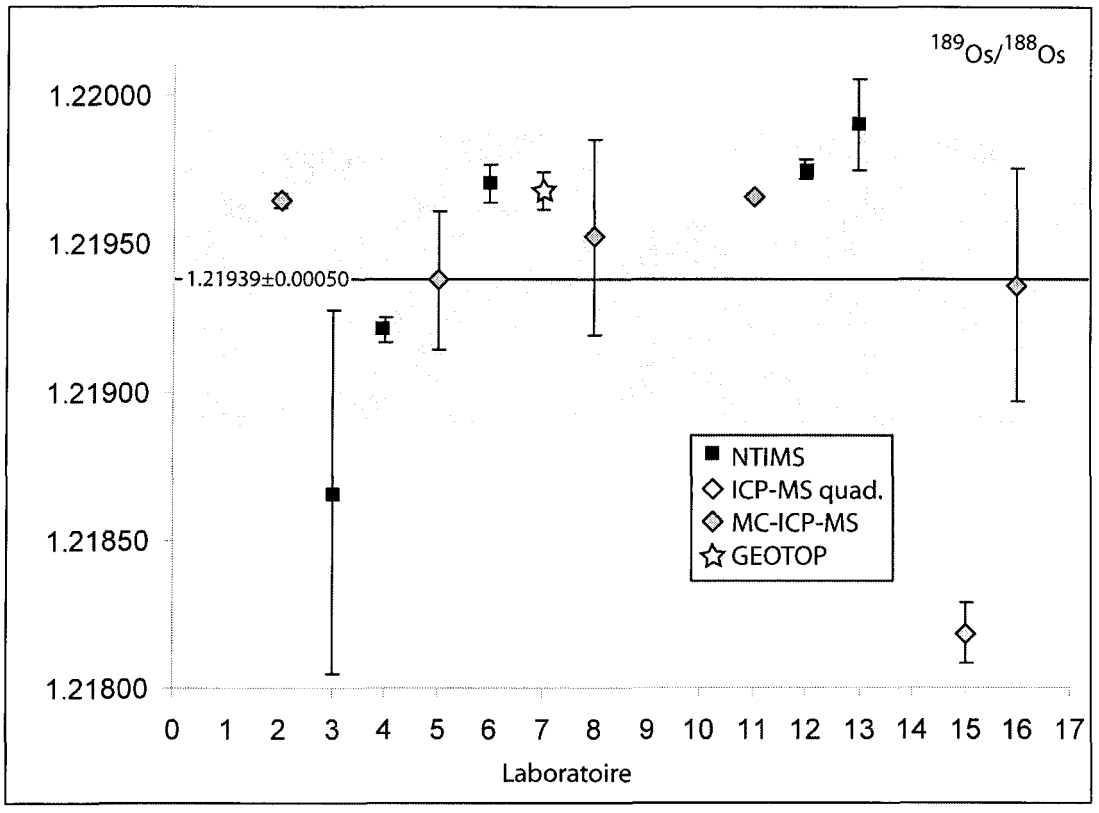

Figure A. 4 Rapports isotopiques $^{189}Os/^{188}Os$ produits par différents laboratoires sur la solution d'osmium LOsTD (valeurs fournies par Dr. T. Meisel). La valeur de la moyenne (±1 écart-type) est indiquée sur la droite horizontale.

En éliminant les données des laboratoires 3 et 15 de la figure A.5, l'écart-type diminue d'un ordre de grandeur, et tous les autres laboratoires sont dans le domaine d'incertitude de la moyenne. Il est surprenant de voir que les laboratoires 9 et 10 ne produisent pas ce rapport ; l'isotope ^{190}Os étant utilisé comme *spike* pour la dilution isotopique par la vaste majorité des études d'osmium.

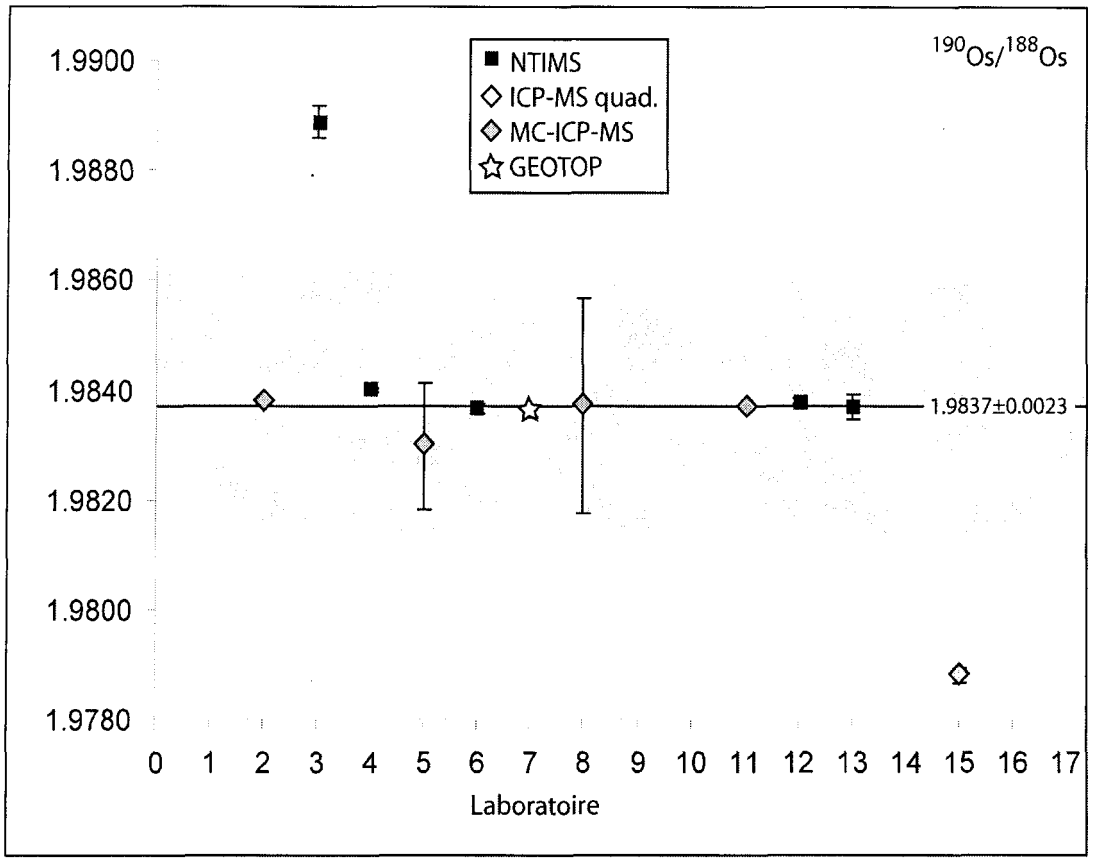

Figure A. 5 Rapports isotopiques $^{190}Os/^{188}Os$ produits par différents laboratoires sur la solution d'osmium LOsTD (valeurs fournies par Dr. T. Meisel). La valeur de la moyenne (±1 écart-type) est indiquée sur la droite horizontale.

Compte tenu des différences obtenues pour cette solution d'osmium par les divers laboratoires, il n'est pas encore possible de certifier les rapports des isotopes d'osmium de cette solution. Beaucoup de problèmes analytiques rapportés dans la littérature semblent provenir de la mise en solution et/ou de l'équilibration avec le spike. Il apparaît ici que l'étape finale de la production de donnée, soit la spectrométrie de masse/dépouillement des résultats bruts, soit porteuse d'une partie de cette divergence. Il est essentiel d'uniformiser les méthodes d'analyses par spectrométrie de masse avant de passer à l'étape de la comparaison des protocoles chimiques.

Dépouillement des données d'osmium

Dans cette section, nous présentons les grandes lignes de notre méthode de traitement des données brutes; celle-ci correspond à la procédure généralement publiée. Malgré cela, un fait étonnant tient en la grande variabilité des résultats issus des différents laboratoires, et ce même pour des appareils analytiques similaires. En supposant que les appareils analytiques fonctionnent bien, on peut donc croire que ce sont les dépouillements mathématiques post-analyses qui induisent de telles différences.

Nos mesures de compositions isotopiques en osmium sont effectuées par spectrométrie de masse à ionisation thermique en polarité inversée, avec une fuite réglable d'oxygène injecté dans la source pendant l'analyse. Par cette technique, l'osmium est oxydé et ionisé sous l'espèce moléculaire OsO_3^-. L'oxygène possédant 3 isotopes (de masses 16, 17 et 18), plusieurs combinaisons sont possibles avec l'osmium. Pour un même isotope d'osmium, plusieurs masses de trioxyde seront obtenues, interférant les une sur les autres, tel qu'exposé au tableau A.1. Afin de corriger ces interférences, nous utilisons les rapports d'abondance d'oxygène suivants : $^{17}O/^{16}O = 0.00037$ et $^{18}O/^{16}O = 0.002047$ (Nier, 1950), en négligeant le fractionnement de l'oxygène (on fait alors l'hypothèse d'un réservoir d'oxygène infini, cas réaliste dans ces conditions). Un calcul de probabilité indique que les combinaisons de deux isotopes mineurs de l'oxygène sont négligeables; seules les combinaisons comportant deux ^{16}O sont prises en considération.

Une fois les intensités des isotopes d'osmium retrouvées (et non plus celles des oxydes), on peut évaluer directement le fractionnement isotopique instrumental. Pour ce faire, nous utilisons le rapport $^{192}Os/^{188}Os$, que nous comparons à la valeur de référence 3.08271. La loi de fractionnement linéaire est utilisée pour corriger les autres rapports isotopiques d'osmium.

L'interférence potentielle de Re à m=187 est vérifiée à la masse 185, mais dans le cas des analyses LOsTD, celle-ci était négligeable. Ajoutons que dans le cas d'échantillon, on doit aussi effectuer une étape de calcul supplémentaire pour extraire la composition de l'échantillon du mélange spike + échantillon. Nous appliquons à nos données l'amplification

d'erreur liée à la sous-addition ou à la sur-addition de spike (telle que décrite dans Sambridge et Lambert, 1997).

Tableau A. 1 Combinaison des isotopes d'Os et O dans la molécule OsO_3. N.B.: les combinaisons avec deux isotopes mineurs de l'oxygène sont négligées, de même que celles avec l'isotope 184 de l'osmium.

Masse 234	Masse 235	Masse 236	Masse 237	Masse 238	Masse 239	Masse 240
$^{186}Os^{16}O_3$	$^{186}Os^{16}O_2{}^{17}O$	$^{186}Os^{16}O_2{}^{18}O$				
	$^{187}Os^{16}O_3$	$^{187}Os^{16}O_2{}^{17}O$	$^{187}Os^{16}O_2{}^{18}O$			
		$^{188}Os^{16}O_3$	$^{188}Os^{16}O_2{}^{17}O$	$^{188}Os^{16}O_2{}^{18}O$		
			$^{189}Os^{16}O_3$	$^{189}Os^{16}O_2{}^{17}O$	$^{189}Os^{16}O_2{}^{18}O$	
				$^{190}Os^{16}O_3$	$^{190}Os^{16}O_2{}^{17}O$	$^{190}Os^{16}O_2{}^{18}O$
						$^{192}Os^{16}O_3$